A CROSSCORRELATION METHOD

FOR

MEASURING THE IMPULSE RESPONSE OF REACTOR SYSTEMS

by

J. DOUGLAS BALCOMB

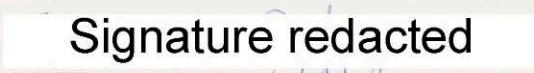B.S., University of New Mexico

(1956)

SUBMITTED IN PARTIAL FULFILLMENT

OF THE REQUIREMENTS FOR THE

DEGREE OF DOCTOR OF PHILOSOPHY

at the

MASSACHUSETTS INSTITUTE OF TECHNOLOGY

June, 1961

Signature of Author   Signature redacted
                    Department of Nuclear Engineering

Certified by   Signature redacted
                    Thesis Supervisor

ABSTRACT

A CROSSCORRELATION METHOD

FOR

MEASURING THE IMPULSE RESPONSE OF REACTOR SYSTEMS

by

J. Douglas Balcomb

Submitted to the Department of Nuclear Engineering on May 12, 1961, in partial fulfillment of the requirements for the degree of Doctor of Philosophy.

By the use of crosscorrelation, the impulse response of a system can be calculated from the system response to a wide-band input signal. The crosscorrelation function of the input and the output signals is equal to the system impulse response. The crosscorrelation method offers advantages over the conventional methods of measuring system dynamics in that it can produce results quickly in the presence of large noise sources. Small input signals can be used which do not excite system non-linearities or interfere with normal system operation. In order to demonstrate the validity of the method for use on nuclear reactor systems, an analog computer study and two sets of experiments on widely differing reactor types have been performed all with satisfactory results. It is concluded that the crosscorrelation method is a useful reactor diagnostic technique, probably the best technique for measuring the dynamic response characteristics of some reactor systems, including rocket propulsion reactors. Included in the work are: a detailed analysis of the theory of the crosscorrelation method, an extensive and exact analysis of errors in the crosscorrelation data due to system noise, a description of a computer code for transforming data from the impulse response of a system to a system transfer function, a description of the equipment which has been built to implement the crosscorrelation method, and a description of the experiments performed and their results.

Thesis Supervisor: Elias P. Gyftopoulos
Title: Assistant Professor of Nuclear Engineering

ACKNOWLEDGEMENTS

Dedication

TO

SARA

TABLE OF CONTENTS

TABLE OF APPENDICES

LIST OF FIGURES AND ILLUSTRATIONS

LIST OF FIGURES AND ILLUSTRATIONS

LIST OF TABLES

CHAPTER I

INTRODUCTION

The advent of new and specialized types of reactor
systems has resulted in increasing difficulties in
performing system dynamics measurements by the convention-
al methods.

The small signal dynamic response of reactor systems
is normally measured either by exciting the reactor with
sinusoidal[2,3] or step changes[4] of reactivity or by auto-
correlating the reactor power fluctuations.[5,6] These
techniques each have inherent restrictions which limit
their use. Oscillation tests require a relatively long
operating time because many frequency components of the
response spectrum must be excited separately. In
addition, the system response to the sinusoidal input
must be appreciably larger than the inherent reactor
noise to obtain accurate results unless input-output
crosscorrelation techniques are employed. Furthermore,
large signals may exceed the linear range of the system.
Step response experiments do not require a long time,
but the requirements for such an experiment cannot
always be met. The minimum step amplitude is determined
by the accuracy required in the presence of the inherent
reactor noise. The maximum step amplitude is determined
either by safety considerations or by system non-lineari-
ties. In many cases the step amplitude required is great-
er than the permissible maximum and the experiment can-
not be performed. Reactor power autocorrelation methods
do not introduce system disturbances and do not require
long experiment time. The autocorrelation function of
the reactor power fluctuations is calculated and some
assumptions are made about the origin of noise within

the system. The system dynamics can then be calculated. In most practical instances, very little is known about the internal system noise and so the autocorrelation function is of little use.

The crosscorrelation method is a means of measuring the impulse response of a system and is particularly useful in applications where the above three methods cannot be used. The method requires a minimum of time and can produce very usable results with system response amplitudes equal to the inherent system noise. The particular motivation for the work described in this writing was the need to make system dynamics measurements on the control systems of nuclear rocket reactors during actual operation. The experimental test conditions are such that conventional methods cannot be used. The reactors are operated for a short time, of the order of minutes, and only once. In addition, the allowable perturbations of reactor power are of the same magnitude as the noise in the measured reactor power. Boiling water reactors are another type of reactor system in which the crosscorrelation method could be used to advantage, since the noise level in these reactors is very large.

The crosscorrelation method consists basically of the following: The system, for which a dynamic response characteristic is desired, is excited by introducing a noise-like input signal. The signal contains, in equal magnitude, each frequency for which the system has a significant response. The crosscorrelation function of the input signal and the system output is computed. This crosscorrelation function is equal to the impulse response of the system. A simplified derivation, which illustrates why this result is obtained, follows.[7]

Consider a system characterized by an impulse

response or weighting function h(t). For an input, a(t), the corresponding system output, b(t), is given by the convolution integral.

$$b(t) = \int_0^\infty d\lambda\, h(\lambda)\, a(t-\lambda) \tag{I-1}$$

The crosscorrelation function, $\phi_{ab}(\tau)$, between the input and the output is defined as:

$$\phi_{ab}(\tau) = \lim_{P \to \infty} \frac{1}{2P} \int_{-P}^{P} dt\, a(t)\, b(t+\tau) \tag{I-2}$$

Substituting equation (I-1) for b(t) and reversing the order of integration, one obtains

$$\phi_{ab}(\tau) = \int_0^\infty d\lambda\, h(\lambda) \lim_{P \to \infty} \frac{1}{2P} \int_{-P}^{P} dt\, a(t)\, a(t+\tau-\lambda) \tag{I-3}$$

The integral with respect to t in equation (I-3) is defined as the autocorrelation function of a(t), the input.

$$\phi_{aa}(\tau) = \lim_{P \to \infty} \frac{1}{2P} \int_{-P}^{P} dt\, a(t)\, a(t+\tau) \tag{I-4}$$

Thus, equation (I-3) reduces to

$$\phi_{ab}(\tau) = \int_0^\infty d\lambda\, h(\lambda)\, \phi_{aa}(\tau-\lambda) \tag{I-5}$$

If the autocorrelation function of the input is a delta function,

$$\phi_{aa}(\tau) = \delta(\tau) \tag{I-6}$$

then the autocorrelation function of the input and the output is the impulse response of the system

$$\phi_{ab}(\tau) = h(\tau) \tag{I-7}$$

Thus, the impulse response of a system can be measured
by applying to the system input an appropriate signal,
satisfying (I-6), and then calculating the input-output
crosscorrelation function. This result holds even if
the system output includes other noise or commanded
signals as long as these signals do not correlate with
a(t). The impulse response is a complete description
of the dynamics of a linear system and from it other
useful descriptions of the system dynamics, such as
the transfer function, can be developed.

The crosscorrelation method and the mathematical
development given above were first suggested by Y.W. Lee.[8]
There have been several studies of techniques to apply
the method; some of this work is reported in the refer-
ences.[9, 10, 11, 12] These approaches differ in the
exact nature of the input signal employed and in the
method used to calculate the crosscorrelation function.
Of the methods of implementation employed, the technique
of Aeronutronic Systems, Inc,[9] who applied the cross-
correlation method to the measurement of airplane
system dynamics, seemed to hold the most promise for
reactor system dynamics measurements. Using an idealized,
binary input signal developed by Aeronutronic Systems,
Inc., the author has carried out a series of experiments
on an analog computer and on two widely different types
of reactor systems, which clearly demonstrate that the
crosscorrelation method can be successfully applied to
reactor systems.

During the same time that the experiments described
in this writing have been carried out, V. Rajagopal[13]
has independently applied the crosscorrelation method
to measure the mean neutron lifetime of a reactor. The
implementation he has employed differs markedly from
that which has been used by the author. He reports having
obtained a number for the mean neutron lifetime in good
agreement with measurements obtained by other means.

Chapters II, III, and IV comprise a detailed description of the work the author has done in applying the crosscorrelation method to the study on reactor system dynamics. Chapter V is a resumé of the conclusions that have been drawn from this experience. The following is a summary of these chapters:

CHAPTER II -

The derivation, leading to equation (I-7), contains two conditions which cannot be implemented in practice: the restriction of equation (I-6) on the input signal, and the infinite crosscorrelation integral of equation (I-2). In II-A and II-B the equations are modified to account for realistic input signals and for finite crosscorrelation time, the characteristics of the idealized binary signal are presented, and the general result for this input signal is derived. The result, for properly chosen input conditions, is:

$$\phi_{ab}(\tau) = K \cdot h(\tau) + C + x(\tau) \tag{I-8}$$

The constants, K and C, can be calculated. The term, $x(\tau)$, is the noise in the measurements due to extraneous system noise; its exact mean-square value is derived in II-D. The appearance of $x(\tau)$ in equation (I-8) is a result of the finite crosscorrelation time. A model is developed and discussed which shows the analogy between the crosscorrelator and a pass-band filter. The filter characteristics are such that $x(\tau)_{rms}$ is inversely proportional to the square root of the crosscorrelation time. Thus, $x(\tau)$ approaches zero as the crosscorrelation time approaches infinity in accordance with equation (I-7).

In Chapter II-E there is a discussion of methods developed by the author to compute a system transfer

function from the impulse response. Included is a
description of a digital computer code to perform the
calculation from impulse response data. The code includes
a Monte Carlo procedure for estimating the standard de-
viation of the calculated transfer function from the
known standard deviations of the data points. Examples
are given for a simple case.

The description in II-A and II-B is parallel with
that given by Aeronutronic Systems, Inc.[9] This author
used a different approach which it is felt more clearly
illustrates the requirements imposed. The analyses
given in II-C, II-D, and II-E are presented here for the
first time. Aeronutronic Systems, Inc. has made an
estimate of the upper bound of $x(\tau)_{rms}$ which is in rough
agreement with the exact solution obtained in II-D.

All of the analyses of Chapter II are valid for any
linear system.

CHAPTER III -

This chapter contains a description of the equipment
built by the author to implement the crosscorrelation
method.

CHAPTER IV -

Three sets of experiments were carried out using
the equipment described in Chapter III. The results of
two analog computer studies are presented in IV-A. In
the first study, typical crosscorrelation data from a
simple linear system are given, and the necessary data
processing steps are described in detail. The rms error
in the impulse response measurement is 1.6%. The second
analog computer study is an investigation of the effect
of the non-linear behavior of a reactor. From data
taken with inputs of $\pm 8\cent$, $\pm 80\cent$, and $\pm 120\cent$ reactivity,

it is concluded that the crosscorrelation method tends
to measure a linearized reactor impulse response in each
case, even though the reactor fluctuations far exceed the
linear region.

The description and results of an experiment on
Godiva II are given in II-B. Godiva II is a bare U^{235}
fast reactor. The crosscorrelation experiment was
performed by introducing the binary input by means of
the motion of a small plastic slug, smoothing the reactor
output signal with a simple filter, and crosscorrelating
the input and filter output signals. The results agree
with the theoretical results although the variance of
the data is large.

The most important experiments were carried out on
Kiwi-A3, a prototype rocket propulsion reactor. Measure-
ments of the reactor dynamics, at low power, at half
power, and at full power are presented in IV-C. The
results are uniformly good; they prove beyond doubt the
feasibility of the crosscorrelation method for use on
reactor systems.

CHAPTER V -

The conclusions are:

1)   The crosscorrelation method has the following
     advantages:

     a)   It yields the entire information about the
          impulse response of the system in the
          shortest possible time, that is, the sys-
          tem settling time.

     b)   The method requires only small amplitude
          perturbations. Consequently it is not
          hazardous, not limited by system non-
          linearities, and does not interfere with
          normal system operation.

      c)   It can be used even in the presence of strong noise sources provided that the crosscorrelation time is increased beyond the system settling time.

2)   The crosscorrelation method is a useful reactor diagnostic technique.

3)   The crosscorrelation method is probably the best dynamics measurement tool for some reactor systems including rocket propulsion reactors.

4)   The method is promising enough to warrant further expenditure of time and money. Professional equipment is being designed for future experiments on rocket propulsion reactors.

5)   No disagreement with the theory has been found.

6)   The original purposes of the thesis have been achieved.

      a)   The feasibility of the crosscorrelation method for use on reactor systems has been demonstrated.

      b)   Data of the performance of a control system of a rocket propulsion reactor have been obtained.

CHAPTER II

MATHEMATICAL FOUNDATIONS

The basic principles of the crosscorrelation method
have been outlined in the introduction. The mathematical
foundations of the method are expressed in the development
of equations (I-1) through (I-7). The important result
is expressed in equation (I-7) shown below

$$\phi_{ab}(\tau) = h(\tau) \qquad (I-7)$$

This result is obtained by specifying that

$$\phi_{aa}(\tau) = \delta(\tau) \qquad (I-6)$$

This development is adequate to illustrate the principles
of the crosscorrelation method, but it is not adequate for
describing an actual experiment. The development contains
two statements which cannot be implemented in practice.
Equation (I-6) states that the autocorrelation function of
the input signal is a delta function; this implies that $a(t)$
contains all frequencies in equal proportion. This is not
a realizable signal. In addition, it is not possible to
implement the calculation of $\phi_{ab}(\tau)$ since the integration
is taken over infinite limits. In order to modify the
equations to be more representative of a real experiment, the
following two changes should be made:

1) The input signal, $a(t)$, is not specified.

2) The crosscorrelation time is finite.

These modifications can be made without impairing the simple,
basic result stated by equation (I-7). There will always be
some error in equation (I-7), but this error can be made
sufficiently small by proper choice of conditions.

It is necessary that the input signal contain, in equal
proportion, all frequencies for which the system has
appreciable response, and that the crosscorrelation time
be greater than the system settling time. The fact that
the integration time is not infinite will result in some
contribution to the crosscorrelation function due to
noise entering the system. This error can be decreased
by increasing the crosscorrelation time beyond the
settling time of the system.

The crosscorrelation method, as discussed above and
in the remainder of this chapter, applies to any linear
system; it is not restricted to reactor systems in any way.

A.   Basic Equations

Figure 1 is a schematic of an experiment in which
noise may enter either at the system input or output.
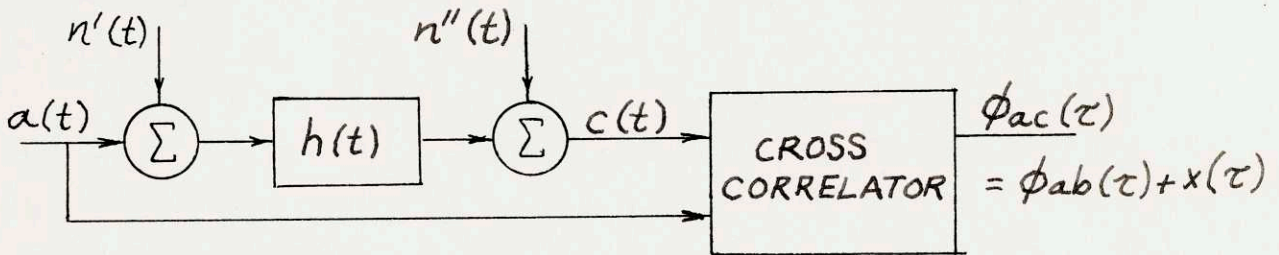
FIGURE 1

The system is assumed to be linear; h(t) is the system
weighting function or impulse response. The quantity,
b(t), is defined as that portion of the system response
due to a(t). The quantity, n(t), is an equivalent noise
referred to the system output

$$n(t) = h''(t) + \int_0^\infty d\lambda\, h(\lambda)\, n'(t-\lambda) \qquad\qquad \text{(II-1)}$$

In an experiment the quantities n'(t), n''(t), and b(t) are not individually observable. An input, a(t), is applied and an output, c(t), is observed. n(t) can be observed separately by setting a(t) equal to zero.

The crosscorrelation function,[*] $\phi_{ac}(\tau)$, is now redefined so that the integration time is finite

$$\phi_{ac}(\tau) = \frac{1}{P} \int_0^P dt\, c(t)\, a(t-\tau) \qquad\qquad \text{(II-2)}$$

This is identical to the usual definition given in equation (I-2) as $P \rightarrow \infty$, since in this case $\phi_{ac}(\tau) = \phi_{ca}(-\tau)$.

If a(t) is applied to the system input starting at $t = t_o$, the system response, b(t), is given by the convolution integral

$$b(t) = \int_{t_o}^t d\lambda\, a(\lambda)\, h(t-\lambda) = \int_0^{t-t_o} d\lambda\, h(\lambda)\, a(t-\lambda) \qquad\qquad \text{(II-3)}$$

Combine (II-2) and (II-3) and c(t) = b(t) + n(t) to obtain the result:

$$\phi_{ac}(\tau) = \frac{1}{P} \int_0^P dt \left[\int_0^{t-t_o} d\lambda\, h(\lambda)\, a(t-\lambda) + n(t) \right] a(t-\tau) \qquad\qquad \text{(II-4)}$$

This result can be split up into two parts

$$\phi_{ac}(\tau) = \phi_{ab}(\tau) + X(\tau) \qquad\qquad \text{(II-5)}$$

where

[*]For a discussion of correlation functions, see reference(14).

$$x(t) \equiv \frac{1}{P} \int_0^P dt \; n(t) \, a(t-\tau)$$

(II-6)

Evaluation of $x(\tau)$ is continued in Section D.

The integration in $\phi_{ab}(\tau)$ is over the shaded part of the t, λ plane in Figure 2.
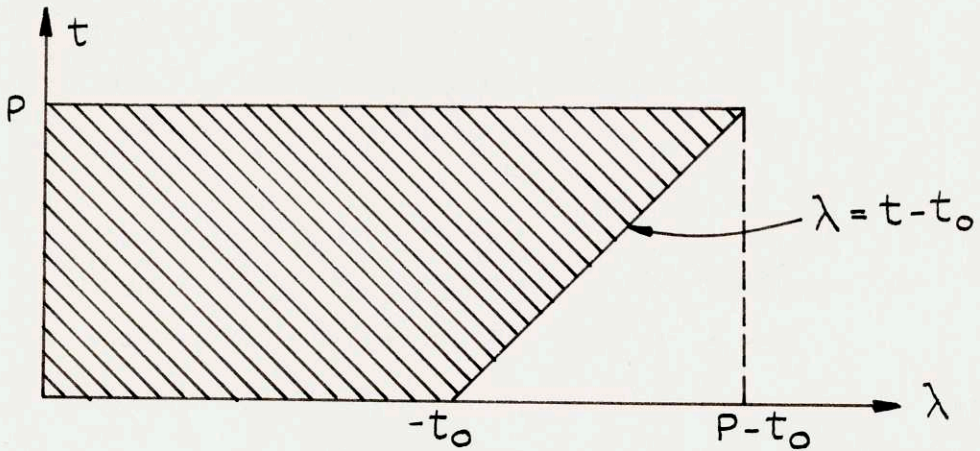
FIGURE 2

Invert the order of integration to obtain

$$\phi_{ab}(\tau) = \int_0^{-t_o} d\lambda \, h(\lambda) \frac{1}{P} \int_0^P dt \; a(t-\lambda) \, a(t-\tau)$$

$$+ \int_{-t_o}^{P-t_o} d\lambda \, h(\lambda) \frac{1}{P} \int_{\lambda+t_o}^P dt \; a(t-\lambda) \, a(t-\tau),$$

(II-7)

$$t_o < 0$$

The integral with respect to t in the first term of
(II-7) is recognized as the input autocorrelation
function:

$$\phi_{aa}(\tau) = \frac{1}{P}\int_0^P dt\, a(t)\, a(t-\tau)$$

(II-8)

If t_o is chosen sufficiently negative so that

$$h(t) = 0, \quad t > -t_o$$

(II-9)

then equation (II-7) becomes

$$\phi_{ab}(\tau) = \int_0^\infty d\lambda\, h(\lambda)\, \phi_{aa}(\tau-\lambda)$$

(II-10)

This equation is the same in form as equation (I-5) but
applies for a finite correlation time P.

In order to continue the evaluation of $\phi_{ab}(\tau)$ as
given in equation (II-10) it is necessary to specify the
input and to calculate its autocorrelation function.

B.   Description of the Input Signal

The first part of Appendix A is a discussion of
possible input signals including a listing of some of
the advantages and disadvantages of each. As a result
of these considerations an input is chosen which has the
following properties;

1)   It is binary; that is, it is either +1 or -1.
2)   It may (but need not necessarily) change sign
     only at intervals spaced Δt apart.
3)   It is periodic with period $T = N\Delta t$, $N \gg 1$.
4)   It has an autocorrelation function as shown
     in Figure 3.

Signals with these properties have been synthesized by
Aeronutronic Systems, Inc.[9]
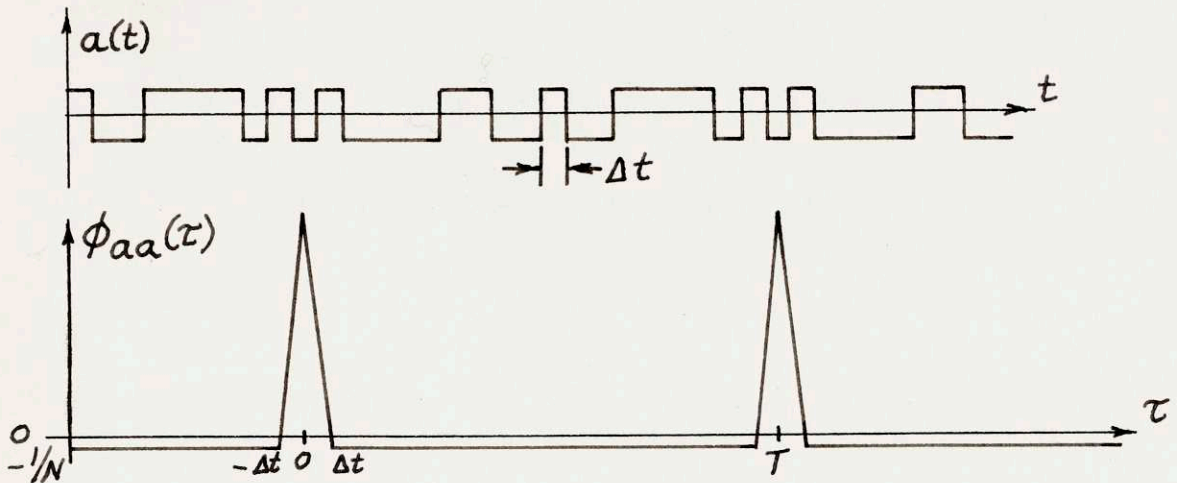
FIGURE 3 - Idealized Binary Signal, N = 19

The binary input is chosen because it affords convenience of storage and delay, and ease of multiplication.

In order to obtain a signal with the "idealized" autocorrelation function of Figure 3, it is necessary to know a "chain", A_1, A_2; A_3, - - - - - - A_N; with A_i = +1 or -1, such that

$$\sum_{i=1}^{i=N} A_i A_{(i+j) \, modulo \, N} = \begin{cases} N, & j=0 \\ -1, & j \neq 0 \end{cases} \qquad (II-11)$$

This chain defines an input signal which will have the desired autocorrelation function. The input signal is equal to A_1 for $0 < t < \Delta t$, A_2 for $\Delta t < t < 2\Delta t$, and so forth, up to t = T, where the sequence repeats.

It is known that chains having property (II-11) can be obtained for values of N which are prime numbers and which are of the form 4k - 1, where k is an integer.[9] The chains for N = 251 and N = 1019 are available and are the ones which have been used.[15]

Some insight into the nature of this signal can be
gained by considering a different signal which has the
same first three properties but, instead of property (4)
has the sign chosen at random during each Δt interval.
Such a signal for N = 19 is shown in Figure 4.
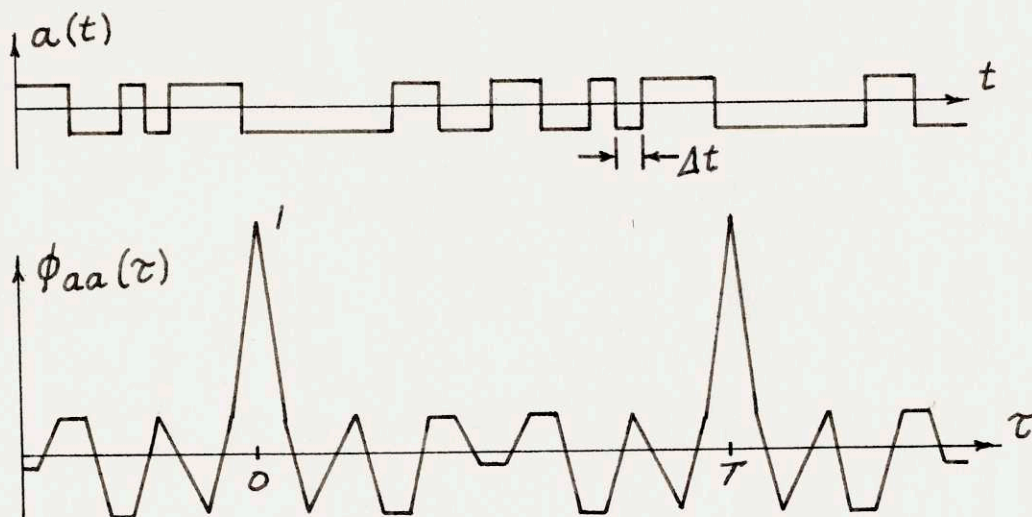
FIGURE 4 - Random Binary Signal, N = 19

The autocorrelation function, also shown in the figure,
does have a shape nearly like Figure 3 within the range
$-\Delta t < \tau < \Delta t$. Outside this range it has side lobes
whose amplitudes are distributed according to a binary
probability distribution, shifted so as to have a zero
average value and a root-mean-square amplitude of $\sqrt{N}$.
There is a close similarity between an idealized signal
and a random signal of the same length. Detailed analy-
sis, performed on the idealized chains for N = 251 and
N = 1019 shows them to be statistically indistinguishable
from random chains of the same lengths. The basic
property which distinguishes the idealized signals from
the random signals is the shape of the autocorrelation
function. The reason that the idealized chains are
better for the crosscorrelation method is that the
contribution to the crosscorrelation function from the

side lobes is small, calculable, and reproducible (see
equation II-10). If random signals are used, the contri-
bution to the crosscorrelation function from these side
lobes must be accepted as a random error in the measure-
ments. In order to obtain accurate results with a
random binary input, N must be made very large (N =
10000 will produce approximately 1% errors).

The function, $\phi_{aa}(\tau)$, of Figure 3 can be said to
be composed of two parts: a constant, -1/N, plus a
series of pyramids of height $(1 + 1/N)$ and width $2\Delta t$
centered at $\tau = kT$, where k is an integer. It is to
be emphasized that even with an idealized binary signal,
this autocorrelation function results only when the
integration time is $T = N\Delta t$ or an integral multiple of
T. If the integration time is not an integral multi-
ple of T, then the autocorrelation function resembles the
autocorrelation function for a random chain as depicted
in Figure 4.

If the integration time, P, in equation (II-2) is
set equal to an integral multiple of T, the resulting
$\phi_{ab}(\tau)$ is given by equation (II-10) using the $\phi_{aa}(\tau - \lambda)$
given in Figure 3. This convolution is shown graphically
in Figure 5. In this figure $\phi_{ab}(\tau)$ is the integral over
λ of the product of the two curves. Essentially, the
pyramid part of $\phi_{aa}(\tau - \lambda)$ samples the $h(\lambda)$ curve
yielding for the integral $\Delta t \cdot h(\tau)$. In addition, the -1/N
portion of $\phi_{aa}(\tau - \lambda)$ yields

$$-(1/N)\int_0^\infty d\lambda\, h(\lambda) \equiv \bar{h}\, \Delta t$$

so that

$$\phi_{ab}(\tau) \approx \Delta t\left[h(\tau) - \bar{h}\right] \tag{II-12}$$
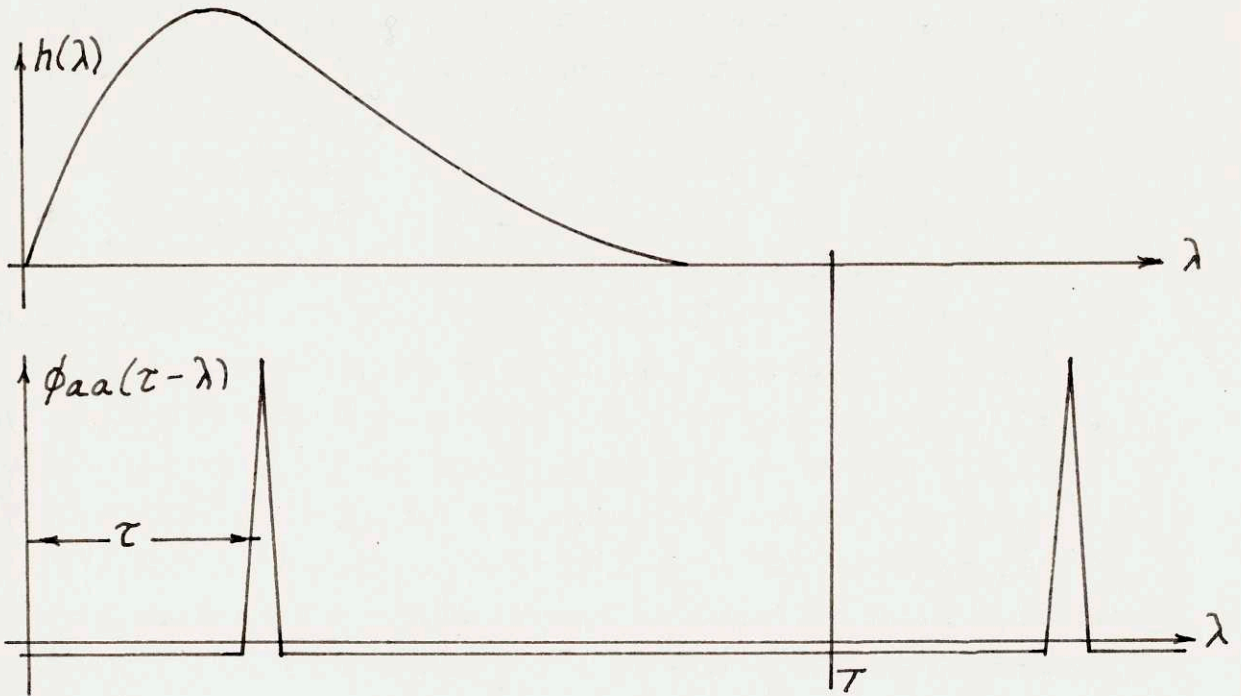
FIGURE 5

If τ is made equal to $-\Delta t$

$$\phi_{ab}(-\Delta t) = -\overline{h}\,\Delta t$$

since $h(t) \equiv 0$ for $t < 0$. Therefore, the equation for the impulse response is

$$h(\tau) = \frac{1}{\Delta t}\left(\phi_{ab}(\tau) - \phi_{ab}(-\Delta t)\right) \qquad (II-13)$$

This is the working equation of the crosscorrelation technique. It states that the shape of the impulse

response is the same as the shape of the crosscorrelation function (shifted by a constant so that $\overline{\phi_{ab}(\tau)} = 0$). The remainder of this chapter deals with corrections, errors, and transformations of this equation.

C.   Correction for Finite Δt

In equation (II-11) it was assumed that the pyramid portion of $\phi_{aa}(\tau - \lambda)$ sampled the $h(\lambda)$ curve (Figure 5). If $h(\lambda)$ curves very much within $\pm \Delta t$ on either side of $\lambda = \tau$, then there will be some error in this assumption. To evaluate this error, and hence to generate a criterion for choosing Δt to make the error negligible, it is necessary to go back to the basic equation (II-10). The constant, $-1/N$, portion of $\phi_{aa}(\tau - \lambda)$ can be integrated out:

let

$$\phi'_{aa}(\tau - \lambda) \equiv \phi_{aa}(\tau - \lambda) + \frac{1}{N} \tag{II-14}$$

$$\phi'_{ab}(\tau) \equiv \phi_{ab}(\tau) - \phi_{ab}(-\Delta t) \tag{II-15}$$

then

$$\phi'_{ab}(\tau) = \int_0^\infty d\lambda \, h(\lambda) \, \phi'_{aa}(\tau - \lambda) \tag{II-16}$$

From here there are two ways to proceed: one can apply an iterative technique to determine $h(\lambda)$ knowing $\phi'_{ab}(\tau)$; or equation (II-16) can be Fourier transformed to yield an explicit equation for the system transfer function. Each of these two methods has its uses depending on whether the impulse response or the transfer function is the desired end.

To apply the first approach, an iterative technique
is employed to determine what curve for $h(\lambda)$ will yield
the measured $\phi_{ab}(\tau)$ from equation (II-16). As a first
guess assume that $h_1(\lambda) = \phi_{ab}(\lambda)/\Delta t$ (refer: equation
II-(13)) and compute $\phi'_{ab1}(\tau)$ from equation (II-16).
Then assume that $h_2(\lambda) = (2\phi_{ab}(\lambda) - \phi'_{ab1}(\lambda))/\Delta t$ and
compute $\phi'_{ab2}(\lambda)$ from equation (II-16). Continue this
process until there is no change, i.e., $h_n(\lambda) = h_{n-1}(\lambda)$.

In practice, $\phi_{ab}(\tau)$ will be given by data points.
If it is assumed that the $\phi_{ab}(\tau)$ curve is a parabola
through three adjacent points, then

$$h_n(\tau_i) = \phi'_{ab}(\tau_i)/\Delta t$$

$$-\frac{\Delta t^2}{6(\tau_{i+1}-\tau_{i-1})}\left[\frac{h_{n-1}(\tau_{i+1})-h_{n-1}(\tau_i)}{\tau_{i+1}-\tau_i} - \frac{h_{n-1}(\tau_i)-h_{n-1}(\tau_{i-1})}{\tau_i-\tau_{i-1}}\right] \quad \text{(II-17)}$$

This iteration technique will always converge if the data
points are spaced at least Δt apart. Equation (II-17)
can serve as a guide for choosing Δt so that the correc-
tion will be negligible. Note that the lowest order
error arises from the <u>curvature</u> of the impulse response
curve and not from the slope.

In the second approach, equation (II-16) is Fourier
transformed

$$\Phi'_{ab}(s) \equiv \mathcal{F}(\phi'_{ab}(\tau)) \equiv \int_{-\infty}^{\infty} d\tau\, e^{-\tau s}\, \phi'_{ab}(\tau) \quad \text{(II-18)}$$

The result of this transformation is

$$\Phi'_{ab}(s) = H(s)\Phi'_{aa}(s) \quad \text{(II-19)}$$

$H(j\omega)$ is the system transfer function and can be found
by division: $H(j\omega) = \Phi_{ab}(j\omega) / \Phi_{aa}(j\omega)$. $\Phi_{aa}(j\omega)$ is a
pure real quantity and is shown plotted in Figure 6.
Methods for obtaining $\Phi_{ab}(j\omega)$ will be discussed in
detail in Section E. The major disadvantage of this
second approach is that $h(\tau)$ is not determined except
by calculating from $H(j\omega)$; this calculation is generally
very difficult.[16]

D.   Errors in the Crosscorrelation Result Due to
         System Noise

The major advantage of the crosscorrelation method
is the improvement in signal-to-noise ratio over other
experimental methods for measuring system dynamics.
Hence, no discussion of the method would be complete
without an evaluation of the errors due to noise. This
section contains an evaluation of the "improvement
factor" obtained by the crosscorrelation method.

In order to define an "improvement factor", it is
necessary to define a figure of merit. For this
purpose, it is convenient to talk in terms of signal-
to-noise ratios defined in terms of root-mean-square
quantities. The signal-to-noise ratio at the system
output (crosscorrelator input) is defined as:

$$(S/N)_c = \frac{\sqrt{\overline{b^2(t)}}}{\sqrt{\overline{n^2(t)}}} \tag{II-20}$$

The signal-to-noise ratio of the crosscorrelation data
is defined as:

FIGURE 6

dimensionless frequency, $f\Delta t \longrightarrow$
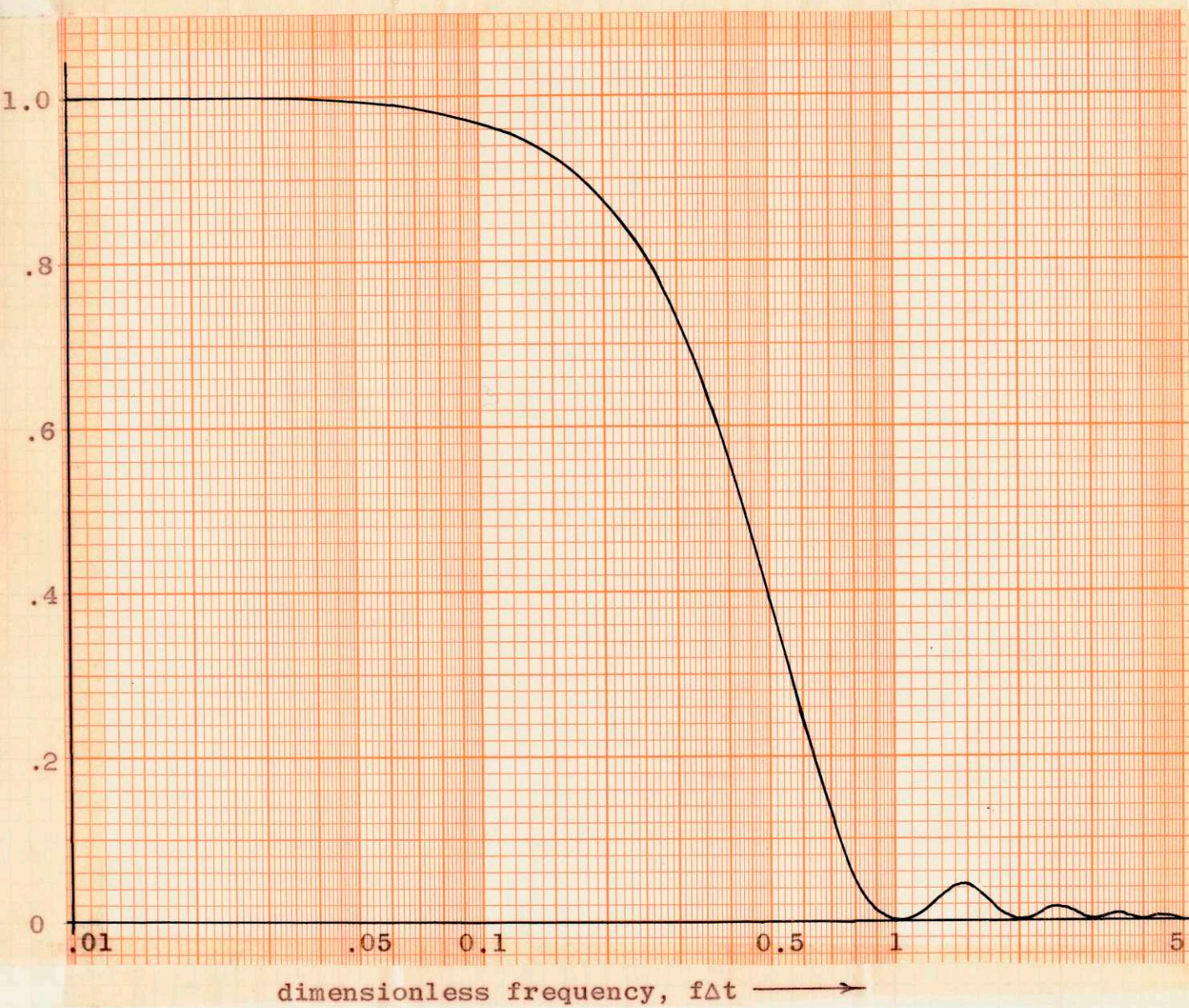
PLOT OF THE FUNCTION $\Phi_{aa}(\omega)/\Delta t$

$$\Phi_{aa}(\omega) = \Delta t \left[\frac{\sin\frac{\omega\Delta t}{2}}{\frac{\omega\Delta t}{2}} \right]^2 \quad , \quad \omega = 2\pi f$$

$$(S/N)_\phi = \frac{\sqrt{\frac{1}{L}\int_0^L dt\, \phi_{ab}^2(\tau)}}{\sqrt{\frac{1}{T}\int_0^T d\tau\, x^2(\tau)}} \qquad\qquad (II\text{-}21)$$

The time, L, is the system settling time. It is smaller
than T by a factor M: T = ML. The improvement factor,
IF, is equal to the ratio:

$$IF \equiv \frac{(S/N)_\phi}{(S/N)_C} = \left\{ \frac{\sqrt{\frac{1}{L}\int_0^L dt\, \phi_{ab}^2(\tau)}}{\sqrt{\frac{1}{T}\int_0^T dt\, b^2(t)}} \right\} \cdot \left\{ \frac{\sqrt{T\, \overline{n^2(t)}}}{\sqrt{T\, \overline{x^2(\tau)}}} \right\} \qquad (II\text{-}22)$$

The general result of this section is that IF is at
least as great as $\sqrt{M}$.

An analogy can be drawn between the crosscorrelator
and a pass-band filter. This equivalent filter has an
attenuation factor of $\sqrt{N}$ and a pass-band roughly equiva-
lent to the spectrum of the a(t) input signal. The
analogy is rigorous only in the mean-square sense: the
rms crosscorrelator output is identical to the rms
filter output. This is true of all signals crosscor-
related with a(t), the informative b(t) signal as well
as the n(t) signal. It is apparent, then, that there is

no improvement in signal-to-noise ratio if the averaging
span of the rms operation is taken to be the same for
both the $x(\tau)$ and the $\phi_{ab}(\tau)$ signals. The improvement
in signal-to-noise ratio obtained by the crosscorrela-
tion method is due to the action of the crosscorrelator
in concentrating the information in the $b(t)$ signal into
a small span compared to the crosscorrelation time.
Stated differently, the crosscorrelator distributes the
total power of $n(t)$ over the entire crosscorrelation
interval, T; the power of $b(t)$ is distributed within the
smaller interval, L.

In order to show that IF is at least as great as
$\sqrt{M}$, it is necessary to calculate each of the four terms
in equation (II-22). It is convenient to treat each of
the bracketed ratios separately. The first ratio is
given approximately by:

$$Z_1 = \frac{\sqrt{\overset{L}{\overline{\phi_{ab}^2(\tau)}}}}{\sqrt{\overset{T}{\overline{b^2(t)}}}} \cong \frac{\sqrt{M}}{\sqrt{N}} \qquad (II\text{-}23)$$

if the input is wide band compared to the system. The
second ratio is

$$Z_2 = \frac{\sqrt{\overline{n^2(t)}}}{\sqrt{\overline{x^2(\tau)}}} \geq \sqrt{N} \qquad (II\text{-}24)$$

The evaluation of Z_1 and Z_2 follows.

1.   Evaluation of Z_1

The numerator is

$$\sqrt{\frac{1}{L} \int_0^L d\tau\, \phi^2_{ab}(\tau)} \cong \sqrt{\frac{M}{T} \int_0^\infty d\tau\, (\Delta t)^2 h^2(\tau)} \qquad (II\text{-}25)$$

To evaluate the denominator, define the autocorrelation function of $b(t)$

$$\phi_{bb}(\lambda) = \frac{1}{T} \int_0^T dt\, b(t)\, b(t+\lambda) \qquad (II\text{-}26)$$

Thus

$$\overline{b^2(t)} = \phi_{bb}(0) \qquad (II\text{-}27)$$

Put this in terms of the inverse Fourier Transform

$$\phi_{bb}(\lambda) = \frac{1}{2\pi} \int_{-\infty}^\infty d\omega\, \Phi_{bb}(\omega)\, e^{j\omega\lambda}$$

$$\phi_{bb}(0) = \frac{1}{2\pi} \int_{-\infty}^\infty d\omega\, \Phi_{bb}(\omega) \qquad (II\text{-}28)$$

From the circuit equations

$$\Phi_{bb}(\omega) = \Phi_{aa}(\omega) \left| H(\omega) \right|^2 \tag{II-29}$$

The spectrum of the input, $\phi_{aa}(\omega)$, is presumed to be constant at frequencies for which $H(\omega)$ has significant value. The constant is Δt. Thus

$$\overline{b^2(t)} \cong \frac{\Delta t}{2\pi} \int_{-\infty}^{\infty} d\omega \left| H(\omega) \right|^2 \tag{II-30}$$

Use Parseval's formula to obtain[17]

$$\sqrt{\overline{b^2(t)}} \cong \sqrt{\Delta t \int_0^\infty dt \, h^2(t)} \tag{II-31}$$

The result is

$$Z_1 \cong \frac{\sqrt{\dfrac{M\Delta t^2}{T} \int_0^\infty d\tau \, h^2(\tau)}}{\sqrt{\Delta t \int_0^\infty dt \, h^2(t)}} = \sqrt{\frac{M}{N}} \tag{II-32}$$

In deriving equation (II-32) several approximations have been made. This is justifiable since Z_1 contains the arbitrary choice for the output "signal" in the signal-

to-noise ratio definition. For this case an approximate, simple answer is preferable to an accurate but complicated answer.

2. Evaluation of Z_2

The ratio, Z_2, is the rms attenuation factor for noise in the crosscorrelation process. To calculate Z_2 it is necessary first to calculate $\overline{x^2(\tau)}$. In order to evaluate $\overline{x^2(\tau)}$ it is convenient to consider two categories of $n(t)$: a) stochastic time functions which will be described by their power spectra, and b) known time functions which will be described by a power series.

a) $n(t)$ is a stochastic time function.

The result of this section is that

$$\overline{x^2(\tau)} = \frac{1}{N} \int_{-\infty}^{\infty} d\omega \, R(\omega) \, \Phi_{nn}(\omega) \qquad (II-33)$$

where $\Phi_{nn}(\omega)$ is the power spectrum of $n(t)$

$$\Phi_{nn}(\omega) = \frac{1}{2\pi} \int_{-\infty}^{\infty} d\tau \, e^{-j\omega\tau} \, \phi_{nn}(\tau) \qquad (II-34)$$

and $R(\omega)$ is a special spectrum defined as

$$R(\omega) = 2 \, \text{Real} \left[\frac{1}{T\Delta t} \int_{0}^{T} d\lambda \, e^{j\omega\lambda} \, \phi_{aa}(\lambda)(T-\lambda) \right] \qquad (II-35)$$

This result states that the crosscorrelator acts as a filter. An equivalent circuit to Figure 1 can be drawn as shown in Figure 7.
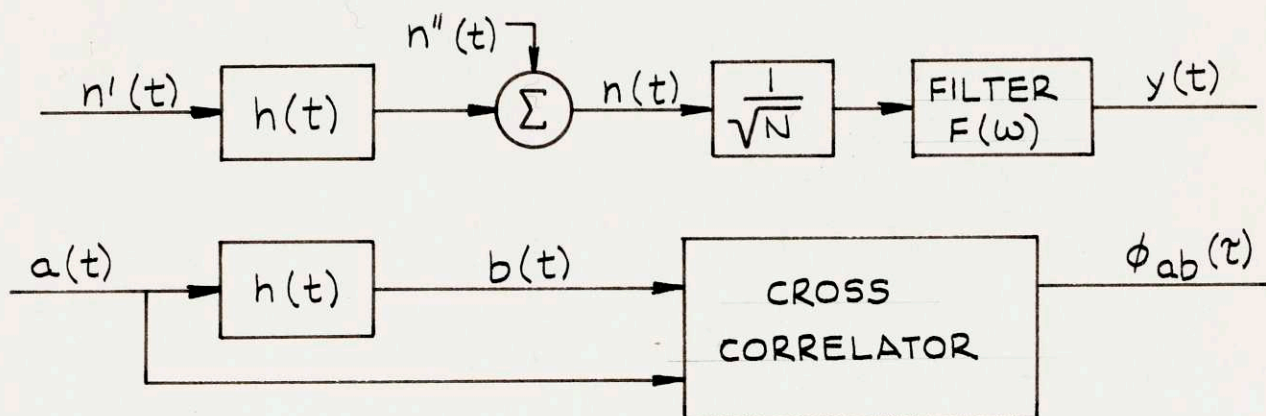
FIGURE 7

The equivalence between the two circuits is in the mean-square sense, namely:

$$\overline{y^2(t)} = \overline{x^2(\tau)} \tag{II-36}$$

The filter shown in Figure 7 is described by its transfer function, $F(\omega)$, given by

$$|F(\omega)|^2 = R(\omega) \tag{II-37}$$

Thus the magnitude of $F(\omega)$ is specified as $\sqrt{R(\omega)}$, but the phase shift is unspecified. This follows from the fact that phase shift of a filter does not affect the rms value of the output.

The function, $|F(\omega)|$, is plotted in Figure 8 for input parameters, $N = 251$, $\Delta t = .02$ sec. In general, $F(\omega)$ is a pass-band filter with

lower cutoff frequency (3db) = $.56/T$ cps
upper cutoff frequency (3db) = $.33/\Delta t$ cps (for $N > 10$)

From the equivalent circuit it is apparent that Z_2 is equal to $\sqrt{N}$ if the noise spectrum lies entirely within the filter pass-band. If some of the noise is attenuated by the filter, then $Z_2 = \sqrt{N}/$(fraction of the noise passed by the filter).

The fact that Figure 7 is an equivalent circuit to Figure 1 follows from the observation that:

$$\Phi_{yy}(\omega) = \frac{1}{N}\,|F(\omega)|^2\,\Phi_{nn}(\omega) \tag{II-38}$$

and

$$\phi_{yy}(0) = \overline{y^2(t)} = \int_{-\infty}^{\infty} d\omega\,\Phi_{yy}(\omega) \tag{II-39}$$

Therefore

$$\overline{y^2(t)} = \overline{x^2(\tau)} \tag{II-36}$$

FIGURE 8

EQUIVALENT CROSSCORRELATION FILTER

$\Delta t = 0.02$ seconds

$N = 251$

MAGNITUDE

$|F(\omega)|$

frequency, cycles/second ———→

1.0

.8

.6

.4

.2

0.1   0.1   1.0   10   100
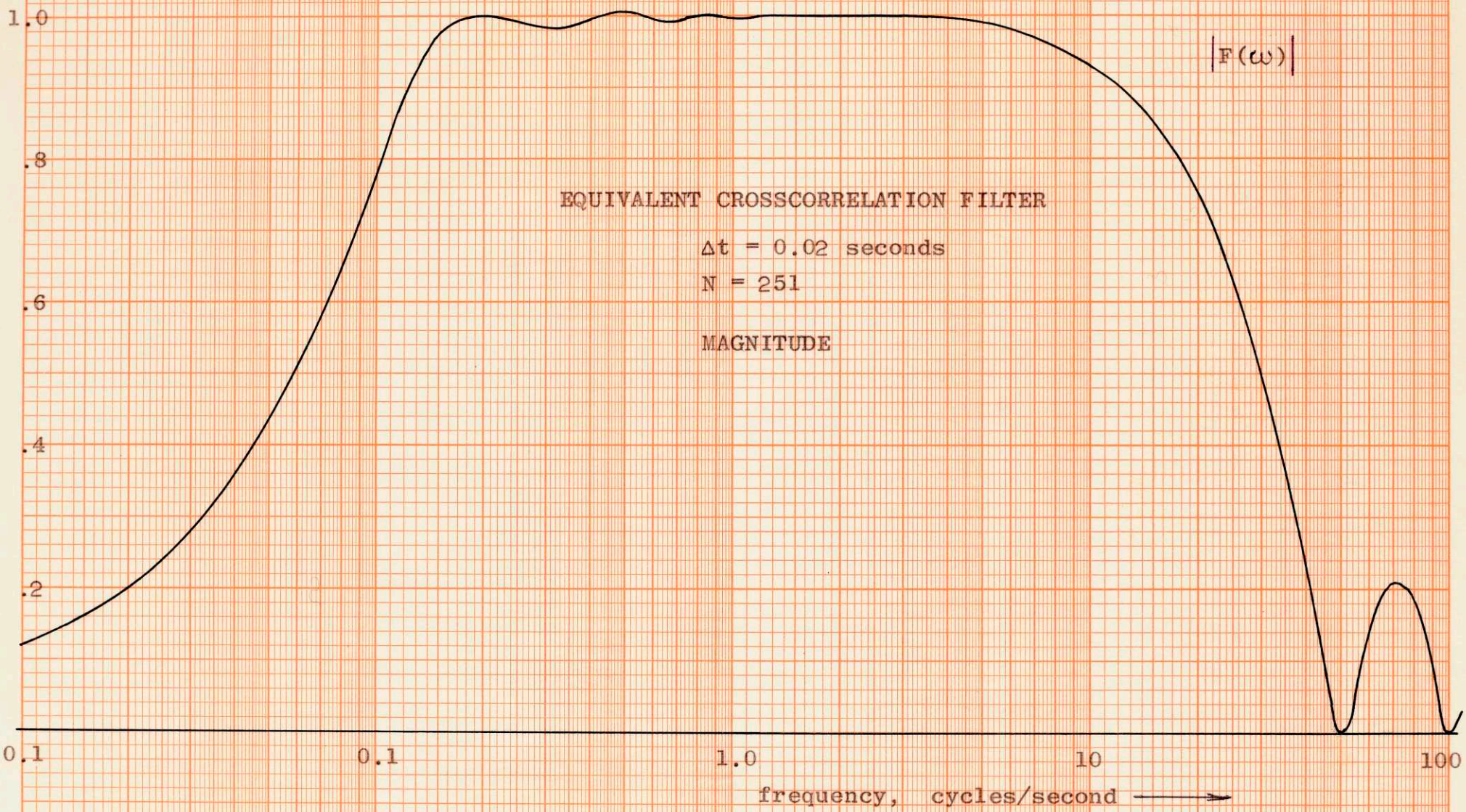
In order to obtain equations (II-33, 34, 35),
start with the definition of $x(\tau)$ from equation (II-6):

$$x(\tau) \equiv \frac{1}{T} \int_{0}^{T} dt\, n(t)\, a(t-\tau)$$

<div align="right">(II-6)</div>

The desired quantity is $\overline{x^2(t)}$; but if this is computed
directly from equation (II-6), the result will depend on
where, within the input cycle, the integration started.
In equation (II-6) the integration is started at time
$t = 0$. Consider that the integration might start at
$t = \delta$ instead of at $t = 0$; equation (II-6) becomes

$$x(\tau, \delta) = \frac{1}{T} \int_{\delta}^{T+\delta} dt\, n(t)\, a(t-\tau)$$

<div align="right">(II-40)</div>

Introduction of this new variable in no way changes the
results which have been obtaind thus far in this chapter.
This shift will have no effect on the equations for
$\phi_{ab}(\tau)$ in sections A and B since $\phi_{aa}(\tau)$ is unaffected
by a shift in the integration range.

If, now, one calculates $\overset{\tau}{\delta}\, \overline{x^2(\tau, \delta)}$ from equation
(II-40)*, the result is independent of starting time,
and, more important, the effects of $n(t)$ and $a(t)$ are
separable.

---

* A bar over a quantity means the average. The symbol
  in front of the bar is the variable with respect to
  which the average is taken.

Start by changing variables $\beta = t - \tau - \alpha$, $\alpha = \delta - \tau$

$$x(\tau, \alpha) = \frac{1}{T} \int_0^T d\beta \, a(\beta + \alpha) \, n(\beta + \alpha + \tau) \qquad \text{(II-41)}$$

Define, in the usual manner,

$$\phi_{xx}(\lambda, \alpha) \equiv \lim_{P \to \infty} \frac{1}{2P} \int_{-P}^{P} d\tau \, x(\tau, \alpha) \, x(\tau + \lambda, \alpha), \qquad \text{(II-42)}$$

so that

$$\overline{x^2(\tau, \alpha)} \equiv \lim_{P \to \infty} \frac{1}{2P} \int_{-P}^{P} d\tau \, x^2(\tau, \alpha) = \phi_{xx}(0, \alpha) \qquad \text{(II-43)}$$

Then

$$\phi_{xx}(\lambda, \alpha) = \lim_{P \to \infty} \frac{1}{2P} \int_{-P}^{P} d\tau \, \frac{1}{T} \int_0^T d\beta \, a(\beta + \alpha) \, n(\beta + \alpha + \tau) \frac{1}{T} \int_0^T dt \, a(t + \alpha) \, n(t + \alpha + \tau + \lambda)$$

$$\text{(II-44)}$$

Reverse the order of integrations to give

$$\phi_{xx}(\lambda,\alpha) = \frac{1}{T}\int_0^T d\beta\, a(\beta+\alpha)\frac{1}{T}\int_0^T dt\, a(t+\alpha) \lim_{P\to\infty} \frac{1}{2P}\int_{-P}^P d\tau\, n(\beta+\alpha+\tau)n(t+\alpha+\tau+\lambda)$$

(II-45)

The last integral is the autocorrelation function of the noise, so that

$$\phi_{xx}(\lambda,\alpha) = \frac{1}{T}\int_0^T d\beta\, a(\beta+\alpha)\frac{1}{T}\int_0^T dt\, a(t+\alpha)\phi_{nn}(\lambda+t-\beta)$$ (II-46)

Now compute the average over α

$$\overline{\phi_{xx}}^{\,\alpha}(\lambda) \equiv \frac{1}{T}\int_0^T d\alpha\, \phi_{xx}(\lambda,\alpha)$$

(II-47)

$$\overline{\phi_{xx}}^{\,\alpha}(\lambda) = \frac{1}{T}\int_0^T d\alpha\, \frac{1}{T}\int_0^T d\beta\, a(\beta+\alpha)\frac{1}{T}\int_0^T dt\, a(t+\alpha)\phi_{nn}(\lambda+t-\beta)$$

(II-48)

Reverse the order of integrations to give

$$^{\alpha}\overline{\phi_{xx}}(\lambda) = \frac{1}{T}\int_0^T d\beta \frac{1}{T}\int_0^T dt\, \phi_{nn}(\lambda+t-\beta)\frac{1}{T}\int_0^T d\alpha\, a(\beta+\alpha)\, a(t+\alpha) \tag{II-49}$$

The last integral is the autocorrelation function of the input; so that

$$^{\alpha}\overline{\phi_{xx}}(\lambda) = \frac{1}{T}\int_0^T d\beta \frac{1}{T}\int_0^T dt\, \phi_{nn}(\lambda+t-\beta)\, \phi_{aa}(t-\beta) \tag{II-50}$$

Now compute the Fourier Transform of $^{\alpha}\overline{\phi_{xx}}(\lambda)$.

$$^{\alpha}\overline{\Phi_{xx}}(\omega) \equiv \int_{-\infty}^{\infty} d\lambda\, ^{\alpha}\overline{\phi_{xx}}(\lambda)e^{-j\omega\lambda} \tag{II-51}$$

$$^{\alpha}\overline{\Phi_{xx}}(\omega) = \int_{-\infty}^{\infty} d\lambda \frac{1}{T}\int_0^T d\beta \frac{1}{T}\int_0^T dt\, \phi_{nn}(\lambda+t-\beta)\, \phi_{aa}(t-\beta)e^{-j\omega\lambda} \tag{II-52}$$

Reverse the order of integrations

$$^{\alpha}\overline{\Phi_{xx}}(\omega) = \frac{1}{T}\int_0^T d\beta \frac{1}{T}\int_0^T dt\, \phi_{aa}(t-\beta)e^{j\omega(t-\beta)}\int_{-\infty}^{\infty} d\lambda e^{-j\omega(\lambda+t-\beta)}\phi_{nn}(\lambda+t-\beta) \tag{II-53}$$

The last integral is 2π times the power spectrum of the
noise (see equation (II-34)), so that

$$\overset{\alpha}{\overline{\Phi}}_{xx}(\omega) = \frac{2\pi}{T}\int_0^T d\beta \, \frac{1}{T}\int_0^T dt \, \phi_{aa}(t-\beta)e^{j\omega(t-\beta)} \overline{\Phi}_{nn}(\omega) \quad \text{(II-54)}$$

Thus

$$\overset{\alpha}{\overline{\Phi}}_{xx}(\omega) = \frac{2\pi}{N} R(\omega) \, \Phi_{nn}(\omega) \quad \text{(II-55)}$$

where

$$R(\omega) = \frac{1}{\Delta t}\int_0^T d\beta \, \frac{1}{T}\int_0^T dt \, e^{j\omega(t-\beta)} \phi_{aa}(t-\beta) \quad \text{(II-56)}$$

With $\overset{\tau}{\underset{\alpha}{\overline{\Phi}}}{}_{xx}(\omega)$ known, $x^2(\tau,\alpha)$, can be calculated from the
inverse Fourier Transform

$$\overset{\alpha}{\overline{\phi}}_{xx}(\lambda) = \frac{1}{2\pi}\int_{-\infty}^{\infty} d\omega \, e^{j\omega\lambda} \overset{\alpha}{\overline{\Phi}}_{xx}(\omega) \quad \text{(II-57)}$$

by setting λ equal to zero.

$$\overset{\tau}{\underset{\alpha}{\overline{x^2(\tau,\alpha)}}} = \frac{1}{N}\int_{-\infty}^{\infty} d\omega \, R(\omega) \, \Phi_{nn}(\omega) \quad \text{(II-58)}$$

This is equation (II-33). This result is significant
in that it represents an explicit, general solution for
the rms effect of noise on the crosscorrelation function.
It is general in two respects:

1) No restrictions on the input have been imposed.
   Changes in the nature of the input change the
   function R (ω). Non-periodic inputs can be
   handled by allowing T to approach infinity.

2) No restrictions have been placed on n(t).
   Indeed, n(t) could be set equal to a(t).

Equation (II-33) is also helpful in that it allows
the simple equivalent circuit of Figure 7 to be drawn.
This mental picture of the crosscorrelator acting as a
pass-band filter with an attenuation of $1/\sqrt{N}$ is fairly
simple to interpret compared to equation (II-6) or
equation (II-33).

The function, R(ω), in equation (II-56), can be
reduced to a form that is easier to calculate. First
change variables, $\lambda = t - \beta$,

$$R(\omega) = \frac{1}{\Delta t} \int_0^T d\beta \frac{1}{T} \int_{-\beta}^{T-\beta} d\lambda \, e^{+j\omega\lambda} \, \phi_{aa}(\lambda) \qquad \text{(II-59)}$$

The double integration is computed over the shaded part
of the β, λ plane in Figure 9.
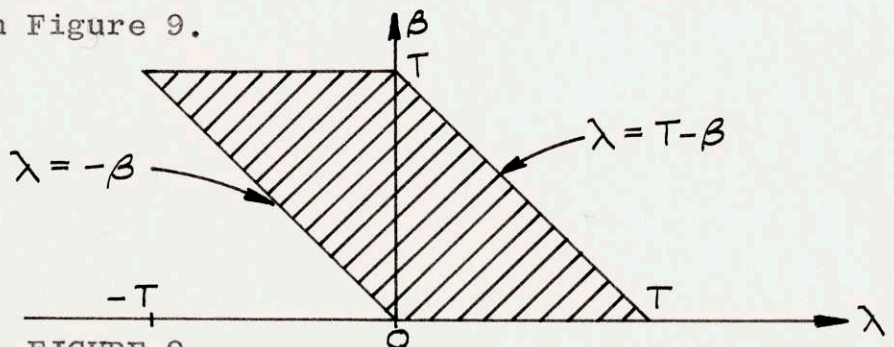
FIGURE 9

Reverse the order of integrations to give

$$R(\omega) = \frac{1}{\Delta t} \int_{-T}^{0} d\lambda\, e^{j\omega\lambda}\, \phi_{aa}(\lambda) \frac{1}{T} \int_{-\lambda}^{T} d\beta$$

$$+ \frac{1}{\Delta t} \int_{0}^{T} d\lambda\, e^{j\omega\lambda}\, \phi_{aa}(\lambda) \frac{1}{T} \int_{0}^{T-\lambda} d\beta \qquad \text{(II-60)}$$

In the first integral, let $-\lambda$ replace λ and compute the integrals with respect to β.

$$R(\omega) = \frac{1}{T\Delta t} \int_{0}^{T} d\lambda\, e^{-j\omega\lambda}\, \phi_{aa}(-\lambda)(T-\lambda)$$

$$+ \frac{1}{T\Delta t} \int_{0}^{T} d\lambda\, e^{j\omega\lambda}\, \phi_{aa}(\lambda)(T-\lambda) \qquad \text{(II-61)}$$

The function, $\phi_{aa}(\lambda)$, is symetric, $(\phi_{aa}(\lambda) = \phi_{aa}(-\lambda))$ so the first integral is the complex conjugate of the second integral.

$$R(\omega) = I(\omega) + I^{*}(\omega) = 2\,\text{Real}\,\left[I(\omega)\right] \qquad \text{(II-35)}$$

$$I(\omega) \equiv \frac{1}{T\Delta t} \int_{0}^{T} d\lambda\, e^{j\omega\lambda}\, \phi_{aa}(\lambda)(T-\lambda)$$

The single integral of $I(\omega)$ is much easier to compute than the double integral of equation (II-56).

Up to this point the treatment is general. $R(\omega)$ is now evaluated for the special case of the idealized binary input.

From Figure 3 there follows:

$$\phi_{aa}(\lambda) = 1 - (1 + 1/N)\, \lambda/\Delta t \, , \quad 0 < \lambda < \Delta t$$

$$\phi_{aa}(\lambda) = -1/N \qquad\qquad , \quad \Delta t < \lambda < T - \Delta t$$

$$\phi_{aa}(\lambda) = -N + (1 + 1/N)\, \lambda/\Delta t, \quad T - \Delta t < \lambda < T \qquad\qquad \text{(II-62)}$$

The integration is a bit tedious. The result is

$$
\begin{aligned}
I(\omega) = \frac{1}{N^2 x^3}\Big[& e^{Nx}(Nx - 2(N+1)) \\
& + e^{(N-1)x}((N+1)\,x + 2(N+1)) \\
& + e^x((N^2 - 1)\,x + 2(N+1)) \\
& + (-N^2 x^2 - N(N+2)\,x - 2(N+1))\Big]
\end{aligned}
\qquad \text{(II-63)}
$$

where $x = j\omega\Delta t$

Take twice the real part to obtain

$$
\begin{aligned}
R(\omega) = \frac{2}{(N^2)\,(y^3)}\Big[& -Ny\cos Ny + 2(N+1)\sin Ny \\
& -(N+1)\,y\cos(N-1)\,y - 2(N+1)\sin(N-1)y \\
& -(N^2 -1)\,y\cos y - 2(N+1)\sin y \\
& +(N^2 + 2N)\,y\Big]
\end{aligned}
\qquad \text{(II-64)}
$$

where $y = \omega\Delta t$

This function has been calculated on the IBM 704 for several values of N. The results (plus an asymptotic approximation) indicate that:

$$R(\omega) \longrightarrow 1/N, \text{ as } y \longrightarrow 0$$

$$R(\omega) \cong \left[\frac{\sin y/2}{y/2}\right]^2, \quad y > 1/N, \quad N > 100$$

Figure 9 is a plot of $\sqrt{R(\omega)}$ for $N = 251$, $\Delta t = .02$ sec.

The results of this section are very useful as a general aid in understanding the crosscorrelator. For example, Figure 8 can be used to observe the range of system transfer function that an input with $N = 251$ and $\Delta t = .02$ sec, is capable of measuring. Frequencies from 0.2 cps to 4.0 cps are passed by the crosscorrelator without distortion; frequencies from .05 cps to 30 cps are passed with a maximum distortion of 50%, etc. The crosscorrelator is an information filter as well as a noise filter.

b) Evaluation of $\overline{x^2}(t)$ if $n(t)$ is a known time function

Express $n(t)$ in a power series:

$$n(t) = \sum_{i=0}^{\infty} n_i(t) = \sum_{i=0}^{\infty} \frac{\Delta n_i}{T^i} t^i, \quad 0 < t < T \qquad \text{(II-65)}$$

where Δn_i is value of the ith component, $n_i(t)$, at $t = T$. The result of putting equation (II-65) into equation (II-6) is

$$\overline{x_i^2}(\tau) \cong (\Delta n_i)^2 / (2i + 1) N \qquad \text{(II-66)}$$

To show this, first perform the substitution

$$x(\tau) = \frac{1}{T} \int_0^T dt \sum_{i=0}^{\infty} \frac{\Delta n_i}{T^i} t^i \, a(t - \tau) \qquad \text{(II-67)}$$

Next reverse the order of summation and integration to give

$$x(\tau) = \sum_{i=0}^{\infty} \Delta n_i \, M_i(\tau) \tag{II-68}$$

where

$$M_i(\tau) = \frac{1}{T^{i+1}} \int_0^T dt \; a(t-\tau) t^i \tag{II-69}$$

Now let $t = x\Delta t$, $\tau = k\Delta t$.

$$M_i(\tau) = \frac{1}{N^{i+1}} \int_0^N dx \, a(x\Delta t - K\Delta t) x^i \tag{II-70}$$

$a(x\Delta t - k\Delta t)$ is a constant, A_{jk}, over the range $j - 1 < x < j$, where $A = +1$ or -1; therefore

$$M_i(\tau) = \sum_{j=1}^{N} \frac{A_{jk}}{N^{i+1}} \int_{j-1}^{j} dx \; x^i \tag{II-71}$$

$$M_i(\tau) = \sum_{j=1}^{N} \frac{A_{jk}}{N^{i+1}} \cdot \frac{j^{+i+1} - (j-1)^{i+1}}{i+1}$$

If $-(j-1)^{i+1}$ is expanded in a binomial series, the first term will cancel j^{i+1}, and the next term, $(i+1)(j)^i$, will be much greater than the sum of the following terms, over most of the summation range (if N is large). Therefore:

$$M_i(K) \cong \sum_{j=1}^{N} A_{jk} \, j^i / N^{i+1} \qquad \text{(II-72)}$$

If a series of numbers x_1, x_2, x_3, $- - - - x_n$ has a sum defined as

$$S_n \equiv \sum_{i=1}^{n} a_i \, x_i \qquad \text{(II-73)}$$

where a_i is +1 or -1 with equal probability, then the average squared sum is:

$$\overline{S_n^2} = \sum_{i=1}^{n} x_i^2 \qquad \text{(II-74)}$$

as can easily be shown by induction. This means that

$$\overline{M_i^2} \cong \left(\frac{1}{N^{i+1}} \right)^2 \sum_{j=1}^{N} j^{2i} \qquad \text{(II-75)}$$

The sum can be approximated closely by an integral

$$\overline{M_i^2} \cong \frac{1}{N^{2i+2}} \int_0^N j^{2i} \, dj = \frac{1}{(2i+1)N} \qquad \text{(II-76)}$$

Therefore: $\overline{x_i^2} \cong (\Delta n_i)^2 / (2i + 1)N$, which is equation (II-66). In order to compute Z_2 from this result, compute $\overline{n_i^2(t)}$:

$$\overline{n_i^2(t)} = \left(\frac{\Delta n_i}{T^i}\right)^2 \frac{1}{T} \int_0^T t^{2i} \, dt$$

$$\overline{n_i^2(t)} = (\Delta n_i)^2 / (2i + 1) \qquad \text{(II-77)}$$

Therefore

$$Z_2 = \frac{\Delta n_i / \sqrt{2i+1}}{\Delta n_i / \sqrt{(2i+1)N}} = \sqrt{N} \qquad \text{(II-78)}$$

The constraint of equation (II-11) on the A_{jk} will have the effect of decreasing $\overline{M_i^2}$ in equation (II-75) and hence will increase the improvement factor.

E. System Transfer Function

The crosscorrelation method measures the system impulse response, $h(t)$, directly. The transfer function, $H(\omega)$ is an equally descriptive measure of system dynamics. These two functions are a transform pair:

$$H(\omega) = \int_{-\infty}^{\infty} dt \, e^{-j\omega t} h(t) \qquad \text{(II-79)}$$

$$h(t) = \frac{1}{2\pi} \int_{-\infty}^{\infty} d\omega \, e^{j\omega t} H(\omega) \qquad \text{(II-80)}$$

This section includes a description of an IBM 704 code to perform the transformation plus a discussion of the propagation of errors from h(t) to H(ω).

A major difficulty in computing the transformation of equation (II-79) is the fact that h(t) is specified by discrete points; hence the curve between these points is ambiguous. Some assumptions must be made about the shape of the entire h(t) curve. A few possibilities are:

1) h(t) is a series of delta functions
2) h(t) is described by straight line segments joining the data points
3) h(t) is given by polynomial interpolation betweem data points
4) h(t) is a least-squares fit of some function to the data points

Each of these possibilities has been explored successfully. The conclusions are, respectively:

1) Much better results can be obtained using method (2).
2) Good results are obtained, even with crude data.
3) Very good results are obtained from very good data. A small amount of error in the data, however, will cause large fluctuations in the interpolated curve. The interpolation order must be decreased as the relative error in the data increases.
4) Excellent results are obtained for data which can be made to fit a polynomial of eighth order or less. Most of the curves studied, however, were not at all suitable to polynomial fitting, and so this method was abandoned. Other types of functions would undoubtedly produce better fits. However, iteration tech-

niques for computing other least-square fits
generally do not converge unless the data are
very good, in which case method (3) is
adequate.

The results of these four methods are presented
in Tables B, C, and D for the three sets of data given
in Table A.

TABLE A

Time (sec)	Set 1 e^{-t}	Set 2 $\sigma = .025$	Set 3 $\sigma = 0.1$
0	1.000	1.015	.947
.051	.950	.915	.847
.105	.900	.892	.977
.162	.850	.844	.796
.223	.800	.831	.703
.287	.750	.736	.735
.356	.700	.748	.725
.431	.650	.680	.922
.511	.600	.593	.593
.597	.550	.575	.601
.692	.500	.515	.505
.797	.450	.450	.597
.916	.400	.448	.364
1.049	.350	.381	.371
1.203	.300	.348	.290
1.383	.250	.227	.244
1.608	.200	.211	.345
1.896	.150	.110	.114
2.300	.100	.091	.254
2.810	.060	.099	-.040
3.510	.030	.040	.166
4.600	.010	.049	.045
6.900	.000	.000	.000

TABLE B— TRANSFORMS DERIVED BY THE FOUR METHODS

DATA — Set #1, Table A

Frequency cps	MAGNITUDE—DECIBLES					PHASE—DEGREES				
	Actual	(1)	(2)	(3)	(4)	Actual	(1)	(2)	(3)	(4)
.00178	− .000	− .000	+ .001	+ .009	+ .001	− .64	− .31	− .66	− .66	− .34
.00316	− .002	− .000	− .001	+ .001	+ .003	− 1.14	− .55	− 1.16	− 1.16	− .60
.00562	− .005	− .002	− .005	− .005	+ .009	− 2.02	− .99	− 2.05	− 2.05	− 1.08
.01000	− .017	− .005	− .017	− .018	+ .026	− 3.59	− 1.75	− 3.65	− 3.65	− 1.93
.0178	− .054	− .015	− .055	− .057	+ .078	− 6.37	− 3.11	− 6.47	− 6.46	− 3.54
.0316	− .168	− .048	− .172	− .178	+ .219	−11.24	− 5.52	−11.41	−11.39	− 6.85
.0562	− .511	− .150	− .529	− .541	+ .471	−19.46	− 9.72	−19.77	−19.67	−14.57
.1000	− 1.445	− .452	− 1.514	− 1.514	+ .153	−32.14	−16.78	−32.52	−32.15	−32.71
0.178	− 3.519	− 1.247	− 3.60	− 3.50	− 3.867	−48.17	−27.61	−48.05	−47.90	−51.96
0.316	− 6.944	− 3.00	− 7.02	− 6.99	− 5.404	−63.28	−41.88	−63.12	−62.83	−67.21
0.562	−11.30	− 6.20	−11.31	−11.31	−10.48	−74.20	−55.57	−74.24	−74.35	−72.36
1.000	−16.07	−10.46	−16.08	−16.09	−15.41	−80.96	−63.80	−80.47	−81.05	−80.13
1.78	−21.00	−14.25	−21.13	−21.03	−20.23	−84.88	−63.38	−85.05	−84.75	−85.51
3.16	−25.97	−17.44	−26.07	−25.99	−25.51	−87.12	−52.62	−87.42	−87.14	−87.03
5.62	−30.97	−19.24	−30.96	−30.98	−30.83	−88.38	+14.80	−88.60	−88.38	−88.26
10.00	−35.96	−11.75	−36.01	−35.98	−37.03	−89.09	−10.01	−89.36	−89.10	−88.56
17.8	−40.96	−10.40	−41.00	−40.98	−48.91	−89.49	+13.33	−89.52	−89.49	−87.88
31.6	−45.96	− 8.29	−46.01	−45.98	−39.22	−89.71	−21.99	−89.81	−89.72	+88.74
56.2	−50.96	− 9.90	−51.01	−50.98	−40.72	−89.84	+22.99	−89.86	−89.84	−88.50
100.0	−55.96	−18.35	−56.01	−55.98	−41.30	−89.91	−61.66	−89.92	−89.91	−88.47

TABLE C - TRANSFORMS DERIVED BY THE FOUR METHODS

DATA - Set #2, Table A (σ = .025)

Frequency cps	MAGNITUDE-DECIBLES					PHASE-DEGREES				
	Actual	(1)	(2)	(3)	(4)	Actual	(1)	(2)	(3)	(4)
.00178	- .000	- .000	- .002	- .002	- .001	- .64	- .33	- .81	- .86	- .81
.00316	- .002	- .001	- .005	- .005	- .003	- 1.14	- .58	- 1.47	- 1.55	- 1.44
.00562	- .005	- .002	- .011	- .012	- .010	- 2.02	- 1.04	- 2.62	- 2.74	- 2.56
.01000	- .017	- .006	- .033	- .038	- .031	- 3.59	- 1.84	- 4.65	- 4.86	- 4.55
.0178	- .054	- .019	- .105	- .119	- .098	- 6.37	- 3.28	- 8.22	- 8.60	- 8.06
.0316	- .168	- .061	- .327	- .373	- .309	-11.24	- 5.79	-14.39	-15.01	-14.12
.0562	- .511	- .186	- .998	- 1.133	- .947	-19.46	-10.13	-24.29	-25.10	-23.95
.1000	- 1.445	- .533	- 2.72	- 2.99	- 2.623	-32.14	-17.20	-36.16	-36.01	-36.10
.178	- 3.517	- 1.31	- 4.49	- 4.38	- 4.464	-48.17	-27.68	-48.08	-43.27	-43.57
.316	-6.944	- 3.02	- 7.48	- 7.72	- 7.513	-63.28	-42.87	-63.62	-62.29	-66.22
.562	-11.30	- 6.62	-13.08	-13.39	-12.07	-74.20	-57.38	-81.77	-83.35	-75.87
1.000	-16.07	-10.78	-16.96	-16.97	-17.01	-80.96	-61.54	-80.76	-81.40	-82.05
1.78	-21.00	-14.55	-22.68	-22.53	-22.02	-84.88	-60.04	-79.35	-79.22	-85.62
3.16	-25.97	-17.81	-27.25	-27.16	-27.13	-87.12	-48.16	-80.84	-76.29	-87.42
5.62	-30.97	-18.32	-31.01	-31.32	-32.47	-88.38	+12.82	-84.58	-84.46	-88.43
10.00	-35.96	-11.59	-36.27	-36.67	-38.71	-89.09	-13.17	-88.26	-91.83	-88.85
17.8	-40.96	-11.00	-41.70	-41.70	-50.53	-89.49	+13.47	-90.69	-86.79	-87.89
31.6	-45.96	- 8.11	-46.74	-46.88	-40.87	-89.71	-22.05	-89.33	-90.41	+88.85
56.2	-50.96	-10.08	-51.73	-51.83	-42.40	-89.84	+26.27	-90.31	-90.08	-88.80
100.0	-55.96	-17.74	-56.75	-56.83	-42.98	-89.91	-48.42	-90.13	-90.35	-88.78

TABLE D— TRANSFORMS DERIVED BY THE FOUR METHODS

DATA — Set #3, Table A
($\sigma = 0.1$)

Frequency cps	MAGNITUDE—DECIBLES					PHASE—DEGREES				
	Actual	(1)	(2)	(3)	(4)	Actual	(1)	(2)	(3)	(4)
.000178	− .000	− .000	+ .009	+ .001	− .001	− .64	− .36	− .95	− .87	− .99
.00316	− .002	− .001	− .003	− .003	− .004	− 1.14	− .64	− 1.65	− 1.43	− 1.77
.00562	− .005	− .002	− .011	− .006	− .013	− 2.02	− 1.14	− 2.94	− 2.58	− 3.14
.01000	− .017	− .007	− .035	− .022	− .043	− 3.59	− 2.02	− 5.20	− 4.58	− 5.58
.0178	− .054	− .023	− .110	− .070	− .135	− 6.37	− 3.58	− 9.21	− 8.13	− 9.87
.0316	− .168	− .073	− .346	− .224	− .425	−11.24	− 6.33	−16.19	− 14.41	−17.28
.0562	− .511	− .225	− 1.08	− .723	− 1.316	−19.46	−11.04	−27.65	− 25.27	−29.10
.1000	− 1.445	− .646	− 3.14	− 2.38	− 3.681	−32.14	−18.58	−42.45	− 42.06	−42.02
.178	− 3.519	− 1.55	− 5.96	− 6.25	− 5.482	−48.17	−29.12	−47.30	− 48.78	−45.53
.316	− 6.944	− 3.29	− 8.01	− 6.92	− 9.170	−63.28	−44.59	−70.25	−74.31	−67.90
.562	−11.30	− 6.24	−10.51	− 9.32	−13.52	−74.20	−53.45	−71.12	− 70.17	−78.24
1.000	−16.07	−11.74	−16.86	−16.35	−18.48	−80.96	−77.68	−109.19	−117.76	−83.35
1.78	−21.00	−15.05	−25.50	−23.68	−23.58	−84.88	−57.64	−69.36	− 46.77	−86.08
3.16	−25.97	−15.38	−24.35	−24.57	−28.61	−87.12	−72.70	−105.80	−106.50	−87.69
5.62	−30.97	−21.31	−32.16	−31.79	−33.96	−88.38	24.51	−119.31	−119.15	−88.55
10.00	−35.96	−10.71	−37.56	−34.14	−40.20	−89.09	−13.39	−80.96	− 78.95	−89.05
17.8	−40.96	−12.30	−44.40	−44.52	−52.03	−89.49	21.79	−93.34	− 81.04	−87.97
31.6	−45.96	− 9.24	−48.40	−47.52	−42.37	−89.71	−21.09	−92.64	− 87.43	+88.91
56.2	−50.96	−11.42	−53.06	−53.02	−43.90	−89.84	21.43	−89.63	− 90.52	−89.02
100.0	−55.96	−18.23	−58.51	−57.67	−44.48	−89.91	−31.42	−90.07	−90.43	−88.99

The first set of data is 23 exact points on the curve $h(t)$ = e^{-t}. The second and third sets of data are for the same curve with simulated errors added to the data; the resulting points are distributed with a normal probability distribution centered about the exact curve. The standard deviation in set 2 is .025, and in set 3 it is 0.1. In each set the last data point is made equal to zero.

Method two is the basic tool that has been adopted for computing transfer functions. If the accuracy of the data warrants its use, method three is also available. In order to derive a formula for computing $H(\omega)$ if $h(t)$ is given by straight line segments, rewrite equation (II-79).[18]

$$H(\omega) = \frac{1}{j\omega} \int_{-\infty}^{\infty} dt \, e^{-j\omega t} \frac{dh(t)}{dt} \qquad \text{(II-81)}$$

The function, $dh(t)/dt$, is a delta function, $h(o)\delta(t)$, corresponding to a step in $h(t)$ at zero, plus a bounded function. Rewrite equation (II-81) as

$$H(\omega) = \frac{1}{(j\omega)^2} \int_{-\infty}^{\infty} dt \, e^{-j\omega t} \frac{d^2h(t)}{dt^2} + \frac{h(o)}{j\omega} \qquad \text{(II-82)}$$

The function, d^2h/dt^2, consists of a series of delta functions

$$\frac{d^2h}{dt^2} = \sum_{i=1}^{m} \left[\begin{array}{l} \text{change in the slope of} \\ \text{the } h(t) \text{ curve at } t = t_i \end{array} \right] \delta(t_i) \qquad \text{(II-83)}$$

Therefore:

$$H(\omega) = \frac{h_1}{j\omega} - \frac{1}{\omega^2}\left[\frac{h_2 - h_1}{t_2} - \frac{h_m - h_{m-1}}{t_m - t_{m-1}} e^{-j\omega t_m}\right.$$

$$\left. + \sum_{i=2}^{m-1}\left(\frac{h_{i+1} - h_i}{t_{i+1} - t_i} - \frac{h_i - h_{i-1}}{t_i - t_{i-1}}\right) e^{-j\omega t_i}\right] \qquad (II-84)$$

where $h_1 = h(o)$, $h_i = h(t_i)$, $t_1 = 0$, and $t_i < t_{i+1} < t_{i+2}$, etc.

An IBM-704 program has been written to compute the magnitude and phase of $H(\omega)$. In addition, the program can perform the following calculations:

1) It can interpolate a large number of points from the data provided. The order of the interpolation polynomial can be set from 1 to 6.

2) It can perform the finite Δt correction discussed in Section C, either by iteration in the time domain or by division in the frequency domain.

3) Given the observed or estimated standard deviation of the data points, the program can compute the theoretical standard deviation of the transfer function according to the propagation of errors formula:

$$\sigma^2(\omega) = \sum_{i=1}^{m}\left(\frac{\partial H(\omega)}{\partial h_i}\right)^2 \sigma_{h_i}^2 \qquad (II-85)$$

4) The program computes the area and the squared-area, $\int_0^\infty h^2(t)\,dt$, of the segmented data curve. The transfer functions are normalized by dividing by the area.

5) Given the h(t) data points and their respective standard deviations, the program can compute a new data curve. Each new point is chosen at random on a normal probability distribution centered about the original data point. The program will then compute the transfer function of this new data curve. The program can compute a large number of such randomized curves and then compute, as a function of frequency, the average and standard deviation of the entire ensemble of curves.

The program is written in FORTRAN; the listings are given in Appendix B. Details of the equations used can be determined by reference to these listings.

The purposes of parts (3) and (5) are the same - to compute the expected standard deviations of the transfer function from the known standard deviations of the impulse response. No reasonable answers are obtained from the method of propagation of errors (part (3)) and hence the Monte Carlo method of part (5) is used exclusively. As an illustration of the type of results that are obtained, the Monte Carlo method has been used to calculate the standard deviations of the transforms of the impulse response data of Table A. Figure 10 shows the data of set 3 of Table A ($\sigma = 0.1$) plotted along with e^{-t} from which it was derived. Figure 11 shows the magnitude, phase, and standard deviations of the transform of h(t) along with the transform of e^{-t}.

PLOT OF DATA SET #3
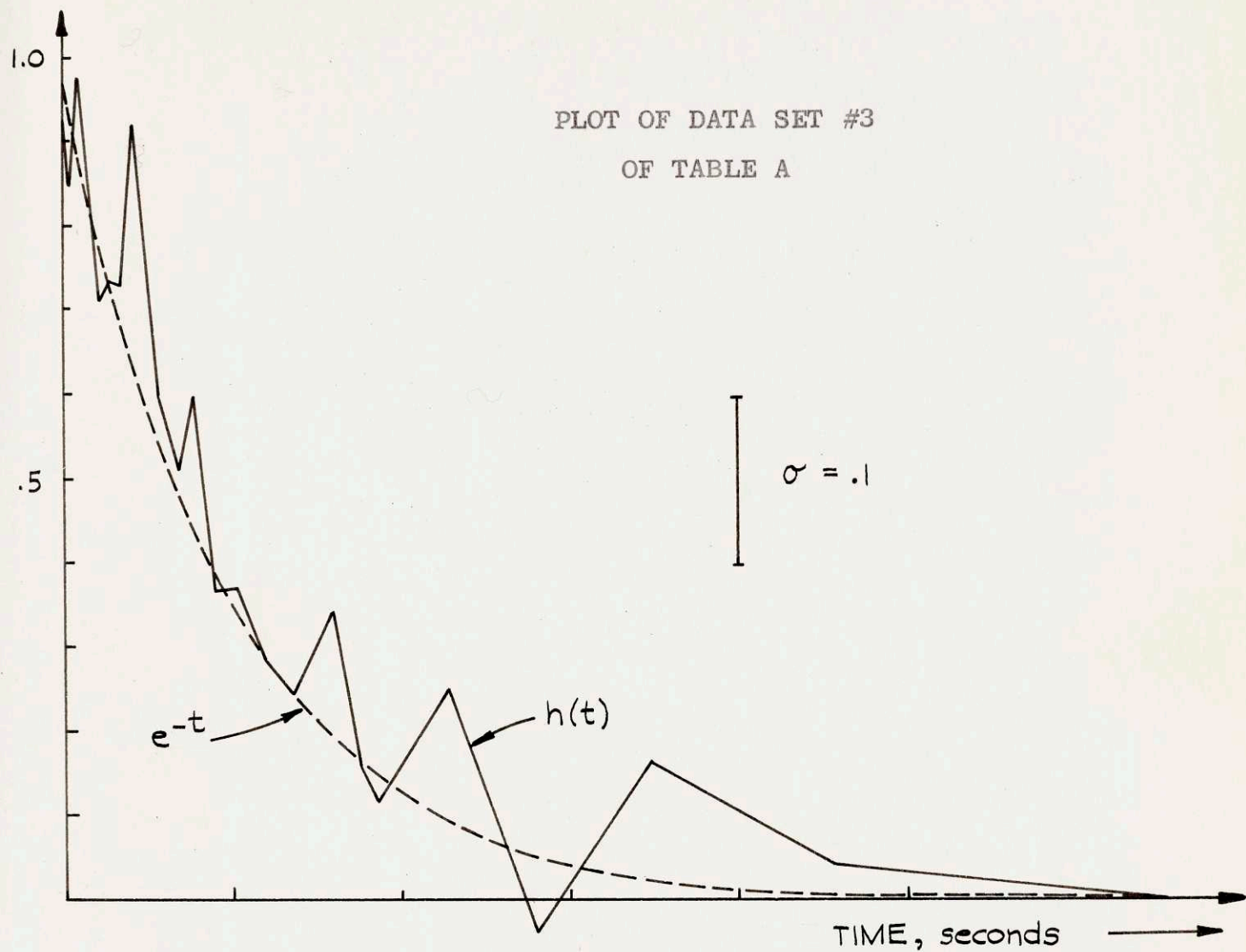
OF TABLE A

FIGURE 10

In Table E are tabulated the corresponding results for data
set 2 of Table A (σ = .025). In both of these calculations,
50 data curves and their transforms were calculated.
Since equation (II-79) is linear it follows that the
transform of the average should equal the average of the
transforms $\overline{F(h(t))}$ = $F(\overline{h(t)})$. This condition is

frequency, cycles/second

MAGNITUDE

transform of e^{-t}

CALCULATED TRANSFORM
OF THE DATA OF SET 3
OF TABLE A

An ensemble of 50 curves
was used to calculate the
rms errors.

FIGURE 11

frequency, cycles/second

transform of e^{-t}

PHASE
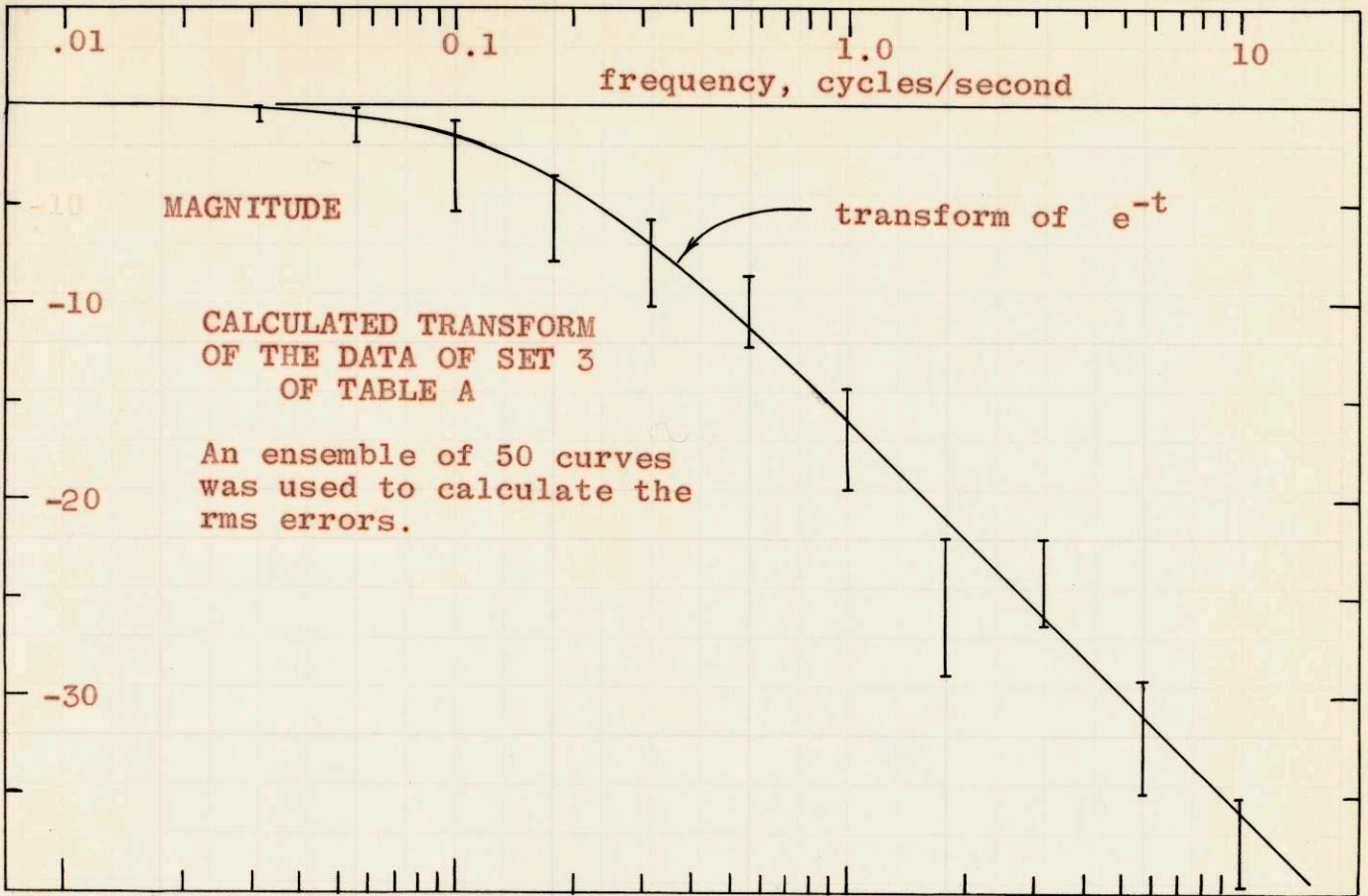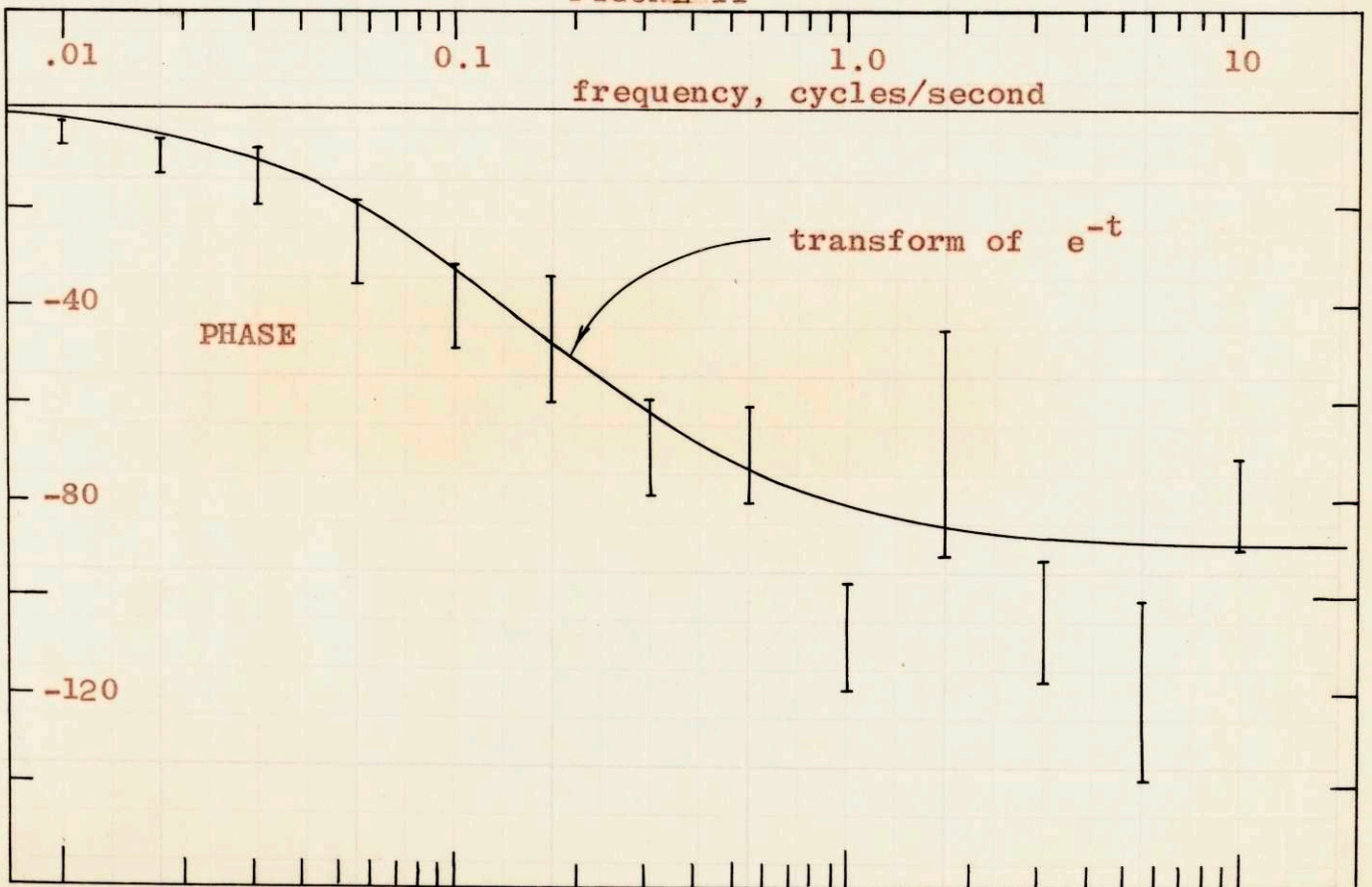
approached reasonably closely for an ensemble of 50
curves and hence the estimated standard deviations are
judged to be a close guess to the true standard deviations.

The transfer function results that are given in
Chapter IV on experiments have all been calculated using
the IBM-704 code described and their standard deviations
have been estimated by the Monte Carlo method of part (5).

TABLE E

EXPECTED ERRORS IN THE TRANSFORM OF DATA SET NO. 2

Frequency cps	Magnitude db	Phase Degrees
.00178	− .002 ± .002	− .81 ± .10
.00316	− .005 ± .001	− 1.47 ± .17
.00562	− .011 ± .003	− 2.62 ± .30
.01000	− .033 ± .009	− 4.65 ± .53
.0178	− .105 ± .027	− 8.22 ± .94
.0316	− .327 ± .086	−14.39 ± 1.61
.0562	− .998 ± .264	−24.29 ± 2.48
.1000	− 2.711 ± .696	−36.16 ± 2.22
.178	− 4.487 ± .539	−44.08 ± 3.39
.316	− 7.486 ± .568	−63.62 ± 2.48
.562	−13.08 ± .68	−81.77 ± 4.19
1.000	−16.96 ± .67	−80.76 ± 3.66
1.78	−22.68 ± .79	−79.35 ± 4.82
3.16	−27.25 ± .73	−80.84 ± 5.18
5.62	−31.01 ± .70	−84.58 ± 4.63
10.00	−36.27 ± .49	−88.26 ± 2.38
17.8	−41.70 ± .49	−90.69 ± .65
31.6	−46.75 ± .47	−89.33 ± .45
56.2	−51.73 ± .47	−90.31 ± .30
100.0	−56.75 ± .47	−90.13 ± .17

CHAPTER III

Implementation of the Crosscorrelation Method

In the previous chapter it has been shown that, for
a properly chosen input signal, the impulse response of
a linear system is given by the crosscorrelation function
of the system input and output. This chapter describes
the equipment that has been built to measure the impulse
response of reactor systems.

There are two basic jobs the equipment must perform:
A) It must supply the input; and, B) it must compute
the crosscorrelation function.

A)   The Input and Delayed Inputs Generator

The input and delayed inputs are stored on punched
paper tape. A small section is shown in Figure 1.
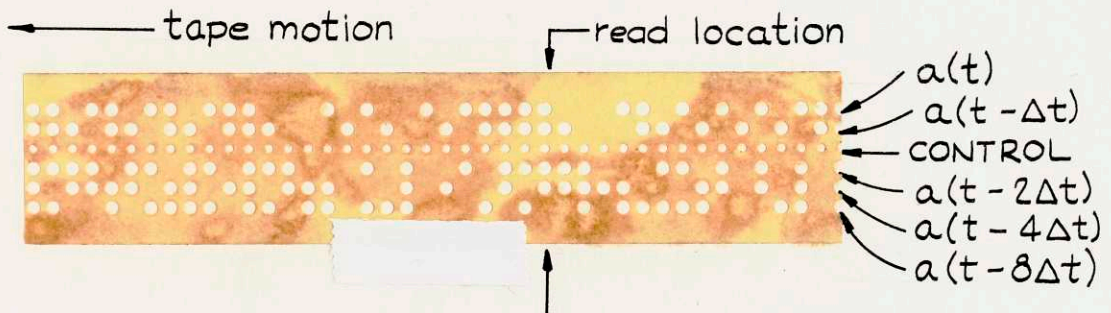
FIGURE 1

The top row is the input signal and the other four rows
are the same signal shifted to the right 1, 2, 4, and 8

places respectively. A multi-vibrator generates one
timing pulse each Δt seconds. This pulse moves the tape
in the tape reader in jerks past the read location. Thus
the output of a register that is set by any one of the
five rows is a discrete-interval, binary square-wave.
In particular, the signal from channel one is taken to
be the input, the signal from channel two is equivalent
to the signal from channel one delayed by Δt, channel
three is equivalent to channel one delayed by $2\Delta t$, etc.
Thus, any delay can be realized by properly punching the
tape as long as the delay is an integer multiple of Δt.

B.   The Crosscorrelator

The function to be computed is:

$$\phi_{ab}(\tau_1) = \frac{1}{T}\int_0^T dt\, b(t)\, a(t-\tau_1) \qquad\qquad (\text{II-2})$$

This involves four steps:

1)   Delay of $a(t)$ by τ_1. This delay has been
      accomplished artificially by the use of second
      channel of the punched paper tape.

2)   Multiplication of $b(t)$ by $a(t - \tau_1)$. This
      multiplication can be accomplished by selecting
      either $b(t)$ or $-b(t)$ depending on the sign of
      $a(t - \tau_1)$.

3)   Integration of the product. This is accomplished
      by a high gain operational amplifier with re-
      sistor input and capacitor feedback.

4)   Termination of the integration at time, T.

A schematic diagram of one channel of the crosscorrelator
is shown in Figure 2.
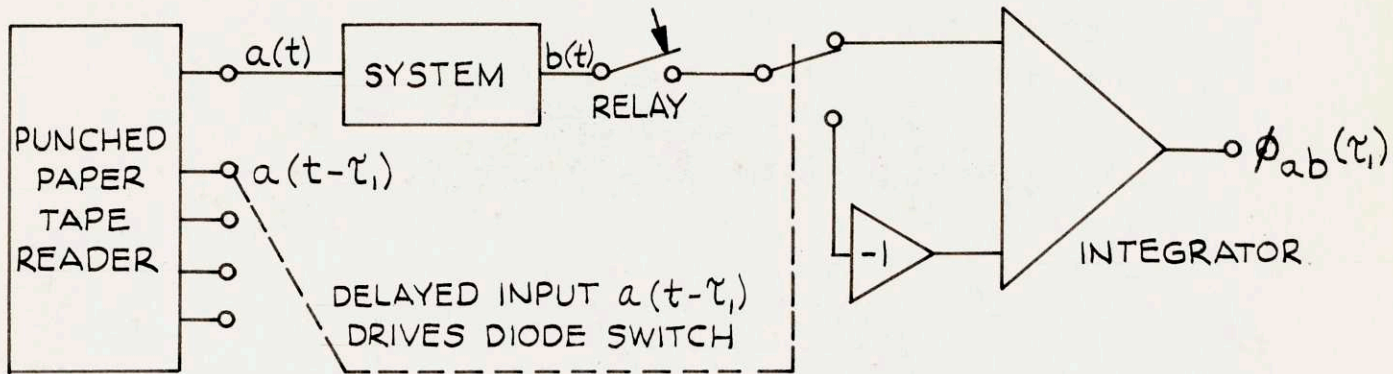
FIGURE 2

The system output is fed through a relay to a pair of six-diode gates. Depending on the polarity of $a(t - \tau_1)$ the gates switch the relay output to either the plus one or the minus one input of the integrator.

The calculation begins when a manual switch is thrown. The relay closes on the next timing pulse and a special scaler begins counting the timing pulses. When the scaler reaches the preset number, $T/\Delta t$, the relay opens and the integrator holds at the final valve, $\phi_{ab}(\tau_1)$.

Figure 2 shows crosscorrelation channel No. 1 which computes $\phi_{ab}(\tau_1)$. Three other identical channels have been built to compute $\phi_{ab}(\tau_2)$, $\phi_{ab}(\tau_3)$, and $\phi_{ab}(\tau_4)$. By using a different punched paper tape with a different set of delays, a different group of four points on $\phi_{ab}(\tau)$ can be calculated. The shape of most curves can be determined by 28 points calculated from seven tapes. Of course, a 28 channel crosscorrelator could be built to perform the same calculations in one seventh the time.

C.   Accuracy and Design

The complete circuit diagrams for all the equipment
that was built especially for this project are given in
Appendix C. A schematic showing how the equipment was
linked to a portable analog computer during use is also
given. Figure 3 is a photograph of the equipment.

Most of the design utilizes switching type circuits
(flip-flops, logic gates, etc.) and once the levels are
set correctly there is no accuracy problem. The diode
gates, however, do present a problem since the continuous
level signal from the system output must pass through
them without distortion. To accomplish this, diodes
are selected in pairs which have the same forward vol-
tage drop. A pair of trimming potentiometers were
designed into the gates so that they could be precisely
balanced. Once balanced, the gates proved to be linear
within ± 0.3% in both switch positions over a range of
-40v. to +40v.

The punched paper tape reader is a rewired photo-
electric model that had served as an input to the Maniac
I computer. It had originally been designed to operate
at 200 bits/second but cannot now be pushed past 50 bits/
second with complete reliability. This is the basic
limitation of this particular implementation of the cross-
correlation method. This means that Δt can be no smaller
than .020 seconds; also that the system under study should
have a bandwidth no greater than 5 cps. This is the point
at which the finite Δt correction, discussed in Chapter
II-C, begins to become significant.

D.   The Punched Paper Tapes

Many paper tapes had to be punched. There are two
chains, $N = 251$ and $N = 1019$, which are used; for each

FIGURE 3
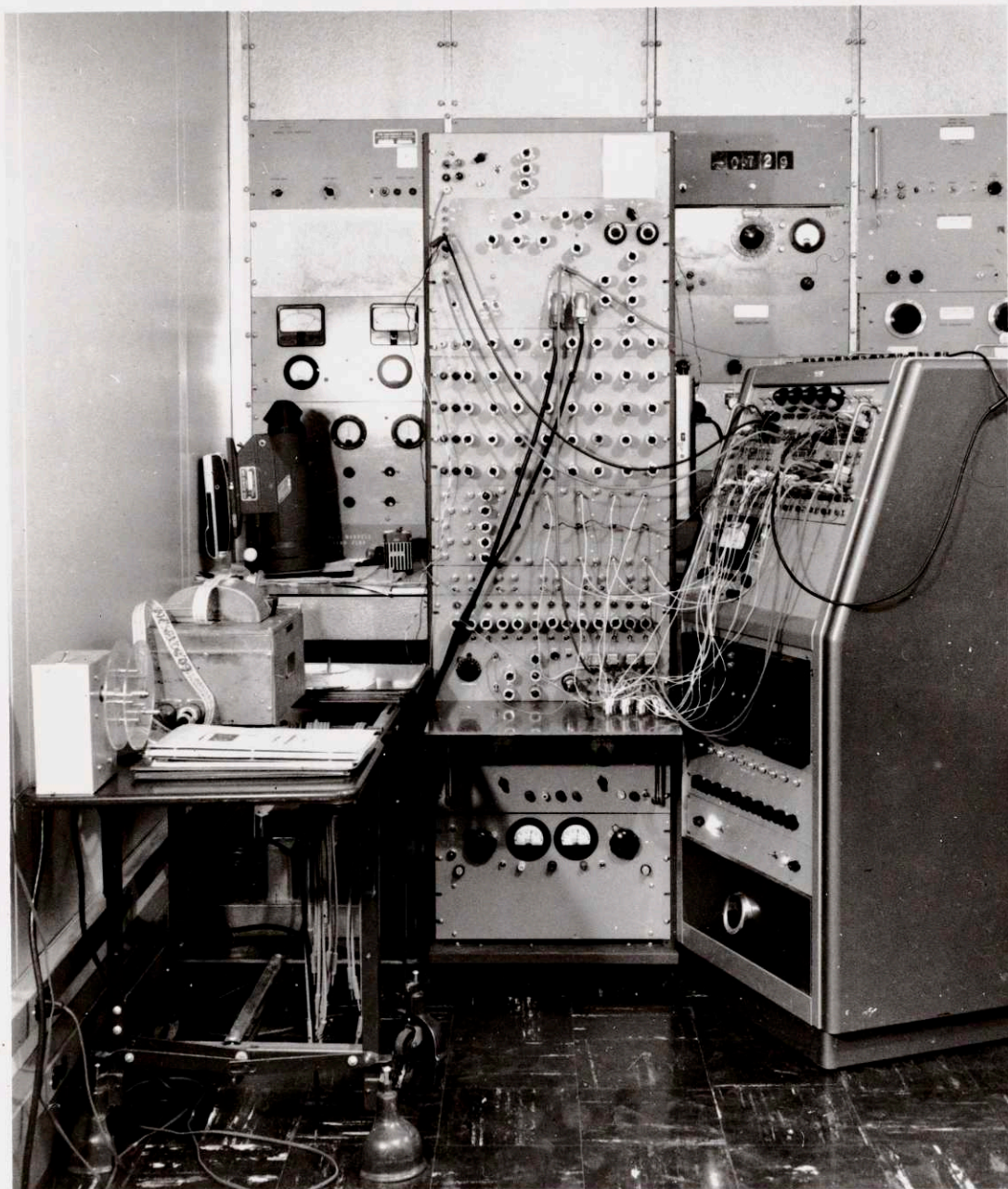
PUNCHED PAPER TAPE AND CROSSCORRELATION EQUIPMENT
The crosscorrelator is in the center, the portable
analog computer on the right, and the punched paper
tape reader on the left.

of these, many different tapes, corresponding to different
sets of delays, are needed. Conveniently, the Maniac
digital computer at Los Alamos can be programmed to
punch paper tapes. Two codes are written which will
accept the input chain, compute the autocorrelation
function, and punch out tapes for any arbitrary sets of
delays.

The first type of tape that is used is a loop. A
tape of length 251 bits, for example, is punched with the
input in channel one and the desired shifted inputs in
the other four channels. The tape is then cut and
glued end to end to form a loop (see Figure 3). When
placed in the reader, the input signal read out auto-
matically has a periodicity of 251 bits. The shifted
channels are punched modulo 251 so that they too form a
continuous, periodic signal equivalent to the input
signal delayed.

In some of the experiments there is not sufficient
time to read the four voltages $(\phi_{ab}(\tau_i))$ from the inte-
grator outputs and to swap loops in the reader between
each integration. For these experiments the punched
paper tapes are continuous and are wound on reels.
Channel one contains the continuous, periodic input
signal. The other channels contain the four shifted
inputs as follows: adjacent to the first several cycles
of the input signal the first four shifted inputs are
punched; adjacent to the next several input cycles the
next set of four shifted inputs are punched, etc. Thus
there is an abrupt change in the delayed channels every
several cycles. The number of cycles of each set of
shifted inputs must necessarily be one greater than the
number of cycles over which the integration is performed
to allow time to reset for the next group. The four in-
tegrator voltages are recorded continuously on a Sanborn

recorder. The values of the crosscorrelation function can be read from the Sanborn record after the experiment.

E.   Post Mortem Crosscorrelation

Any one cycle of the system response and of the input signal contains all the information needed to construct the crosscorrelation function. If these two signals are recorded, then the crosscorrelation can be performed at leisure afterward. The only equipment available to compute the crosscorrelation function, however, is that which has already been described. This equipment can be used to perform the crosscorrelation function of recorded signals as follows:

1) In addition to the input signal and the system output signal, the timing pulse is recorded on magnetic tape.

2) After the experiment, the magnetic tape is played back and the recorded timing pulses are used to control the punched paper tape reader.

3) The recorded input signal and the signal from paper tape channel No. 1 are recorded on a high speed Sanborn recorder and the relative shift between the two is noted.

4) Four points on the crosscorrelation function are computed using the other four paper tape channels to drive the diode switches as usual.

5) The total effective delays, τ_i (corresponding to the points on crosscorrelation function calculated in step 4), are computed: each τ is the sum of the shift observed in step 3 and the shift of the respective punched paper tape channel.

6)   Steps 2) - 4) are repeated many times to obtain as wide a variety of delays as desired.

CHAPTER IV

EXPERIMENTS

As soon as the equipment described in Chapter III was completed it was tried out on analog computer simulations of simple systems. These analog computer studies gave experimental verification of the theoretical predictions and indicated the accuracy capabilities of the crosscorrelation method. During the time that the crosscorrelator was being built, an input device for a reactor was being designed and built. When this was ready, a set of experiments was carried out on the Godiva II fast reactor at Los Alamos. The results were not quite what had been hoped for, but they did establish the feasibility of using the crosscorrelation method on reactor systems. The data do agree with the theoretical predictions, but the variance is very large. The experience gained by experimenting on Godiva was invaluable.

The affirmative results of the Godiva experiment and the analog computer studies provided enough confidence in the crosscorrelation technique to permit its use on Kiwi A3. Kiwi A3 is a prototype nuclear rocket engine built and tested by the Los Alamos Scientific Laboratory. The original reason for the development of the method had been to measure the response characteristics of Kiwi type reactors. There are better methods of measuring the impulse response of Godiva because neither short experiment time nor small excursions are a requirement for experiments on that reactor.[*] But in the case of rocket propulsion reactors the crosscorrelation method is the only method which seems feasible. The experiments were carried out on Kiwi A3 at the Nevada Test Site during October, 1960. The results were uniformly quite good;

[*]See, for example, reference (19).

they prove beyond doubt the feasibility of the crosscorrelation method for use on reactor systems.

Up to this point, the effect of system nonlinearities had not been investigated, either analytically or experimentally. The particular type of nonlinearity of most interest is that of the reactor kinetics equations. An analog computer study was carried out on a reactor simulation to see if any adverse effects could be found. None were found.

The analog computer studies and the two sets of experiments will now be taken up one at a time in some detail.

A. The Analog Computer Studies

A great deal of data have been taken using the analog computer simulations; most of this was for practice. A few results are presented here to indicate the accuracy capabilities of the crosscorrelation method and to show in detail how the data are processed. In both examples given, the system noise was negligible.

The first system chosen for study is a second order system with a natural frequency of 2 rad/sec. and a damping factor of one half. Its characteristics are:

$$h(t) = 4/\sqrt{3} \ e^{-t} \sin(\sqrt{3} \ t)$$

$$H(\omega) = \frac{4}{(4-\omega^2) + 2j\omega} \tag{IV-1}$$

On the analog computer, this system can be simulated as shown in figure 1.[20]
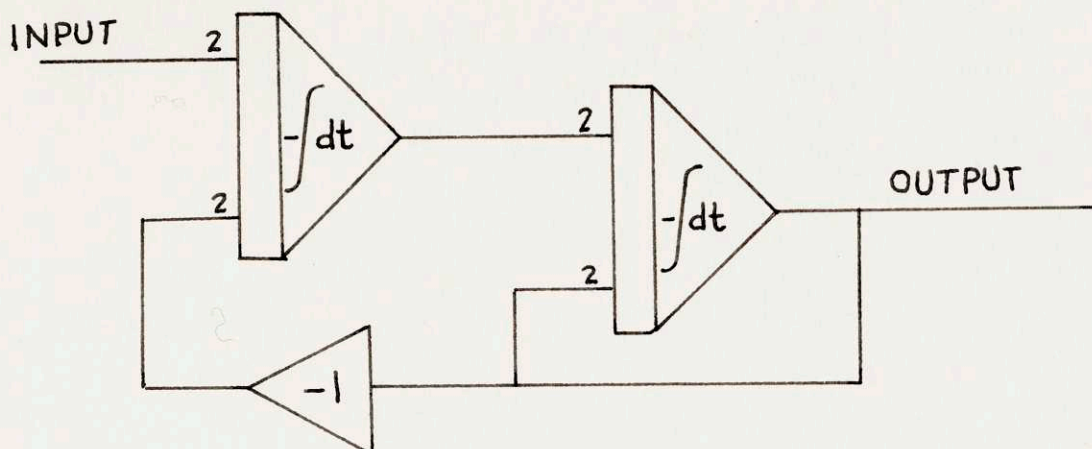
FIGURE 1.

Data were taken under the following conditions:

a(t) = ± 56.7 volts

Δt = .0203 seconds

Integration time = 2T = 502 Δt = 11.5 seconds

Gain from system output to diode gates = 2

Integration rate constant = 0.956

Table A lists the data. Explanation of each column of the table follows:

Column 1 - Lists the channel number.

Column 2 - Lists the delay, τ , in units of Δt. This corresponds to the number of bits the signal was shifted on the punched paper tape.

Column 3 - Lists the delay, τ , in seconds; column 2 times .0203 seconds.

Column 4 - Lists T $\phi_{ab}(\tau)$. This is the voltage at the integrator output at the end of the integration. Repeated measurements indicate that the standard deviation of these voltages is about 0.05 volts, independent of τ.

TABLE A

1 Channel Number	2 τ bits	3 τ sec.	4 $T\psi_{ab}(\tau)$ Volt-sec	5 $T\psi'_{ab}(\tau)$ Volt-sec	6 $P(\tau)$ Volt-sec	7 $h(\tau)$ Sec^{-1}	8 $h(\tau)$ normalized Sec^{-1}	9 $h(\tau)$ true Sec^{-1}
1	- 1	- .0203	- 3.98					
2	- 1	- .0203	- 4.01					
3	- 1	- .0203	- 4.08					
4	- 1	- .0203	- 4.00					
1	1	.0203	- 2.28	1.70	1.704	.076	.082	.079
2	2	.0406	- .65	3.36	3.363	.150	.163	.155
3	3	.0609	.90	4.98	4.989	.222	.241	.228
4	4	.0812	2.50	6.50	6.504	.290	.314	.297
1	6	.122	5.41	9.39	9.398	.419	.454	.426
2	8	.162	7.90	11.91	11.914	.531	.576	.542
3	10	.203	10.14	14.22	14.227	.634	.688	.646
4	12	.244	12.21	16.21	16.214	.723	.784	.737
1	15	.304	14.82	18.80	18.808	.838	.910	.853
2	18	.365	16.56	20.57	20.571	.917	.995	.943
3	21	.426	18.11	22.19	22.197	.990	1.074	1.011
4	25	.507	19.26	23.26	23.263	1.037	1.125	1.066
1	30	.609	19.71	23.69	23.693	1.056	1.146	1.089
2	40	.812	17.86	21.87	21.872	.975	1.058	1.010
3	50	1.015	13.85	17.93	17.931	.800	.867	.823
4	65	1.319	6.09	10.09	10.090	.450	.488	.471
1	80	1.624	- .81	3.17	3.169	.141	.153	.153
2	95	1.928	- 5.67	- 1.66	- 1.661	- .074	- .080	- .060
3	110	2.233	- 7.93	- 3.85	- 3.851	- .172	- .186	- .160
4	130	2.639	- 7.92	- 3.92	- 3.920	- .175	- .190	- .163
1	150	3.045	- 6.44	- 2.46	- 2.460	- .110	- .119	- .094
2	180	3.654	- 4.37	- .36	- .360	- .016	- .017	+ .001
3	200	4.060	- 3.80	.28	.280	+ .012	+ .014	+ .026
4	230	4.669	- 3.81	.19	.190	+ .008	+ .009	+ .021

63

Column 5 - Lists $T\phi'_{ab}(\tau)$. Equation (II-13) indicates that the value of $\phi'_{ab}(-\Delta t)$ should be sub-tracted from each of the other values of $\phi_{ab}(\tau)$ to give an answer proportional to $h(\tau)$. It is observed that the four values of $\phi'_{ab}(-\Delta t)$ are different. These differences are due to small inaccuracies in the diode gate operation; the differences will repeat with repeated measurements. Thus the practice was adopted of subtracting the value of $T\phi_{ab}(-\Delta t)$, as measured by each channel, from the other measurements made by that same channel. These values are listed in the column.

Column 6 - Lists the data of column 5 corrected for finite Δt. This correction has been discussed in Chapter II-C. (Refer: equation (II-17)). Thus, each value satisfies the relation:

$$P(\tau_i) = T\phi'_{ab}(\tau_i)$$

$$-\frac{\Delta t^2}{6(\tau_{i+1} - \tau_i)}\left[\frac{P(\tau_{i+1})-P(\tau_i)}{\tau_{i+1} - \tau_i} - \frac{P(\tau_i)-P(\tau_{i+1})}{\tau_i - \tau_{i-1}}\right]$$

$$(IV-2)$$

To satisfy this condition within 0.0001 required five iterations. Column 6 is listed to five signifigant figures in order to show the magnitude of the correction. In this particular example this correction was not actually necessary, since Δt was chosen adequately small.

Column 7 - Lists 1/K times column 6. K is the
theoretical constant between impulse
response and $T \phi'_{ab}(\tau)$ corrected.

K =2TΔt (input)(output gain)(Integration constant)
K = $(502)(.0203 \text{ sec})^2 (56.7 \text{ volts})(2)(.965 \text{ sec})$
K = 22.4 volt seconds

Column 8 - Lists column 5 normalized to an area of
unity. For any system, the D-C gain
(gain at zero frequency) is given by the
area under the impulse response: D-C
gain= $\int_0^\infty h(t)dt$. It is a simple matter to
determine the D-C gain very accurately;
in this case it is unity. The normaliza-
tion constant is 20.67 volt-seconds.

Column 9 - Lists the function $4/\sqrt{3} \; e^{-\tau}\sin(\sqrt{3}\tau)$,
the true analytical system impulse response.

It is usually much easier to use a normalization
constant than try to calculate K accurately. For some
systems the D-C gain is zero or infinite and the normaliza-
tion method cannot be used.

The data of column 8 in Table A have been used to
calculate a system transfer function using the techni-
ques discussed in Chapter II-E. For this purpose two
points were added; the values of $h(\tau)$ at $\tau = 0$ and at
$\tau = 251\Delta t$ were set equal to zero. The results are tabula-
ted in Table B along with the theoretical results. Two
hundred equally spaced points were machine interpolated
(3rd order) and from these the transfer function was
calculated, using equation (II-84).

The data of Tables A and B are plotted in Figures
2 and 3 respectively.

TABLE B
MEASURED AND ACTUAL TRANSFER FUNCTION
OF A SECOND ORDER SYSTEM

Frequency Cps	Magnitude - DB		Phase - Degrees	
	Measured	Actual	Measured	Actual
.00100	− .035	.000	− .15	− .18
.00178	− .011	.000	− .22	− .32
.00316	− .002	.000	− .40	− .57
.00562	+ .003	.001	− .73	− 1.01
.01000	+ .011	.004	− 1.30	− 1.80
.0178	+ .036	.013	− 2.33	− 3.20
.0316	+ .112	.042	− 4.24	− 5.73
.0562	+ .337	.133	− 8.05	− 10.33
.1000	+ .902	.404	− 16.76	− 19.22
.178	+ 1.755	1.049	− 39.00	− 39.08
.316	+ .472	.056	− 89.34	− 89.24
.562	− 8.366	− 8.819	−139.83	−140.21
1.000	−18.916	−19.471	−159.42	−160.50
1.78	−29.386	−29.749	−171.02	−169.52
3.16	−39.020	−39.842	−176.76	−174.19
5.62	−48.436	−49.871	−181.68	−176.75
10.00	−60.112	−59.881	−174.02	−178.17
17.8	−69.635	−69.884	−180.58	−178.97
31.6	−79.238	−79.884	−190.35	−179.42
56.2	−89.452	−89.885	−177.37	−179.68
100.0	−99.469	−99.885	−182.72	−179.82

CALCULATED FROM THE DATA OF TABLE A, COLUMN 8.
TWO HUNDRED EQUALLY SPACED WERE INTERPOLATED
(3RD ORDER) AND EQUATION (II-84) WAS USED TO
CALCULATE THE VALUES.

FIGURE 2

MEASURED IMPULSE RESPONSE OF A SECOND ORDER SYSTEM

theoretical

MEASURED FREQUENCY RESPONSE OF A SECOND ORDER SYSTEM
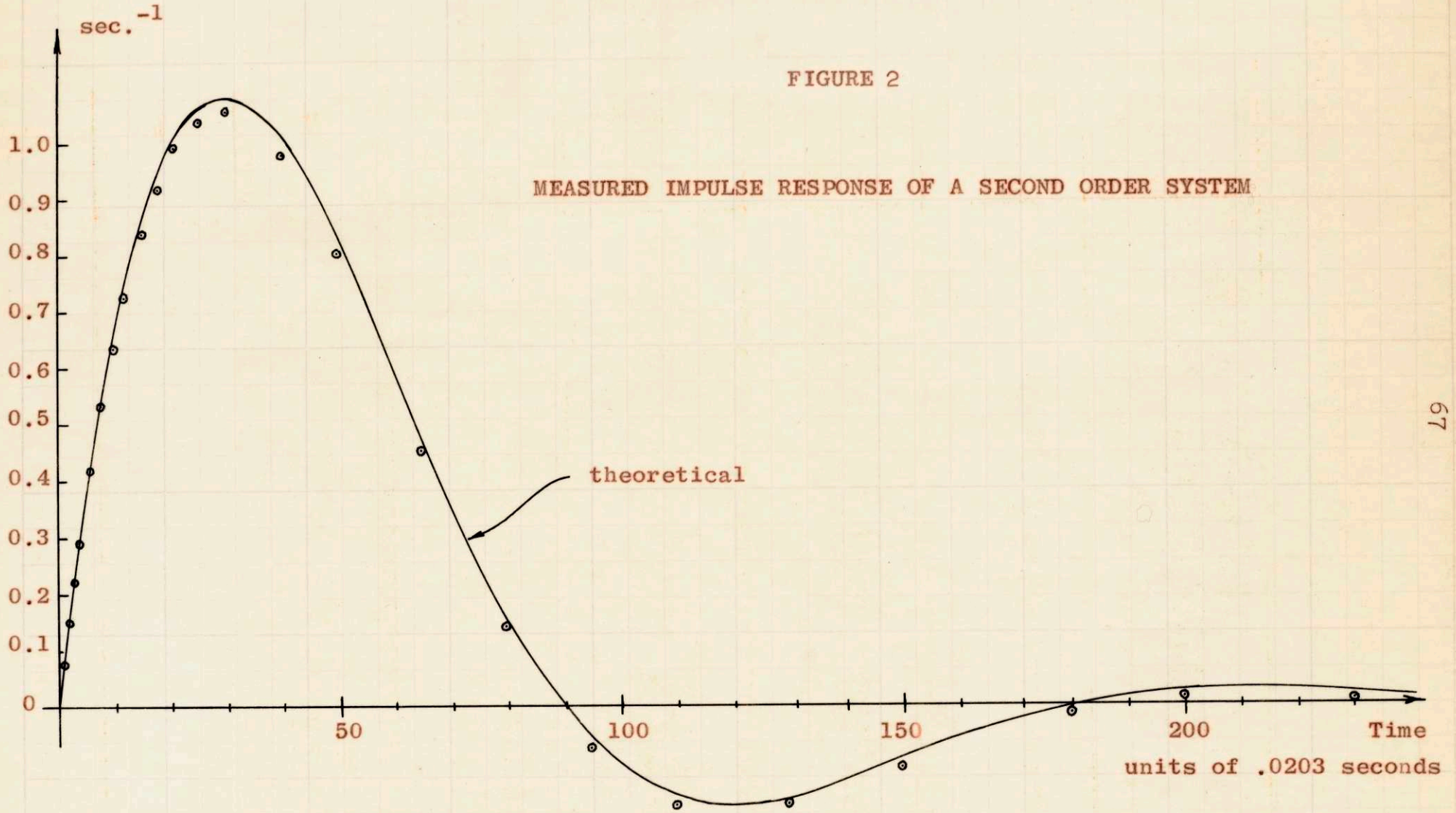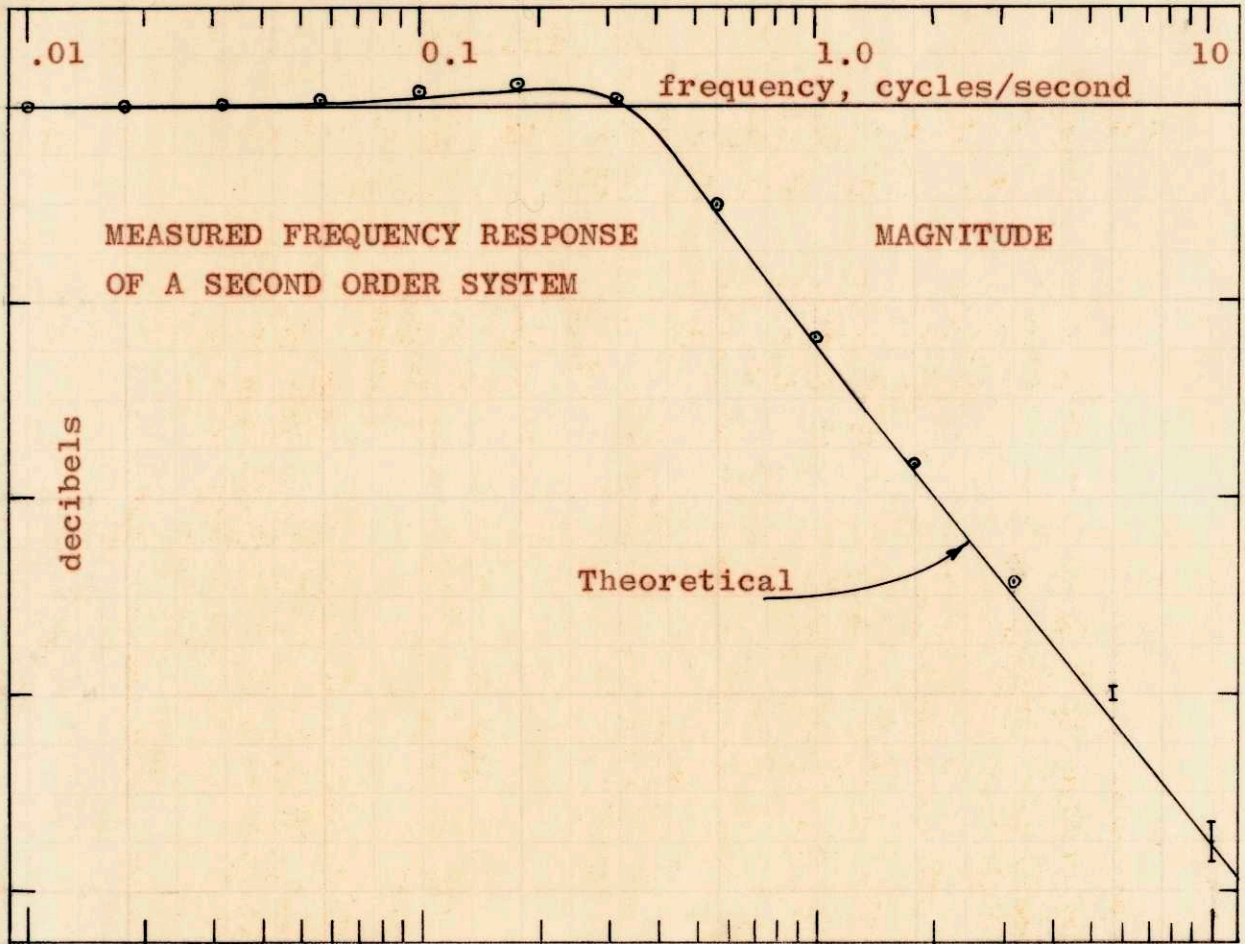
FIGURE 3
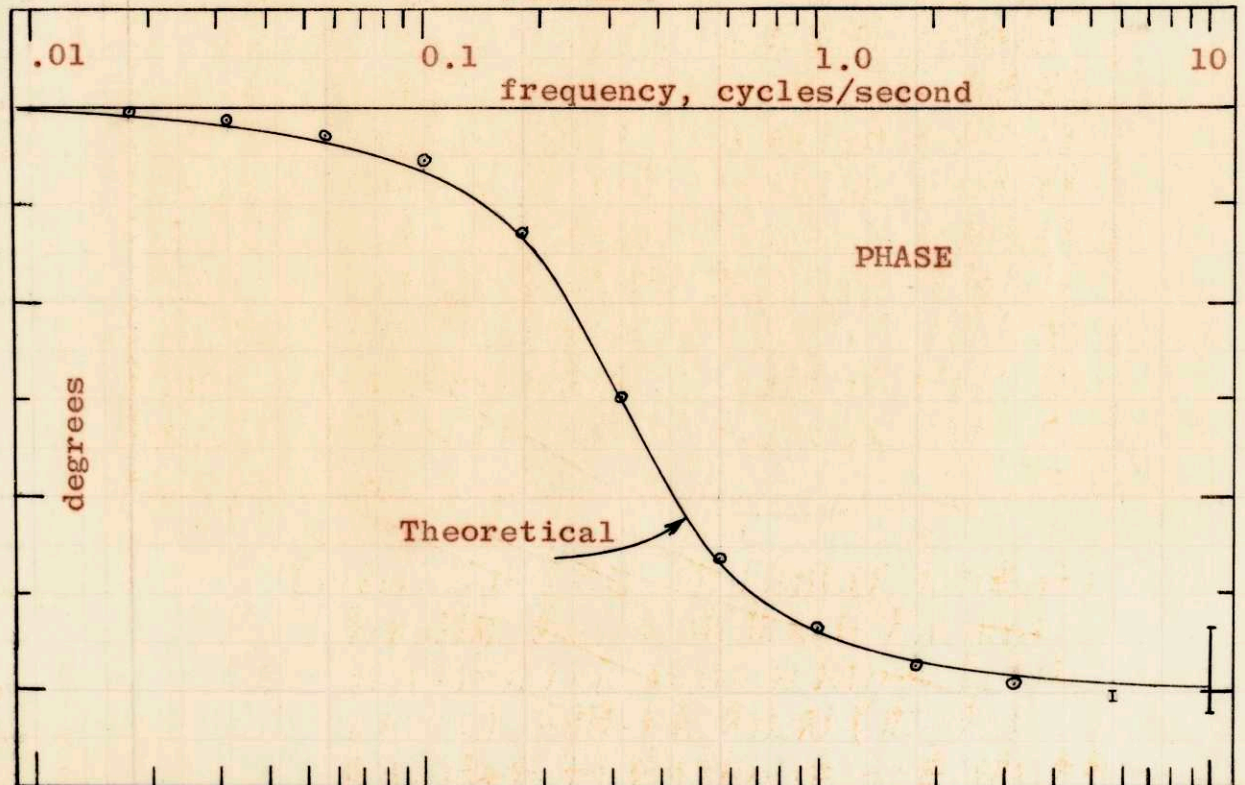
From these results a few general error indexes can be calculated:

Impulse response:

$$\frac{\text{Maximum error}}{\text{Maximum value}} = .035/1.09 = 3.2\%$$

$$\frac{\text{RMS error}}{\text{Maximum value}} = .018/1.09 = 1.65\%$$

Frequency response derived from impulse response:

	OUT TO 1 CPS	OUT TO 100 CPS
Maximum magnitude error	.7 decibels	1.5 decibels
Maximum phase error	2.5 degrees	10.9 degrees

The second system chosen for study is a reactor simulation. The equations used are:[4]

$$\frac{dn}{dt} = \frac{\rho - \beta}{\ell^*} n + \sum_{i=1}^{k} \lambda_i c_i$$

$$\frac{dc_i}{dt} = \frac{\beta_i n}{\ell^*} - \lambda_i c_i \quad , i = 1, 2, \text{----} k$$

$$(IV-3)$$

The non-linearity begins to become important when ρ is significantly different from zero during a time that n is significantly different from its initial value, n_0. A series of three experiments were carried out to ascertain whether the non-linearity is an important limitation to the application of the crosscorrelation method to reactors. For simplification, ℓ^* was made numerically equal to β, ρ was measured in units of 2β, and two groups of delayed neutrons were used.[21]

$$\lambda_1 = .00386 \text{ sec}^{-1} \qquad \lambda_2 = .512 \text{ sec}^{-1}$$

$$\beta_1/\beta = .425 \qquad \beta_2/\beta = .575$$

On the analog computer, time was speeded up by a factor of 10. The linearized transfer function, which is valid for small perturbations, is:

$$\frac{\Delta n}{\Delta \rho} = \frac{2n_o \ (s+0.512)(s+.00386)}{s \ (s+1.353)(s+0.163)}$$
(IV-4)

The corresponding theoretical impulse response is

$$n(t) = 60(.009 + .705 \ e^{-1.353t} + .286 \ e^{-.163t}) \text{ volts}$$
(IV-5)

Three experiments were carried out; the conditions are tabulated in Table C below.

TABLE C

EXPERIMENT NO.	1	2	3
Input-Reactivity	± 8¢	± 80¢	± 120¢
Peak-To-Peak Power Fluctuation	14.3%	147%	230%
Δt (seconds)	.2017	.2021	.1951
T	502Δt	502Δt	502Δt
ρ_o	-0¢	-5¢	-16¢
Noise in Data – % of Max. Data Point	.3%	1.0%	1.7%
Output Gain	10	1	2/3
$\int_0^T h(\tau) \, d\tau$	149	164	167
K	.783	.784	.731

$$K = (.956)(T)(\Delta t)\frac{\Delta \rho}{2\$}(\text{Output gain})$$

If the binary input is imposed on a just-critical reactor, the power level will rise exponentially due to the non-linearity. Figure 4 is a plot of the power level

REACTOR POWER FLUCTUATIONS
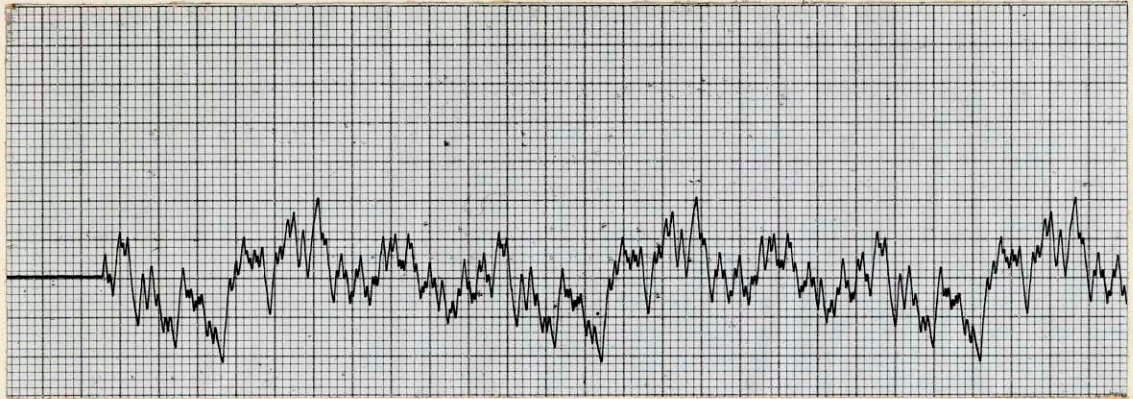
REACTIVITY = ± 8¢ N_0 = 150 chart lines
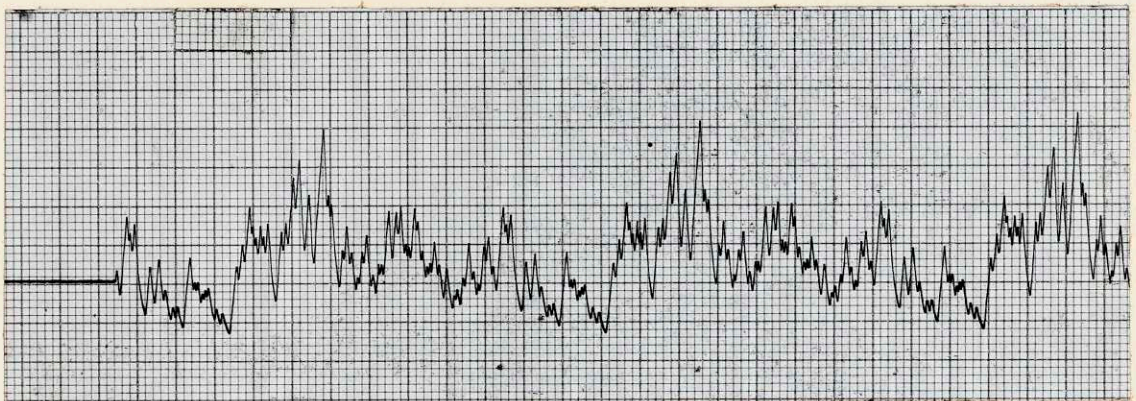
Reactivity = ± 80¢ N_0 = 15 chart lines
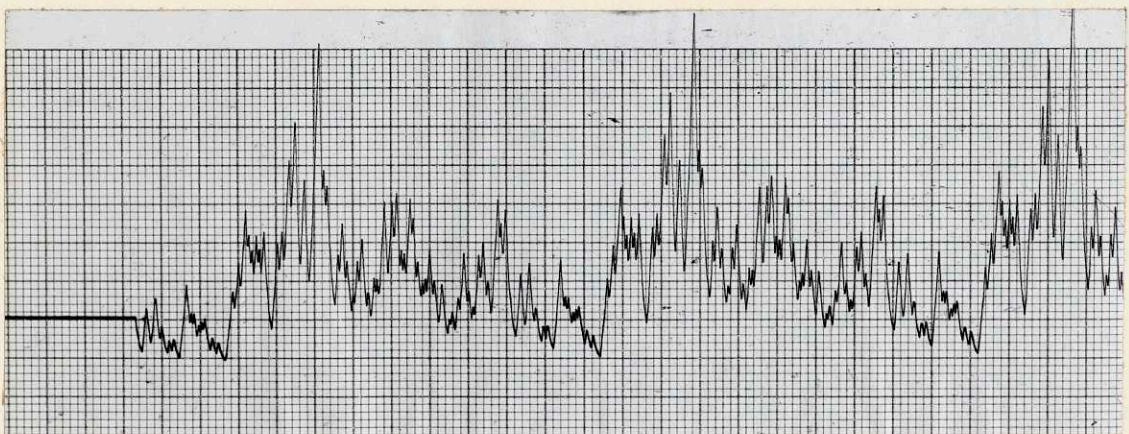
Reactivity = ± 120¢ N_0 = 10 chart lines

Time ⟶   one chart line = one second

for the three different reactivity input levels.
The rise in power for ± 8¢ is undetectable; for ± 80¢
it is clearly noticeable, and for ± 120¢ the signal
quickly goes off the scale. The quantity, ρ_o is that
value of negative reactivity which will maintain the
power at a constant average level. Figure 5 shows the
power level traces with this reactivity imposed. The
scaling of the traces in Figures 4 and 5 is in inverse
ratio to the binary reactivity input level. Thus, if
the system were linear, the traces would be identical.
The increasing asymetry of the signal, with increasing
reactivity, is clearly noticeable.

Data taken during the three experiments are plotted
and tabulated in Figures 6, 7, and 8. The values have
been corrected and divided by K.

The important conclusion that can be drawn from
these figures is that the impulse response data are not
badly impaired by the non-linear effect. Indeed, it
appears that the crosscorrelation method tends to minimize
errors due to finite signal size.

It is apparent that the largest error in the data
is in the scaling constant K. The data of all three
experiments could be made to fit the theoretical curve
very closely by adjusting the value of K a few percent.
The least accurate quantity in the calculation of K is
the true average power level, n_o. In each of these
experiments, the value of ρ_o was established by trial.
The computer was then reset with n_o = 30 volts and
started again at an arbitrary point in the input cycle.
A shift in the average power level is entirely possible.
Since it is the system dynamics that the crosscorrelation
method measures, this inaccuracy in K is not particularly
relevant; the system dynamics are given by the shape of
the impulse response; the value of K leads to the system
gain. This system property can generally be better
measured by some other experimental technique.

REACTOR POWER FLUCTUATIONS
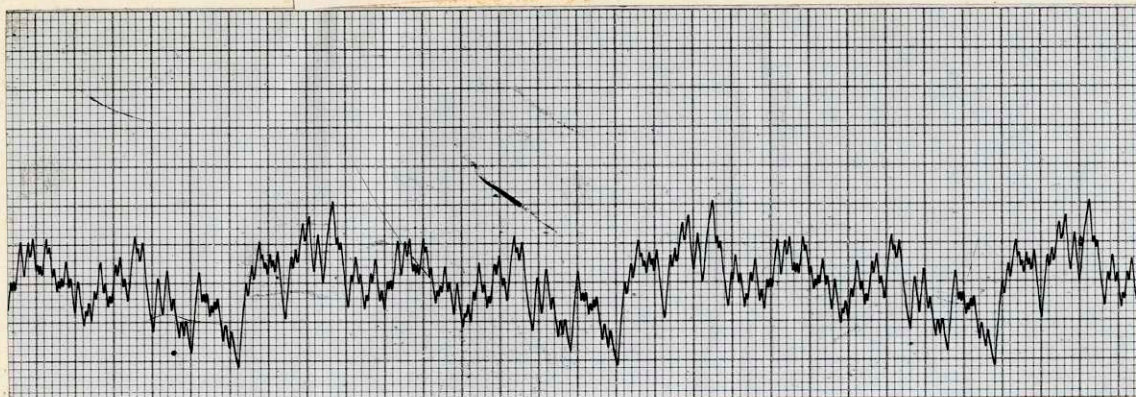
Reactivity = -0 ± 8¢ N_o = 150 chart lines
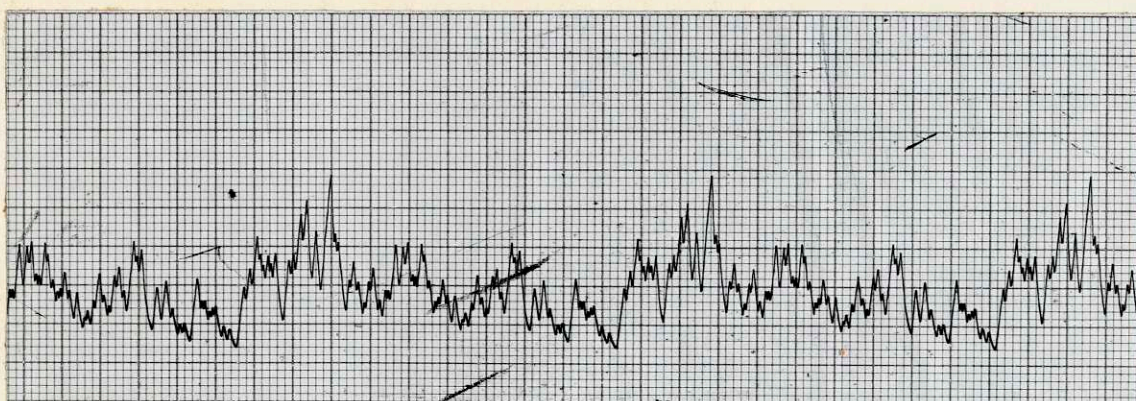
Reactivity = -5¢ ± 80¢ N_o = 15 chart lines
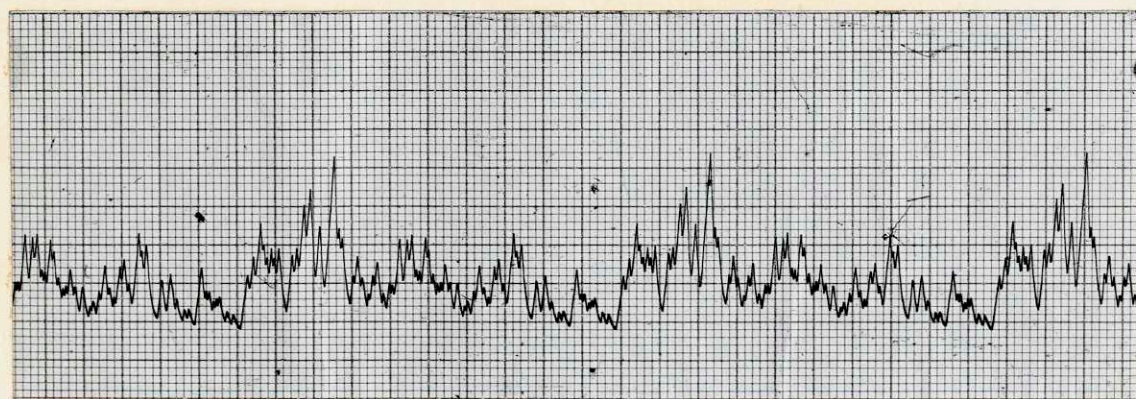
Reactivity = -16¢ ± 120¢ N_o = 10 chart lines

Time ⟶   one chart line = one second

FIGURE 6

MEASURED REACTOR IMPULSE RESPONSE

$$\beta / \ell^* = 1.0$$

INPUT $= \pm 8 \, \cancel{c}$

Theoretical
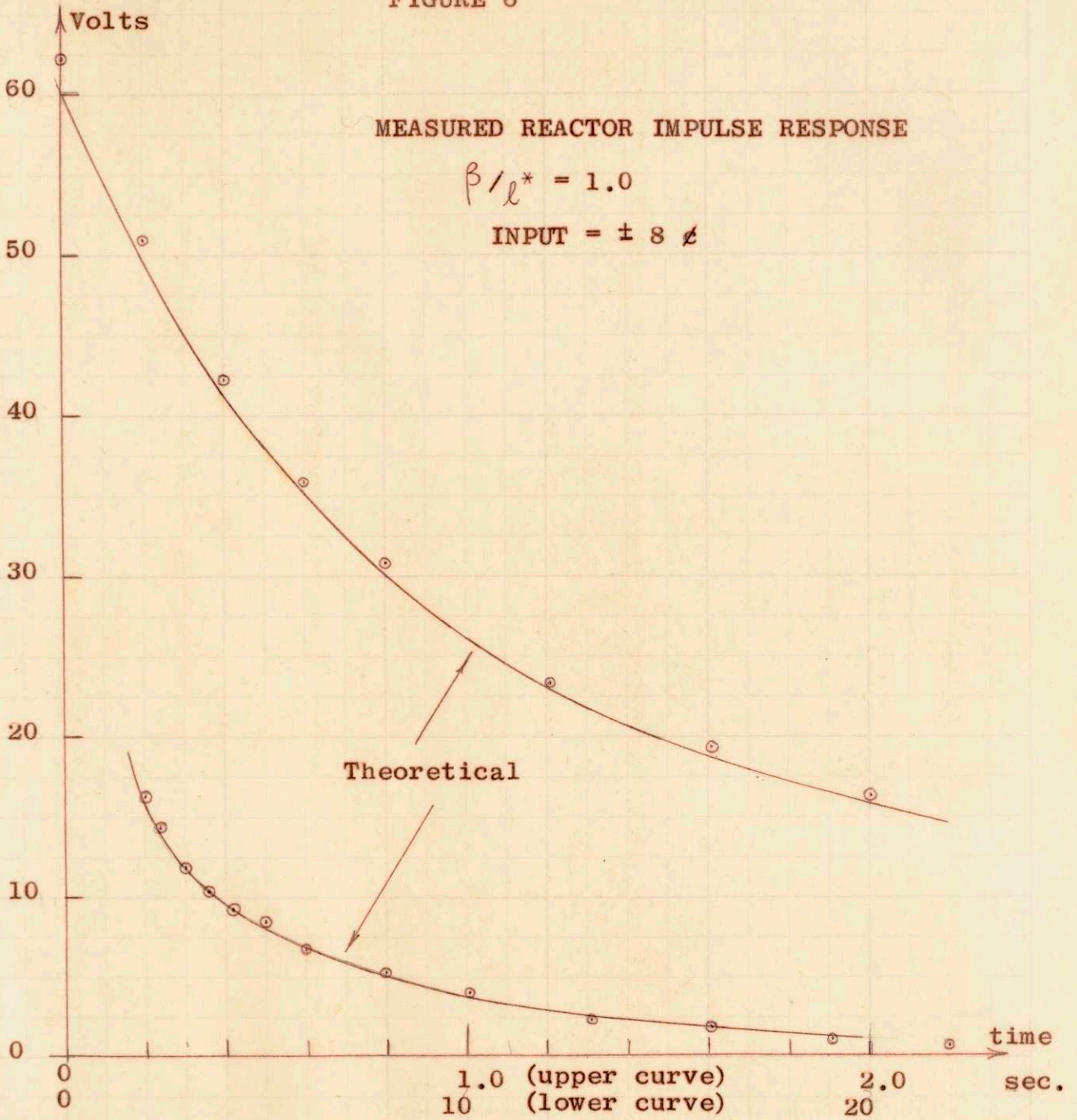
TIME	VALUE	TIME	VALUE	TIME	VALUE	TIME	VALUE
.000	62.08	2.017	16.28	8.07	5.36	30.26	.12
.202	50.48	2.420	14.34	10.09	4.04	36.31	.24
.403	42.34	3.025	12.20	13.11	2.30	40.34	-.32
.605	35.96	3.631	10.37	16.14	1.72	46.39	-.24
.807	30.81	4.236	9.24	19.16	1.05	50.63	.00
1.210	23.35	5.042	8.54	22.19	.77		
1.614	19.33	6.051	6.78	26.22	.44		

FIGURE 7

MEASURED REACTOR IMPULSE RESPONSE

$\beta/\ell^* = 1.0$

INPUT = ± 80 ¢

Theoretical
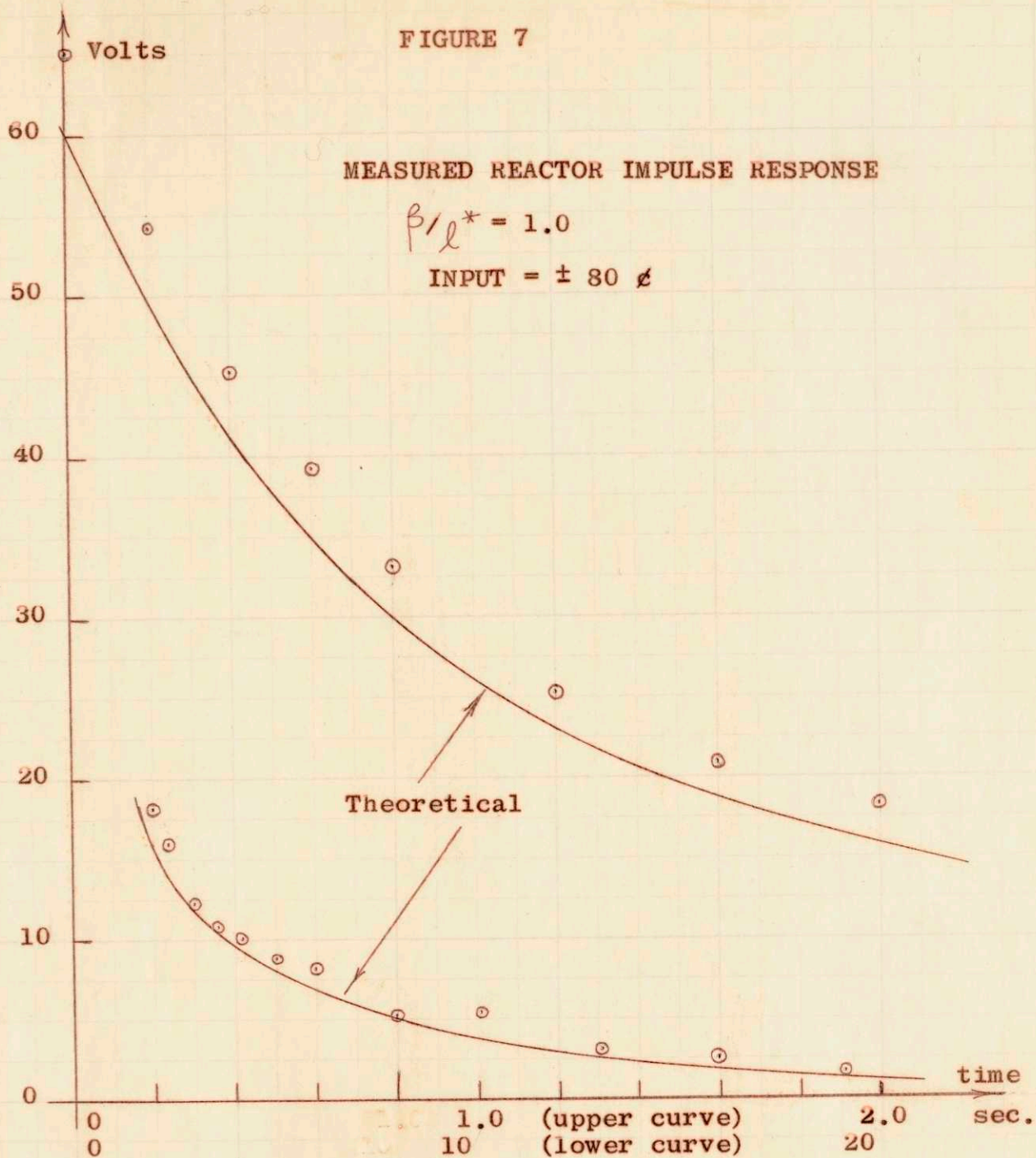
TIME	VALUE	TIME	VALUE	TIME	VALUE	TIME	VALUE
.000	65.05	2.021	18.21	8.08	5.34	30.32	.70
.202	54.18	2.425	16.03	10.10	5.43	36.38	-1.61
.404	45.14	3.031	12.36	13.13	3.10	40.42	-2.12
.606	39.40	3.638	10.83	16.17	3.00	46.48	-.06
.808	33.24	4.244	11.05	19.20	1.79	50.73	.00
1.213	25.31	5.052	8.78	22.23	1.98		
1.617	20.96	6.063	8.27	26.27	.77		

FIGURE 8

MEASURED REACTOR IMPULSE RESPONSE

$\beta / \ell^* = 1.0$

INPUT $= \pm 120$ ¢

Volts (y-axis), time sec. (x-axis)

0 ... 1.0 (upper curve) ... 2.0
0 ... 10 (lower curve) ... 20

Theoretical
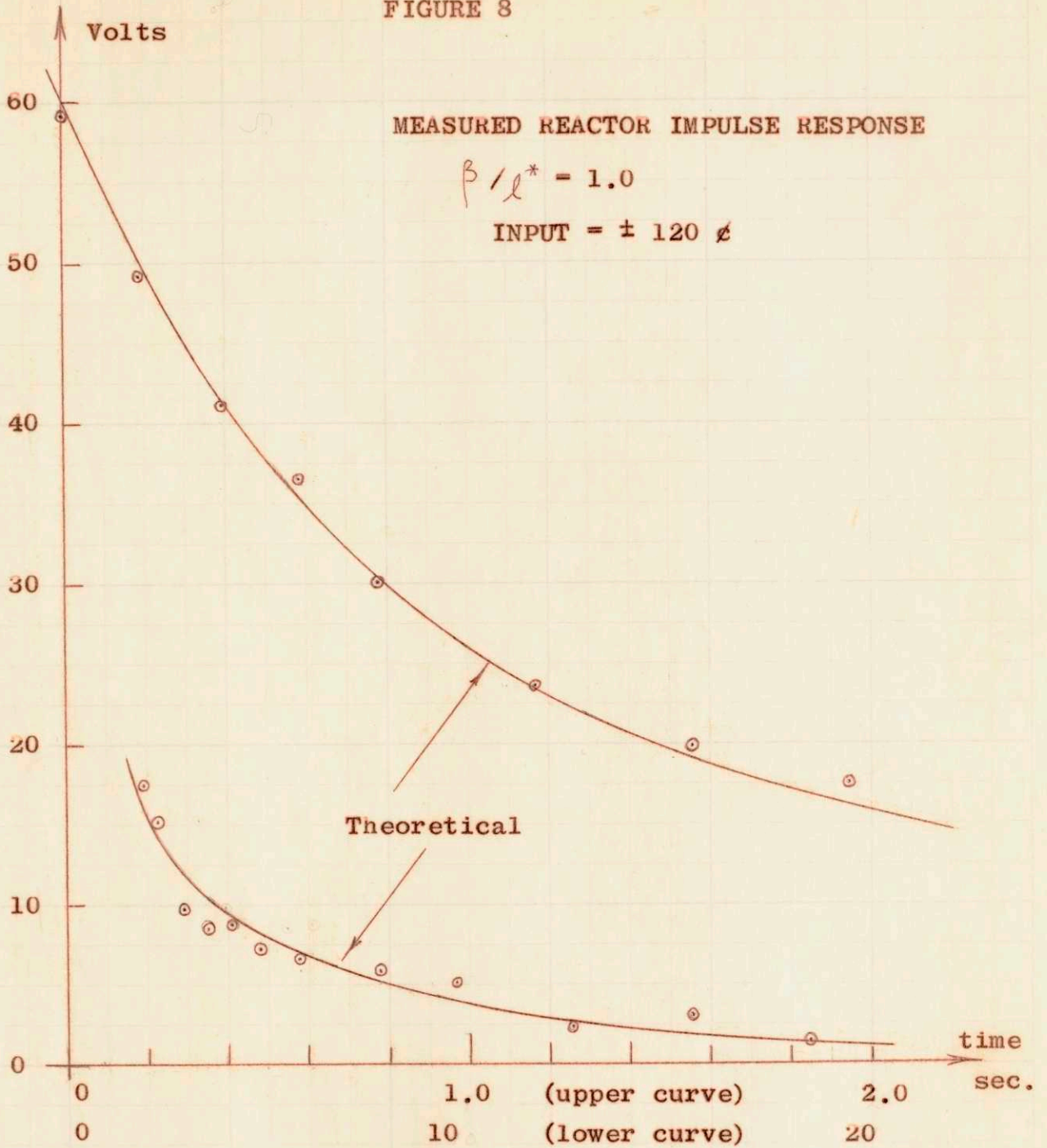
TIME	VALUE	TIME	VALUE	TIME	VALUE	TIME	VALUE
.000	59.26	1.951	17.50	7.80	5.99	29.27	1.89
.195	49.20	2.341	15.40	9.76	5.19	35.12	1.18
.390	42.18	2.926	9.95	12.68	2.49	39.02	-2.05
.585	36.57	3.512	8.58	15.61	3.08	44.87	.48
.780	30.55	4.097	8.81	18.53	1.40	48.97	.00
1.171	23.69	4.877	7.45	21.46	2.68		
1.561	19.91	5.853	6.67	25.36	.47		

B.   The Godiva Experiment

Godiva II is a bare U^{235} fast critical assembly at
Los Alamos. It is a near-cylinder 7.5" in diameter and
has a critical mass of approximately~57.7 kg. A complete
description of the reactor can be found in reference (22).

The main difficulty in performing a crosscorrelation
experiment on a reactor like Godiva is in providing an
input signal. There are two choices of input signal type,
reactivity or neutron source. A neutron source that could
be programmed to produce the idealized binary input
signal was not available, so a reactivity input system
was devised. Basically, this system consists of a
pneumatic mechanism that positions a small plastic slug
(called a rabbit) either at the reactor center or outside
the reactor. If the rabbit position corresponds to the
signal from the punched paper tape, then the desired
binary reactivity input signal is realized.

The one gram plastic rabbit used is worth + 2.4¢ of
reactivity at the reactor center due to moderation of
the fast flux. Thus the reactivity signal imposed is
± 1.2¢.

Figure 9 is a photograph of a reactor mockup with
the rabbit transfer device in place. The 5/8" stain-
less steel tube runs through the center of the reactor.
The rabbit (shown in the foreground) slides freely in
the tube; it is stopped at both ends by springs mounted
inside the tube. The springs are so positioned that the
rabbit is dead center in the reactor at one extreme and
about 1-1/2" outside the reactor at the other extreme.
The rabbit is propelled from end to end and held against
the ends by 50 psi air pressure. A servo valve controls
the direction of the air flow and thus positions the rabbit.

FIGURE 9
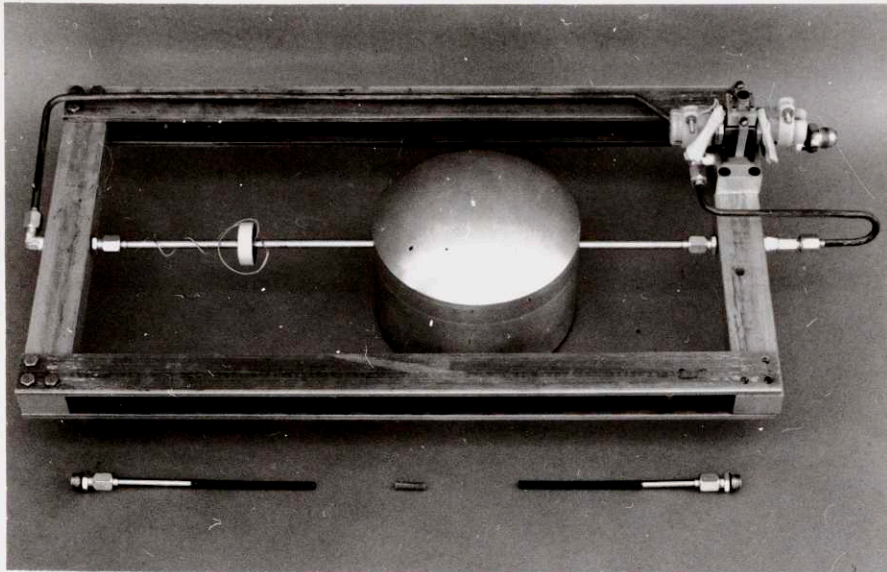
RABBIT TRANSFER DEVICE SHOWN ON A GODIVA MOCKUP

A rabbit is shown in the foreground with two extra
springs which have been removed from the transfer
tube.   The servo valve is on the upper right of
the frame.
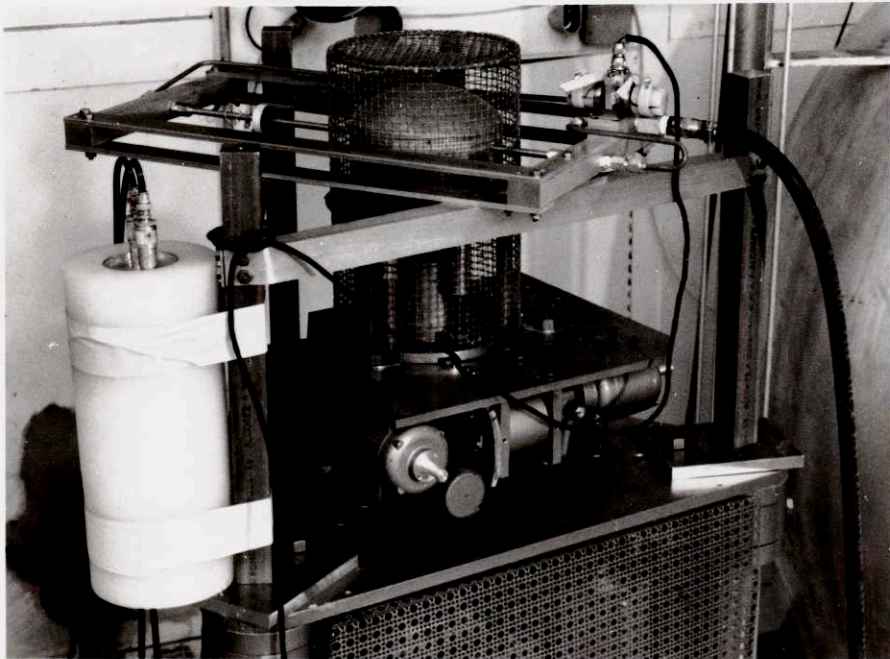
RABBIT TRANSFER DEVICE MOUNTED ON GODIVA II

The rabbit transfer device is built to be as fast as the available techniques and equipment will allow. The servo valve available requires 10 msec. to actuate. Since the valve ports are small, the time required to fill the volume of the piping is appreciable. A larger valve would have a longer actuation time. Determinations of the total time for the rabbit transfer are made with a magnetized steel rabbit in a plastic tube. A coil around the tube produces a voltage pulse as the rabbit passes by; this pulse is observed on an oscilloscope. The sequence of events after a change in sign of the binary command voltage is as follows:

$t = 0$	Change in command - outside to inside Servo valve receives voltage command
$t = 10$ msec.	Servo valve completes stroke
$t = 30$ msec.	All air passages filled up Rabbit begins to move
$t = 35 \pm 5$ msec.	Rabbit hits inside spring, oscillates about two inches and stops
$t = 50$ msec.	End of one Δt time interval
$t = 0$ (return trip)	Change in command- inside to outside
$t = 12$ msec.	Servo valve receives voltage change
$t = 22$ msec.	Servo valve completes stroke
$t = 30$ msec.	All air passages filled up Rabbit begins to move
$t = 35 \pm 5$ msec.	Rabbit stops - outside
$t = 50$ msec.	End of another Δt time interval

The asymetry of the piping requires an electrical delay on the outward trip to balance the greater pneumatic delay on the inward trip. The delay circuit is diagram No. 8 of Appendix C.

The rabbit gets to traveling about 40 feet per second just as it hits the spring and thus the springs

take quite a beating. With Δt set at 50 msec the average number of collisions at one end is 5 per second. Spring life under these conditions is about 1 to 2 hours. The rabbits, by contrast, last much longer. They are 3/4" long by 1/4" in diameter cloth-bound phenolic plastic and are very resilient.

The photograph of Figure 9 (**lower**) shows the rabbit transfer device mounted on Godiva II.

The transfer function of a cold reactor is [23]

$$\frac{\Delta n/n_o}{P/\beta} = \frac{1}{s\left[\frac{\ell^*}{\beta} + \sum_i \frac{a_i}{s+\lambda_i}\right]}$$

$$= \frac{\prod_i (s+\lambda_i)\,\beta/\ell^*}{s\prod_i (s+r_i)}$$

For Godiva, $\beta = .0064$ and $\ell^* \cong .6 \times 10^{-8}$ sec. [24] This will yield $r_1 = \beta/\ell^*$; thus the reactor has a break frequency of $\beta/2\pi\ell^* = 170{,}000$ cps. The impulse response is a high spike, which decays exponentially with a relaxation time of ℓ^*/β sec, plus a sum of very small, slow-decaying exponentials. The crosscorrelation equipment available could not be used to measure the shape of this impulse response, since the width of the response is 20,000 times narrower than Δt. The information about the delayed neutron behavior is masked by the prompt behavior. A filter was employed, in series with the reactor, to confine the impulse response to a bandwidth that could be measured by the crosscorrelator. The experimental setup is shown in Figure 10. The filter transfer function is:

$$H(\omega) = \frac{s}{(s + .058)(s + 1.063)}$$

Reactor

Transfer Tube

Plastic slug positioned by a(t) command

Ion Chamber

Micro-micro-ammeter

Filter

8μ 1M

2μ

Cross-Correlator

1M
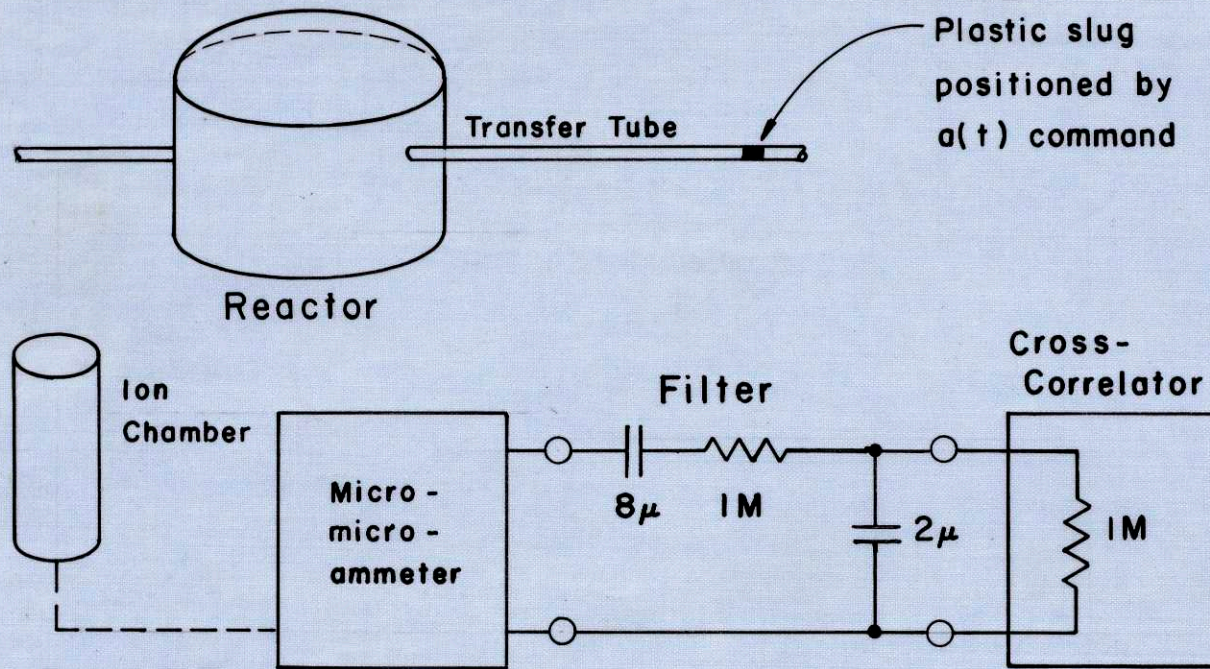
FIGURE 10

and the impulse response is

$$h(t) = 1.058 \; e^{-1.063} - .058 \; e^{-.058t}$$

If one assumes a simplified, two-group reactor with [21]

$$\lambda_1 = .334, \qquad \lambda_2 = .027$$
$$\beta_1/\beta = .656 \qquad \beta_2/\beta = .344$$

The reactor transfer function is

$$\frac{\beta/\ell^*(s + .027)(s + .334)}{(s + \beta/\ell^*)(s + .113)}$$

At frequencies of interest the β/ℓ^* terms cancel. The reactor-filter transfer function is

$$H(\omega) = \frac{(s + .027)(s + .334)}{(s + .113)(s + .058)(s + 1.063)}$$

and the corresponding impulse response is:

$$h(t) = .790 \; e^{-1.063t} + .364 \; e^{-.113t} - .154 \; e^{-.058t}$$

Experiments were carried out on four separate days. Due to difficulties with the rabbit transfer device, only one set of data is meaningful, that of 10/8/60. At this point the equipment had to be shipped to Nevada for the Kiwi experiments. Further experiments would surely have produced more meaningful results, but it was not felt later that they were warranted.

The data of the 10-8-60 experiment are shown in Figure 11 and are tabulated in Table D. Also plotted in the figure are crosscorrelation data, taken the same day, of the impulse response of the filter alone. The important conclusions to be drawn from this experiment are:

1) Meaningful data were taken in spite of the fact that the system output noise was equal to the response signal to the rabbit input.

TABLE D

GODIVA IMPULSE RESPONSE DATA - (10-8-60)

Δt = .05 Sec., N = 1019

T = 1019 $\Delta t \simeq$ 50 Sec.

Delay Sec.	Volts	Delay Sec.	Volts
.150	67.91*	4.75	3.63
.30	63.01*	5.00	.73
.45	59.23*	5.50	4.41
.60	46.69	6.00	4.21
.75	43.23	6.50	4.69
.90	37.44	7.0	2.49
1.05	38.89	11.0	-.69
1.20	33.29	12.0	.19
1.35	32.84	13.0	.49
1.50	27.56	14.0	1.52
1.65	24.26	15.00	-1.21
1,80	20.99	17.5	-1.52
1.95	20.34	20.0	.34
2.10	15.30	22.5	-2.26
2.25	11.23	25.0	2.05
2.50	7.81	27.5	-4.61
2.75	7.29	30.0	.30
3.00	10.25	32.5	3.09
3.25	6.89	35.0	-2.64
3.50	6.65	37.5	-3.13
3.75	5.39	40.0	.72
4.00	5.07	42.5	-1.74
4.25	-6.54	52.45	0
4.50	-4.30		

OBSERVED $\sigma \simeq$ 2.6 VOLTS

*AVERAGE OF TWO READINGS

Theoretical response of the reactor - filter system

Theoretical response of the filter alone

● **Measured response of the reactor - filter system**

○ **Measured response of the filter alone**

h(t), normalized

Time, seconds

0.1   0.2   0.4   0.6   0.8   1.0   2   4   6   8   10   20   40   50   60

84
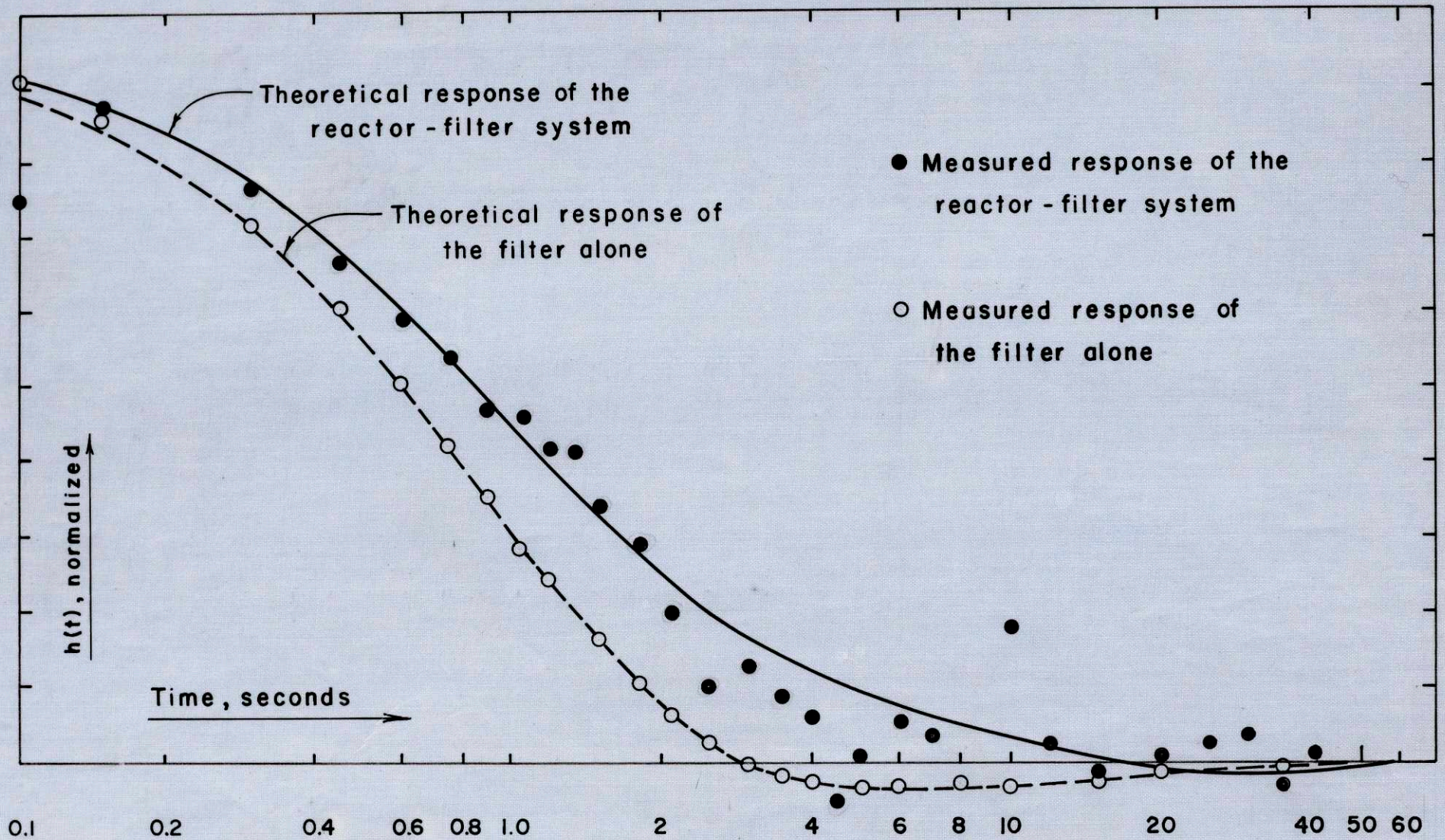
FIGURE II

2)   The data obviously indicate the presence of
the reactor. The theoretical impulse response
of the reactor-filter is a possible fit to the
data; the theoretical filter response alone is
not.

3)   The signal-to-noise ratio in the data is less
than is theoretically predicted. Since the
settling time is the same as the crosscorrela-
tion time, M is equal to unity, and there is
no improvement in signal-to-noise ratio expec-
ted. The signal-to-noise at the system output
is about unity. The observed signal-to-noise
at the crosscorrelator output is 0.41. (See
equation (II-21) Therefore, a decrease in
signal-to-noise ratio is observed. Also,
the noise seems to increase with τ; this is not
predicted theoretically. Perhaps this indicates
that there was some malfunction in the equip-
ment, possibly in the rabbit system.

Data of the quality of Figure 11 cannot be used to
deduce much about the reactor dynamics. A reactor-
filter system transfer function was calculated from this
data and is shown in Figure 12 along with the theoretical
transfer function.

C.   The Kiwi-A3 Experiments

The Kiwi-A reactors are a series of non-flying proto-
types of rocket engines which utilize fission to produce
heat. Hydrogen gas, flowing through the core under pres-
sure, is heated to a high temperature and released through
a sonic nozzle to produce thrust. Kiwi-A3, the third
reactor of this series, was successfully tested at the
Nevada Test Site on October 19, 1960. All three reactors
were built and tested by the Los Alamos Scientific

FIGURE 12

GODIVA – FILTER

MEASURED TRANSFER FUNCTION

MAGNITUDE

decibels

0

.001   .01   0,1   1.0   10

frequency, cycles/ second

−10

Theoretical

−20

FIGURE 12

GODIVA – FILTER

MEASURED TRANSFER FUNCTION

PHASE

frequency, cycles/second

Theoretical

.001   ,01   0.1   1.0   10

0
−20
−60
−100
−140
−180
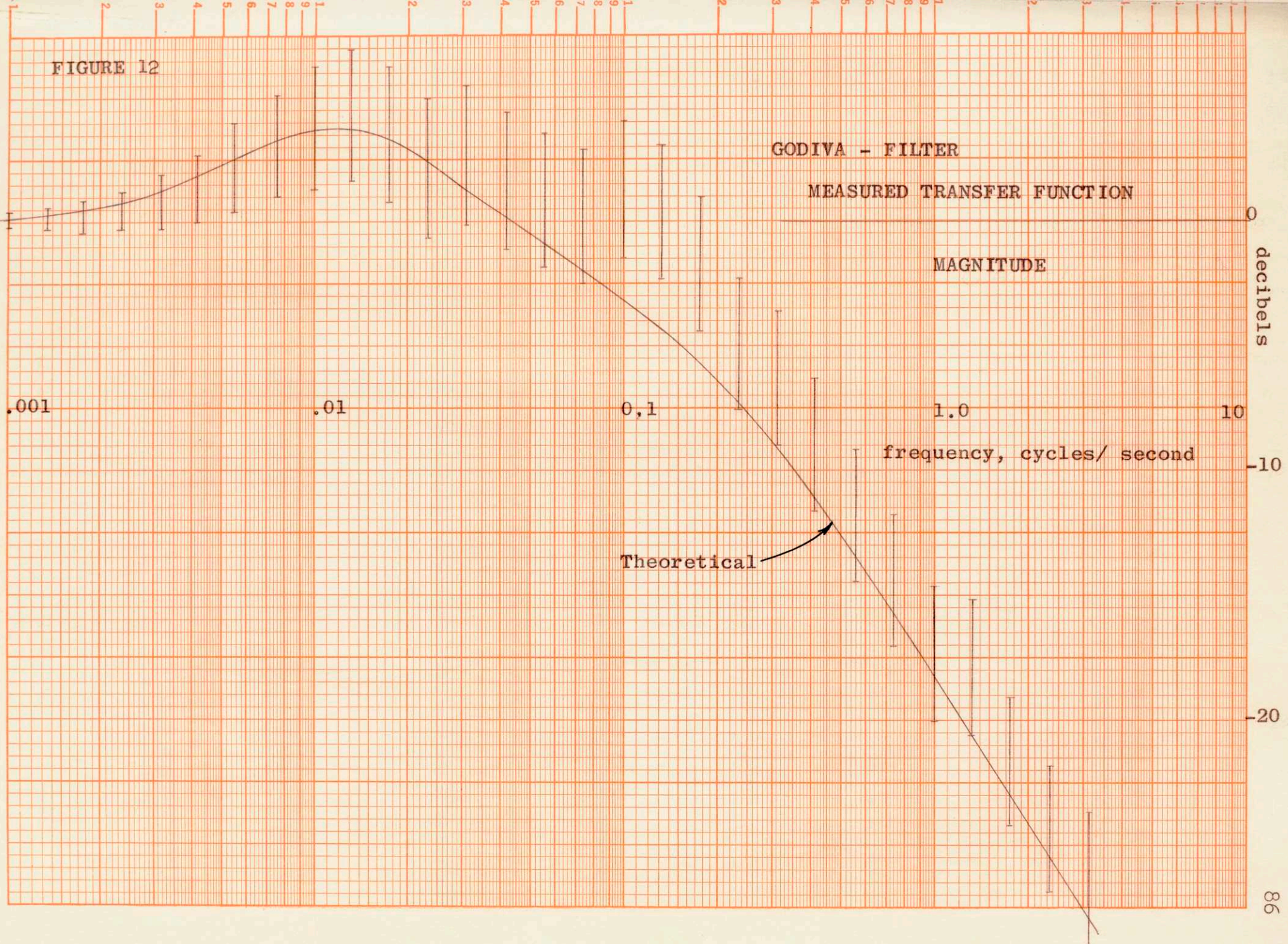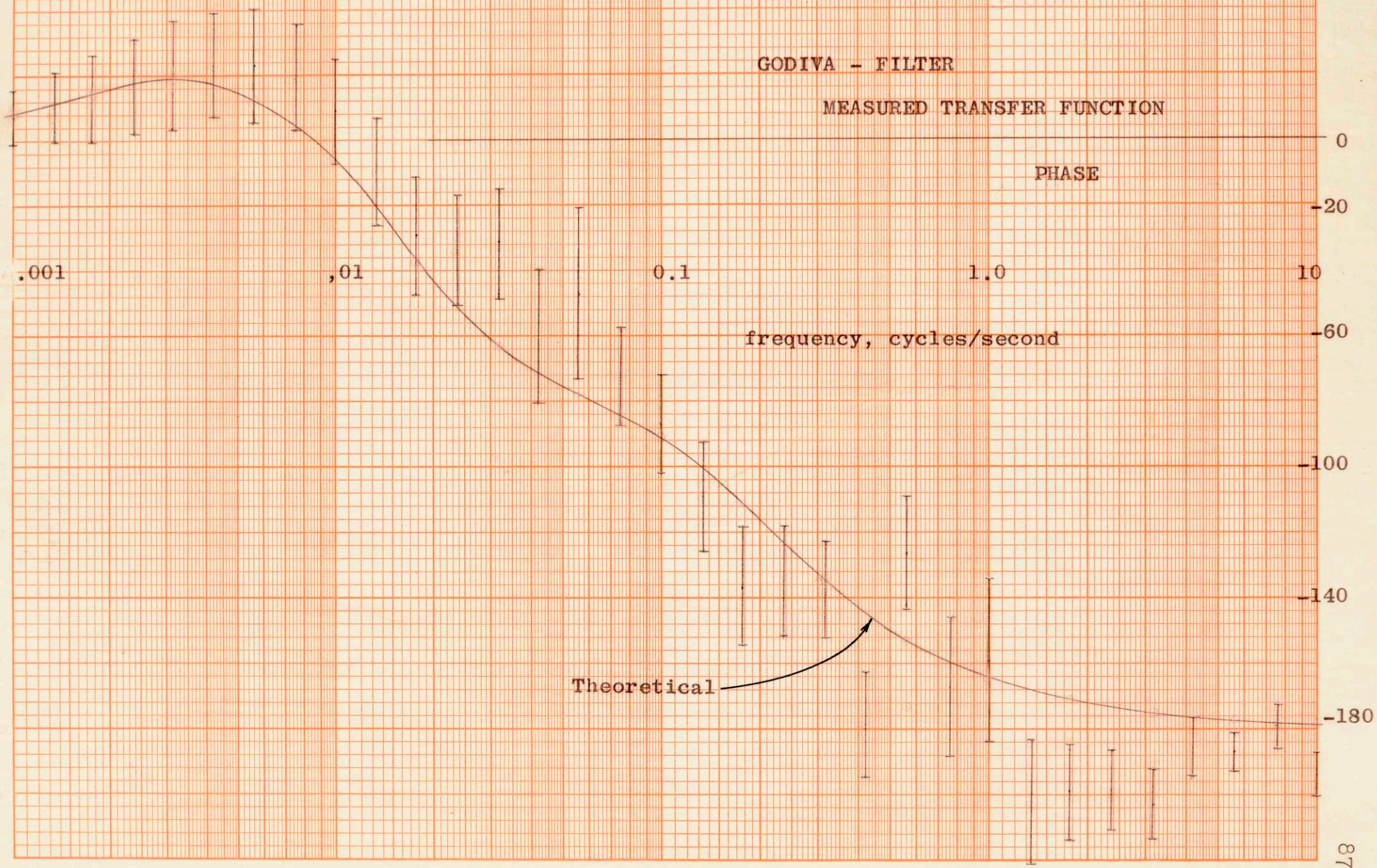
Laboratory.

The operating characteristics of these reactors are:

1) They operate at high temperature and very high power density. The core material is enriched uranium in a graphite matrix.

2) They are unshielded; control operations are two miles from the reactor.

3) The power control system is a closed loop. The reactor is brought up to power on a program and held at constant power for the test.

4) They are operated at full power for a short time, of the order of minutes, and only once.

5) Perturbations of the power for diagnostic purposes may not exceed about ± 2% of the power level. The noise content of the measured reactor power (ionization chamber) is about ± $\frac{1}{2}$%.

It was desired to measure the performance of the control system at full power. The last two operating conditions listed preclude the normal methods of measuring system dynamics. Condition 5 rules out step response techniques. Condition 4 rules out methods utilizing sinusoidal inputs. The crosscorrelation method remains as the only technique which seems feasible. Confidence that the method would work was obtained from experiments on an analog computer simulation of Kiwi-A3 and from the experiments on Godiva.

1. Low Power Experiment

As a prelude to the full power experiment, an experiment was performed at low power (10 kw) with the reactor operating open loop, with no power feedback signal. The purposes of this experiment were to give the equipment a trial run, to check that the neutronics

instrumentation was performing properly, and to obtain a value for the reactor mean neutron lifetime.

The idealized binary signal was supplied as a position command to a control rod servo system. With the command input to this control rod servo set at ± 7¢ reactivity, the combined impulse response of the rod servo-reactor-instrumentation system was measured. It was during this experiment that the post-mortem method (see Chapter III-E) was first tried. Data taken on-line agree with the data taken post-mortem. The impulse response is shown plotted in Figure 13 and the corresponding transfer function is Figure 14. Table E lists the impulse response data of Figures 13 and 15. The errors shown in the transfer function are due to the indeterminacy of the curve through the measured points on the impulse response; the errors in the points themselves are negligible.

In order to make a correction for the rod servo dynamics, its impulse response was measured alone, using the crosscorrelation method. The impulse response is shown plotted in Figure 15 and the transfer function in Figure 16.

The transfer function of the reactor alone can be calculated from the equation

$$\text{Reactor Transfer Function} = \frac{\text{Rod Servo-Reactor-Instrumentation Transfer Function}}{\text{Rod Servo Transfer Function}}$$

since the instrumentation transfer function was equal to unity over the range of interest. The calculated reactor transfer function is shown plotted in Figure 17. For frequencies greater than 0.5 cps, the theoretical transfer function is basically:

$$\frac{\Delta n}{\Delta \rho} = \frac{\beta/\ell^*}{s + \beta/\ell^*}$$

MEASURED IMPULSE RESPONSE OF THE
ROD SERVO, KIWI A3 REACTOR, and
INSTRUMENTATION ALL IN SERIES

$\Delta t = 0.02$ sec.

$N = 251$

$P = 3T = 753\Delta t \cong 15$ sec.

Time , seconds

FIGURE 13

MEASURED IMPULSE RESPONSE OF THE
ROD SERVO
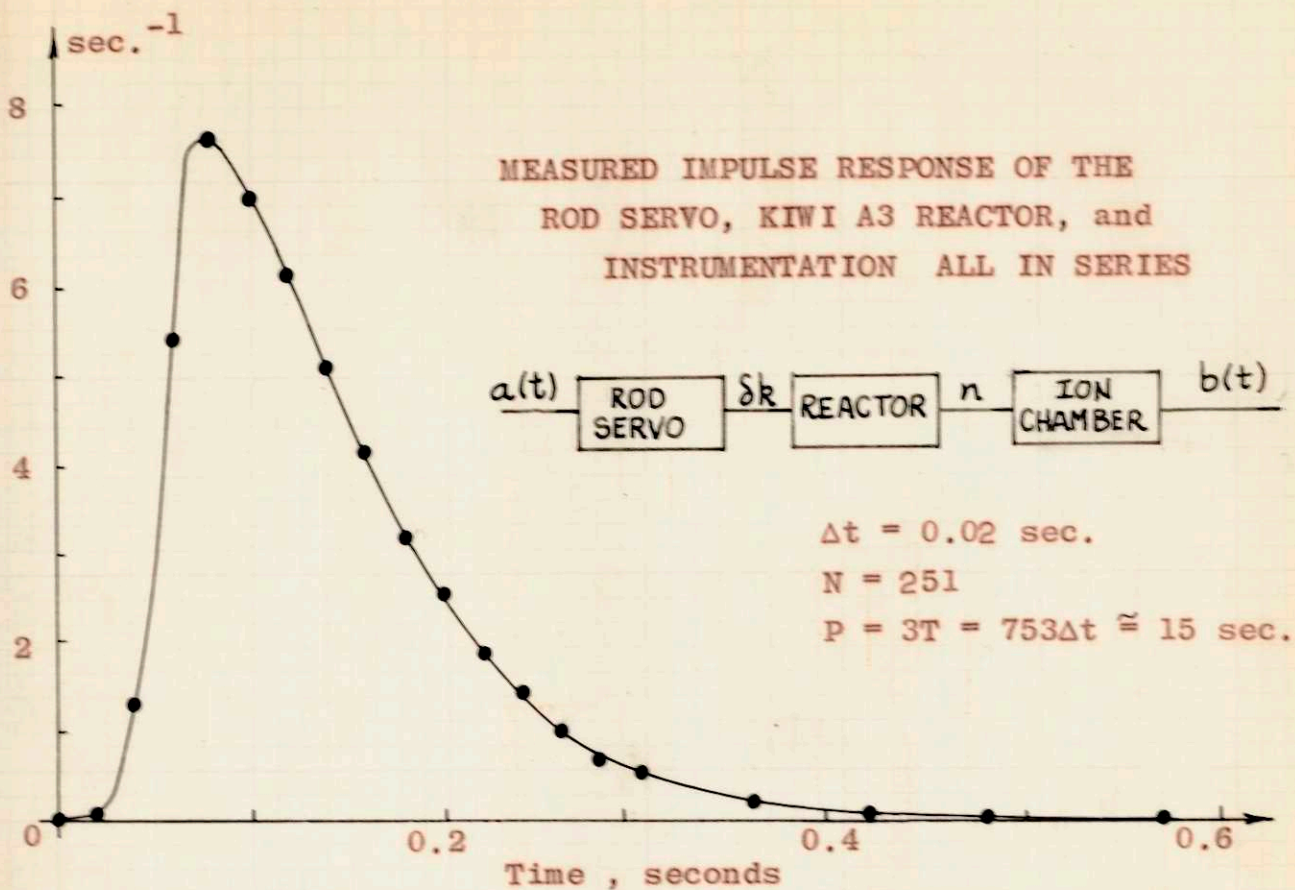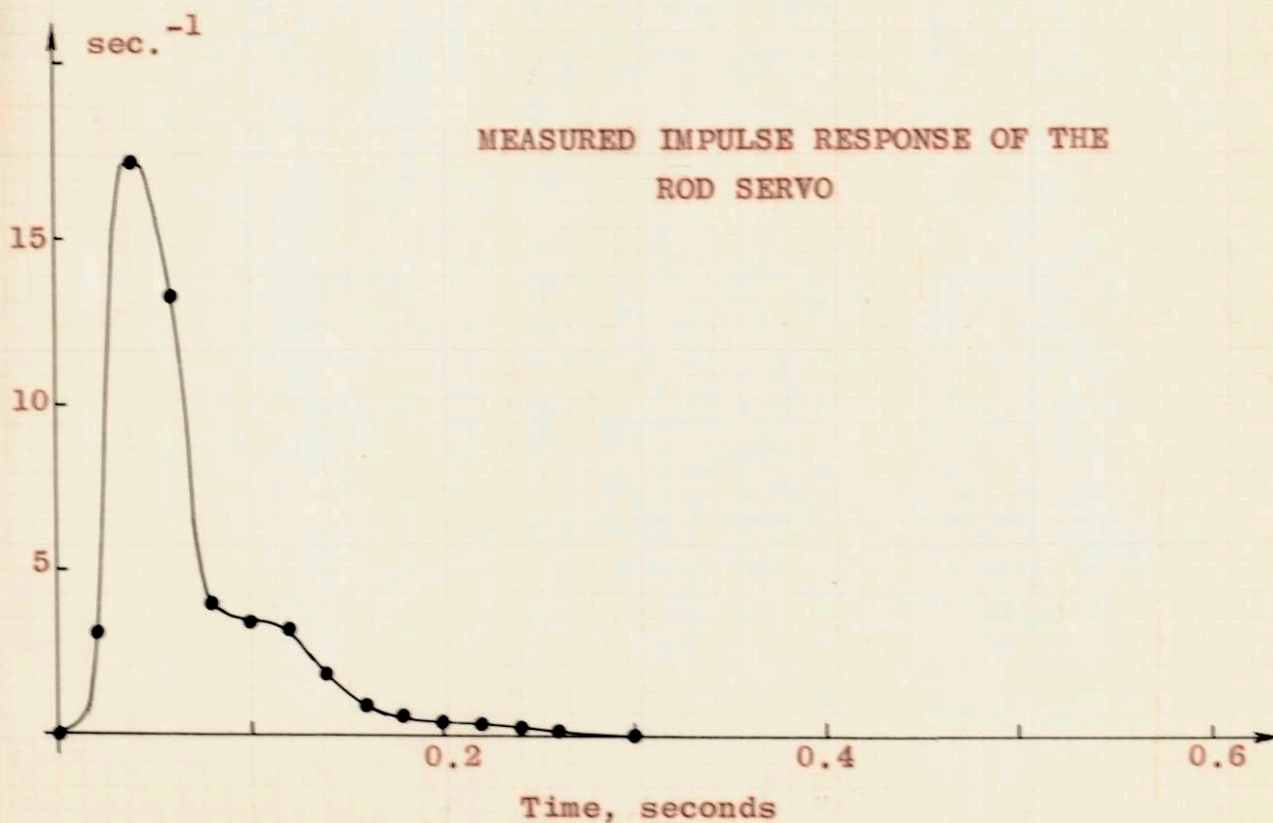
Time, seconds

FIGURE 15

TABLE E
IMPULSE RESPONSE DATA

KIWI-A3
+
ROD SERVO
+

TIME Seconds	INSTRUMENTATION Volts	ROD SERVO Volts
0.020	0.700	5.200
0.040	15.200	29.900
0.060	74.600	22.900
0.080	88.300	6.800
0.100	80.500	5.800
0.120	70.500	5.400
0.140	58.800	3.200
0.160	47.600	1.600
0.180	36.300	1.000
0.200	29.100	0.600
0.220	21.200	0.500
0.240	16.600	0.400
0.260	11.500	
0.280	7.900	
0.300	6.100	0.000
0.360	2.400	
0.420	0.900	
0.480	0.400	

NORMALIZATION CONSTANT

Kiwi-A3 + Rod Servo + Instrumentation = 11.6 volt-sec
Rod Servo = 1.728 volt-sec

TRANSFER FUNCTION
of the

ROD SERVO
KIWI A3 REACTOR (10 kw.)
INSTRUMENTATION

ALL IN SERIES

MAGNITUDE

FIGURE 14

PHASE

ROD SERVO
TRANSFER FUNCTION

MAGNITUDE

FIGURE 16

PHASE

TRANSFER FUNCTION
of the
KIWI A3 REACTOR AT 10 kw.

MAGNITUDE

$$\frac{17.6}{s + 17.6}$$

FIGURE 17

PHASE

$$\frac{17.6}{s + 17.6}$$
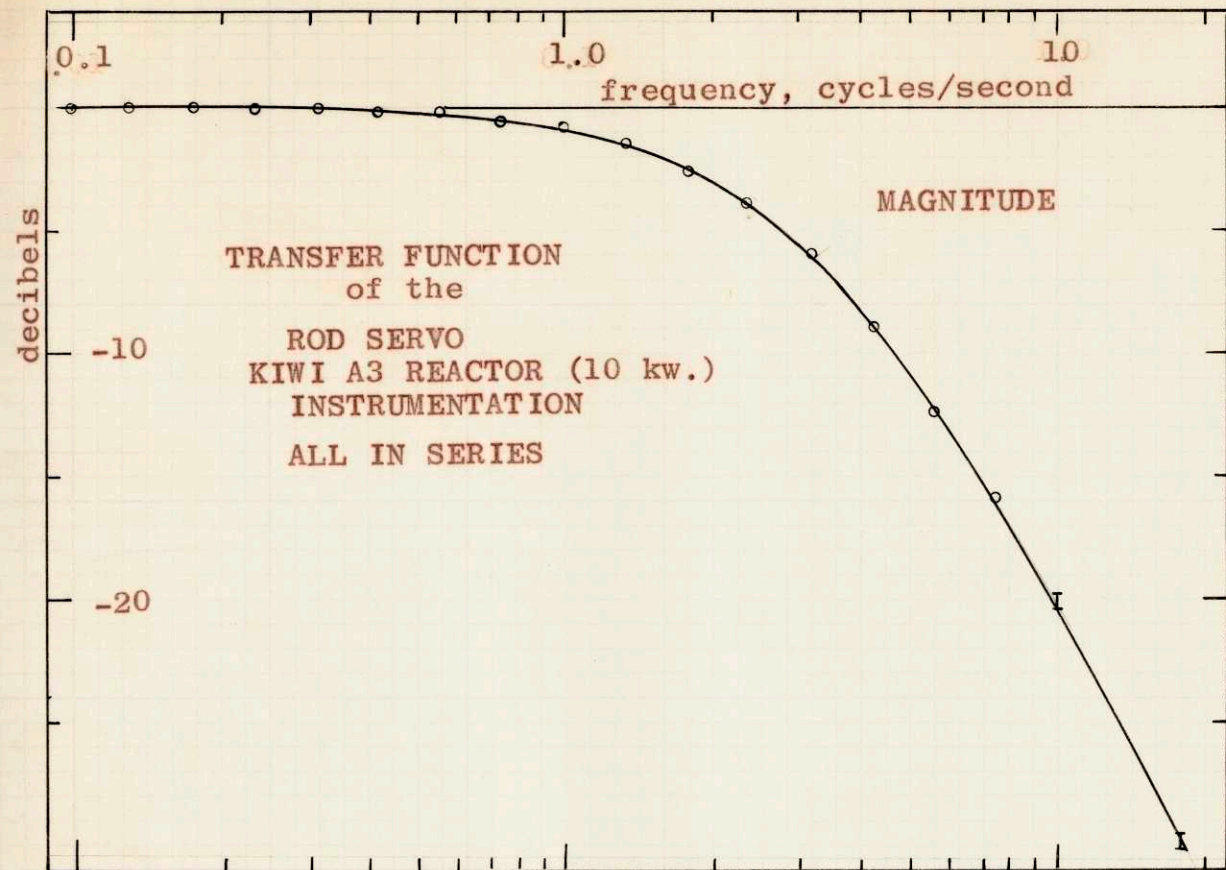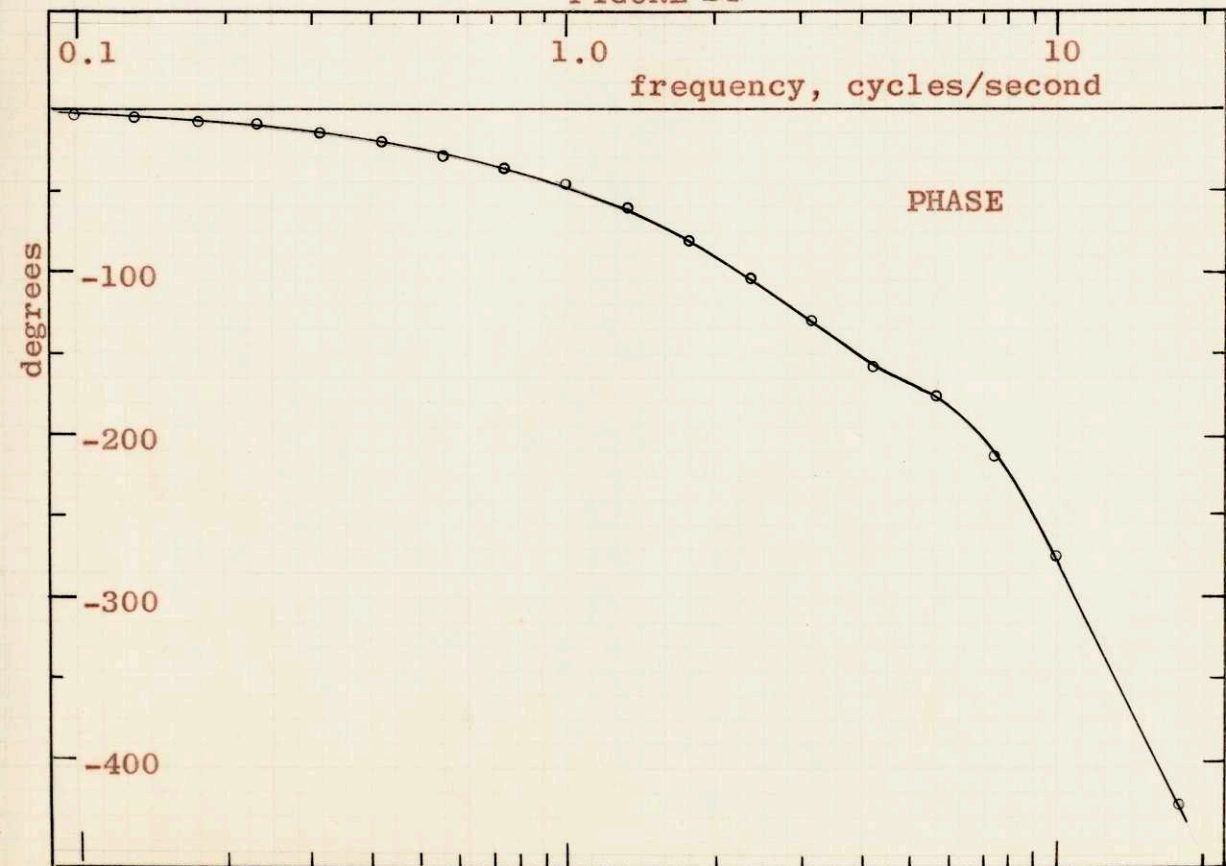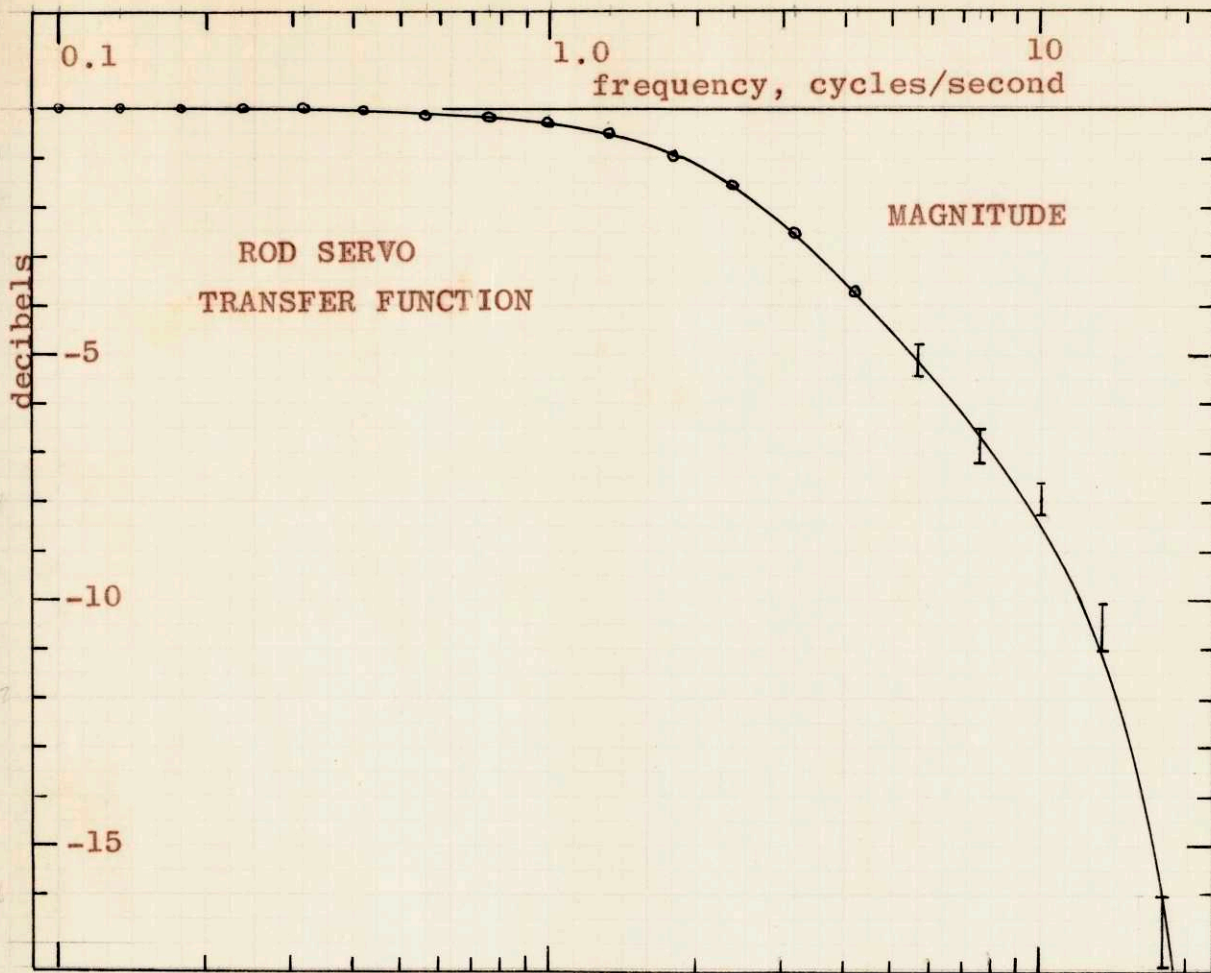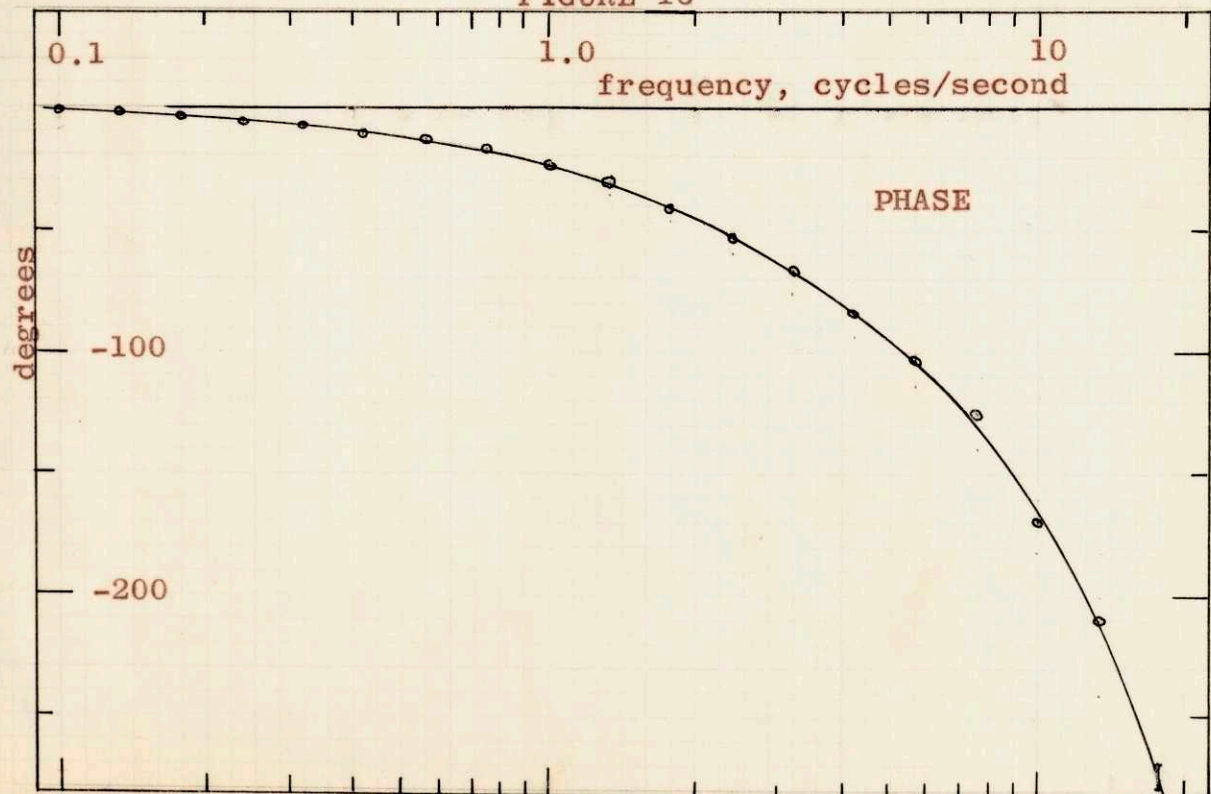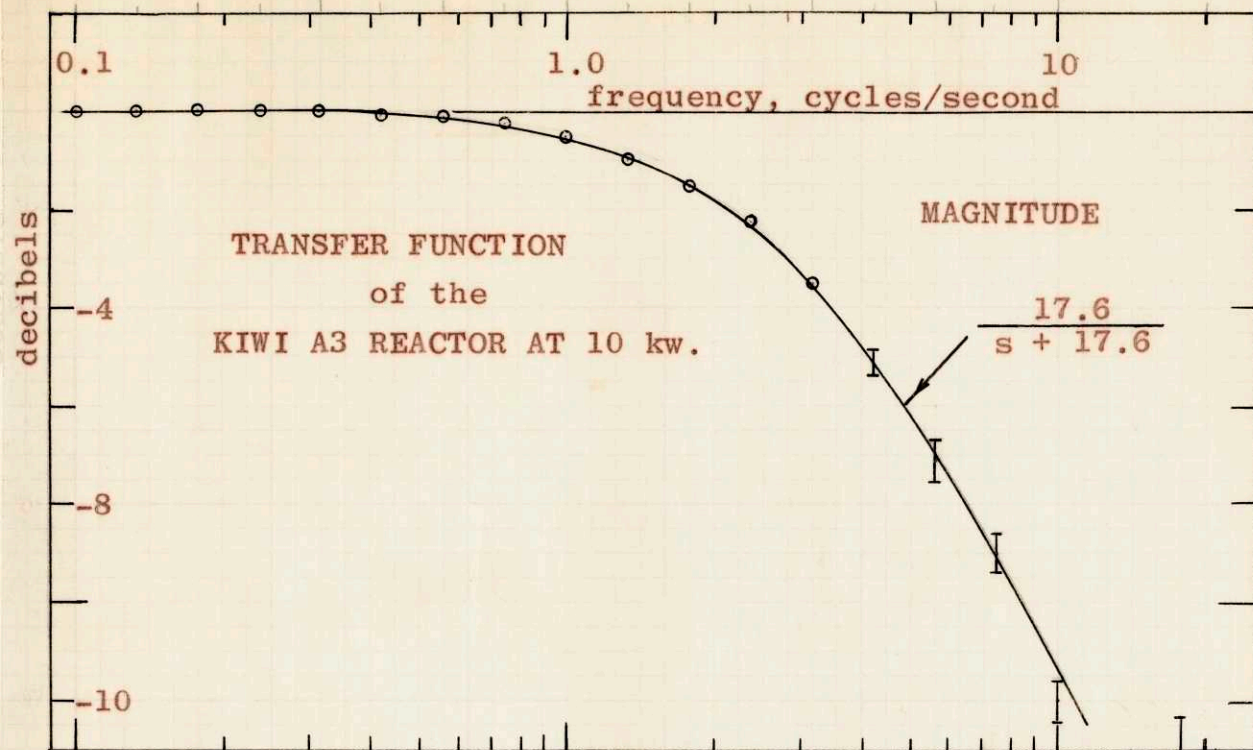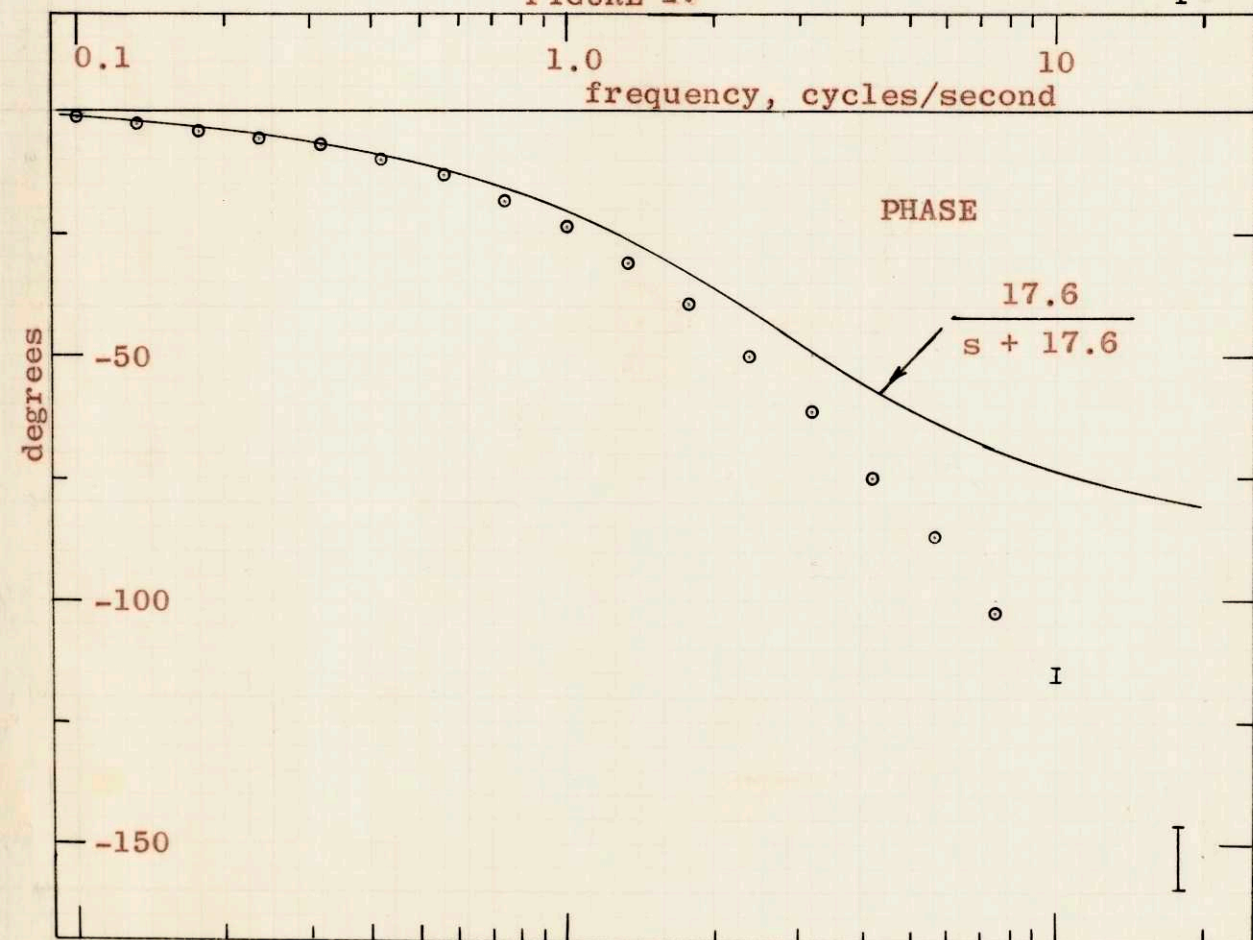
The magnitude curve of Figure 17 gives a very close fit
to this form where

$$\beta/\ell^* = 17.6 \pm 1.0 \ \frac{radian}{second} = (2.8 \pm .16 \ cps)$$

Thus

$$\ell^* = (3.63 \pm .21) \times 10^{-4} \ sec.$$

The phase curve indicates more phase lag than the theory
predicts. If the point at which the phase is equal to
$-45°$ is chosen as a break frequency, then the value
obtained for the mean neutron lifetime is

$$\ell^* = 4.9 \times 10^{-4} \ sec.$$

However, it is apparent that some unknown system delay
is contributing an additional phase lag ($12°$ at 2.8 cps).
It is simply not consistent to use this measured phase
for a measure of neutron lifetime since it does not fit
the theoretical form. Neither is it proper to quote the
error in the ℓ^* measurement derived from the fit to the
magnitude curve. A compromise is to quote the value of
ℓ^* from the magnitude curve fit but assign to it a higher
error:

$$\ell^* = (3.6 \pm .7) \times 10^{-4} \ sec.$$

The weakest link in the chain of measurements is that of
the rod servo system. Due to operating procedures, this
impulse response measurement was made several days before
the reactor system measurements were made. It has been
stated by the designers that the rod servo system
characteristics could change by the amount of the phase
discrepancy over a period of hours.

An ℓ^* measurement made on the Kiwi-A reactor, which
was of similar neutronic design, gave: $\ell^* = 2 \times 10^{-4}$ sec.

An oscillator-rod transfer function measurement at low power was also performed on Kiwi-A3. From the last three measured points there is obtained:

$$\ell^* = (3 \pm 1) \times 10^{-4} \text{ sec.}$$

The value obtained by the crosscorrelation method seems reasonable in light of these other measurements.

2.   High Power Experiments

A block diagram of the Kiwi-A3 power control system is shown schematically in Figure 18.[*]
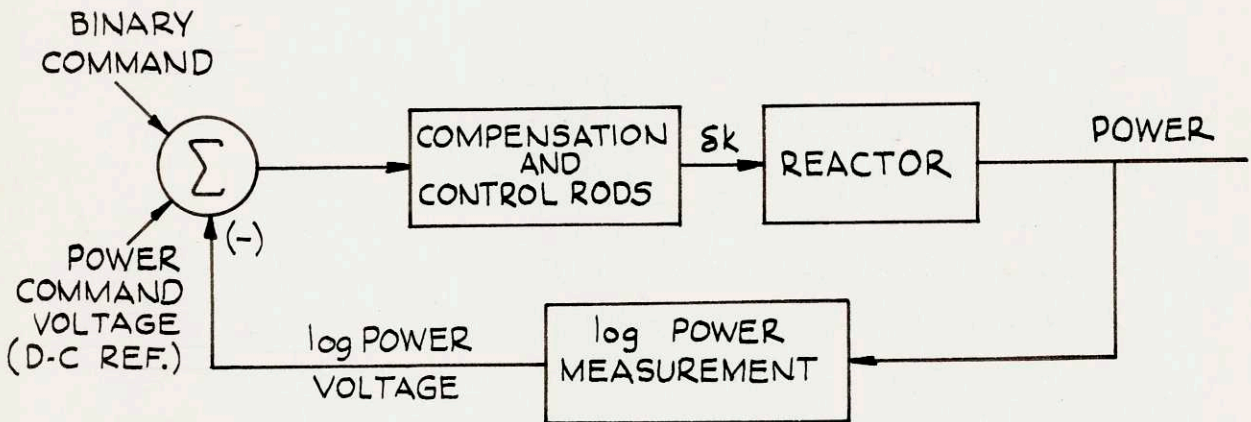
FIGURE 18

The purpose of the high power crosscorrelation experiment was to measure the dynamics of this control loop during actual test at full power.

The log power control system worked very well. The usual problem in reactor control, the fact that the reactor gain is proportional to power level, is just compensated by the log power measuring system, in which the gain is inversely proportional to power level. Thus, the system

[*]For a description of the control systems of the Kiwi reactors, see reference (25)

dynamics are independent of power. In addition, a four-decade operating range is feasible. The log power measuring system consists basically of an ionization chamber and a hot diode. The voltage-current relationship for a diode is logarithmic for small currents.

The crosscorrelation experiment was carried out with an input of $\pm$ .0162 volts introduced as a log power demand. The scaling of log power is set at 1.88 volts per decade. If $V = 1.88 \log_{10} P$, then

$$\frac{dP}{P} = \frac{dV}{1.88 \log_{10} e} = 1.23 \ dV$$

where P is the power and dV is a small voltage change. Thus for a demanded binary input of $\pm$ .0162 volts the demanded power change is $\pm$ 2%. With Δt set at .02 sec, the control system could not follow the binary input exactly; the observed power fluctuations were about $\pm$ 1%.

The impulse response measured is that of the closed loop power control system. The log power measuring system, for small variations, has a constant gain. Therefore, the closed loop impulse response of log power to log power demand can be found by measuring the closed loop impulse response of linear power to log power demand and then normalizing the curve to have an area of unity. It was desired to use the measured linear power as the system response signal instead of the measured log power since the noise in the linear signal was appreciably less.

It was necessary to subtract the steady-state power level from the measured linear power level signal and then amplify the difference to obtain the signal, c(t) which was actually used for crosscorrelation. (See Figure 1, Chapter II) The steady-state power level signal is

obtained from a simple battery-supplied voltage-divider
that can be manually adjusted to obtain a zero-mean signal
for c(t). The amplifier gain needed is fairly high (160
at full power).

The data which are to be presented were taken under
the following conditions:

$$N = 251$$
$$\Delta t = .02 \text{ sec}$$
$$P = 3 \text{ cycles} = 753 \, \Delta t \cong 15 \text{ sec.}$$

During the startup, the program held for about
one minute at "half power".[*] Throughout this period,
the binary input signal was on, the signals were being
recorded, and crosscorrelations were being calculated.
The noise in the linear power signal was observed to
be approximately $\pm 1\%$. This is equal in magnitude to
the system response to the binary input. The data,
taken with the post-mortem technique from the recorded
signals, are given in Table F and in Figure 19.

The errors are observed to be fairly large; analysis
reveals that the standard deviation is $\pm .41 \text{ sec}^{-1}$ for
a single measurement. Many of the values in the table,
particularly of the first points, are averages of as
many as five readings and hence have a smaller standard
deviation. In order to calculate the observed improvement
factor, as defined in Chapter II-D, it is necessary to
relate the observed facts:

a)   The rms noise in the c(t) signal is approxi-
     mately equal to the rms response to the binary
     input signal.

$$\left(S/N \right)_c \cong 1.0$$

[*] More nearly 0.7 of full power

TABLE F

IMPULSE RESPONSE DATA
of the
KIWI A-3 POWER RUNS

TIME Seconds	FULL POWER	HALF POWER	TIME Seconds	FULL POWER	HALF POWER
.020	0.4	−4.2	.580	11.3	16.9
.040	10.6	13.2	.600		12.3
.060	25.9	40.9	.640	10.8	
.080	35.4	61.1	.680		14.2
.100	40.2	61.6	.700	11.1	
.120	43.6	54.3	.740	8.4	9.6
.140	42.1	49.5	.760	7.1	
.160	40.1	45.6	.780	7.9	10.2
.180	37.6	39.2	.800		5.0
.200	31.6	27.9	.840	11.3	
.220	27.0	19.2	.860	7.7	11.7
.240	25.6	14.9	.880		9.1
.260	21.6	18.3	.940	1.7	8.6
.280	17.1	18.3	.960	0.8	
.300	15.8	13.8	1.000		−0.1
.320	9.6	9.0	1.040	3.4	
.340	10.6	11.0	1.060	6.6	6.3
.360		16.4	1.080		−0.8
.380	9.9	19.4	1.100		−3.2
.400	11.1	16.0	1.180		−2.1
.420	9.0	14.9	1.240	−0.0	4.4
.440	11.8	18.5	1.260	−0.2	
.460	13.1	21.2	1.300		−4.0
.480	13.5	20.0	1.340	−0.5	
.500		16.1	1.360		−0.8
.520		14.4	1.420		0.0
.540	13.3	16.9	1.560	0.0	
.560	11.1				

NORMALIZATION CONSTANTS

Full Power   15.37   volt-seconds

Half Power   17.88   volt-seconds

MEASURED IMPULSE RESPONSE
of
KIWI A3 at FULL POWER

FIGURE 20

Note: The curve is just for help
in visualisation; the transfer
function was calculated from
the data points.

100
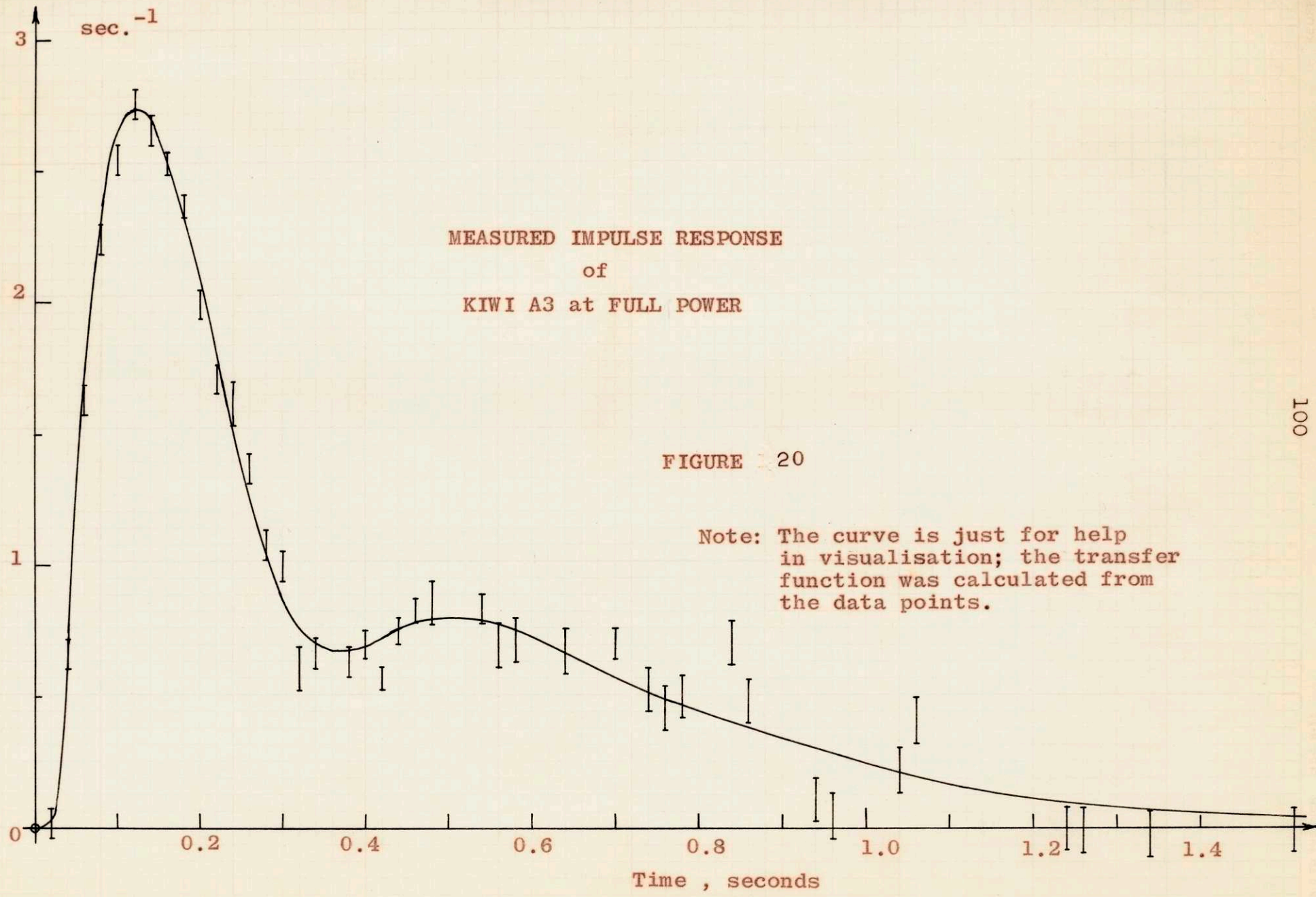
b)   The observed, normalized rms value of the
crosscorrelation function is $.412 \ sec^{-1}$.

$$(S/N)_\phi \quad \frac{\sqrt{\frac{1}{L}\int_0^L h^2(t)dt}}{\sqrt{\overline{x^2(\tau)}}} = \frac{\sqrt{\frac{1}{1.4}}\ (1.685)}{.412} = 2.7$$

The value for the system settling time, L, is taken to
be 1.4 seconds. The crosscorrelation time is 15 seconds.
Therefore M = 15/1.4 = 10.7. The expected improvement
factor is IF $\geq \sqrt{M}$ = 3.3. The observed improvement factor
is approximately 2.7, in very good agreement.

Following the "half power" hold, the program
continued to full power. Data obtained (again post-
mortem) are tabulated in Table F and plotted in
Figure 20. The errors in the data are much smaller
than at "half power" because the relative noise in the
reactor power was much less.

Closed loop transfer functions derived from the
impulse response data of Table F are plotted in Figures
21 and 22.

If a closed loop system has a transfer function
$H(\omega)$, then the open loop transfer function is given by
$G(\omega) = H(\omega)/(1 - H(\omega))$. This function has been calcula-
ted from the transfer functions of Figures 21 and 22, and
the results are plotted together in Figure 23. These
are the projected open loop transfer functions at "half"
and full power. The only difference that one would
expect to find between the two open loop transfer func-
tions is a change in gain corresponding to a change in
differential control rod worth. The control rod system
is constructed so as to command a control rod displace-
ment proportional to the compensated error voltage.
Hence, the reactivity change produced by an error voltage

MEASURED IMPULSE RESPONSE
of
KIWI A3 at HALF POWER

FIGURE 19

Note: The curve is just for help in
visualisation; the transfer
function was calculated from
the data points.

102

TRANSFER FUNCTION
OF KIWI A3 AT FULL POWER

FIGURE 21

frequency , cycles / second

MAGNITUDE

TRANSFER FUNCTION
OF KIWI A3 AT HALF POWER

FIGURE 22

frequency, cycles/second

PHASE

FIGURE 23

OPEN LOOP TRANSFER FUNCTIONS
of the
KIWI A3 POWER LOOP

(deduced from closed loop data)

● FULL POWER

○ HALF POWER

decibels

frequency, cycles/second
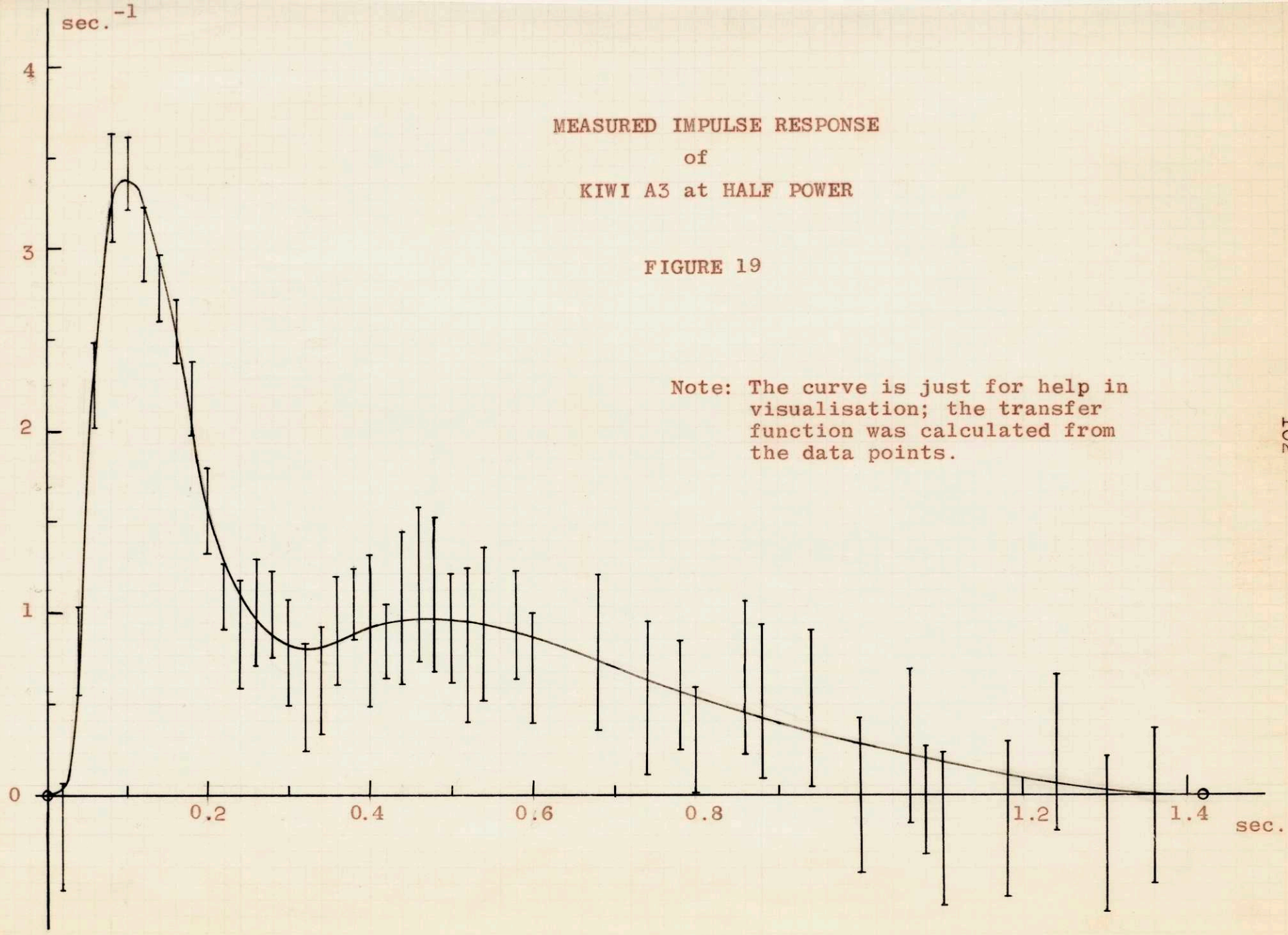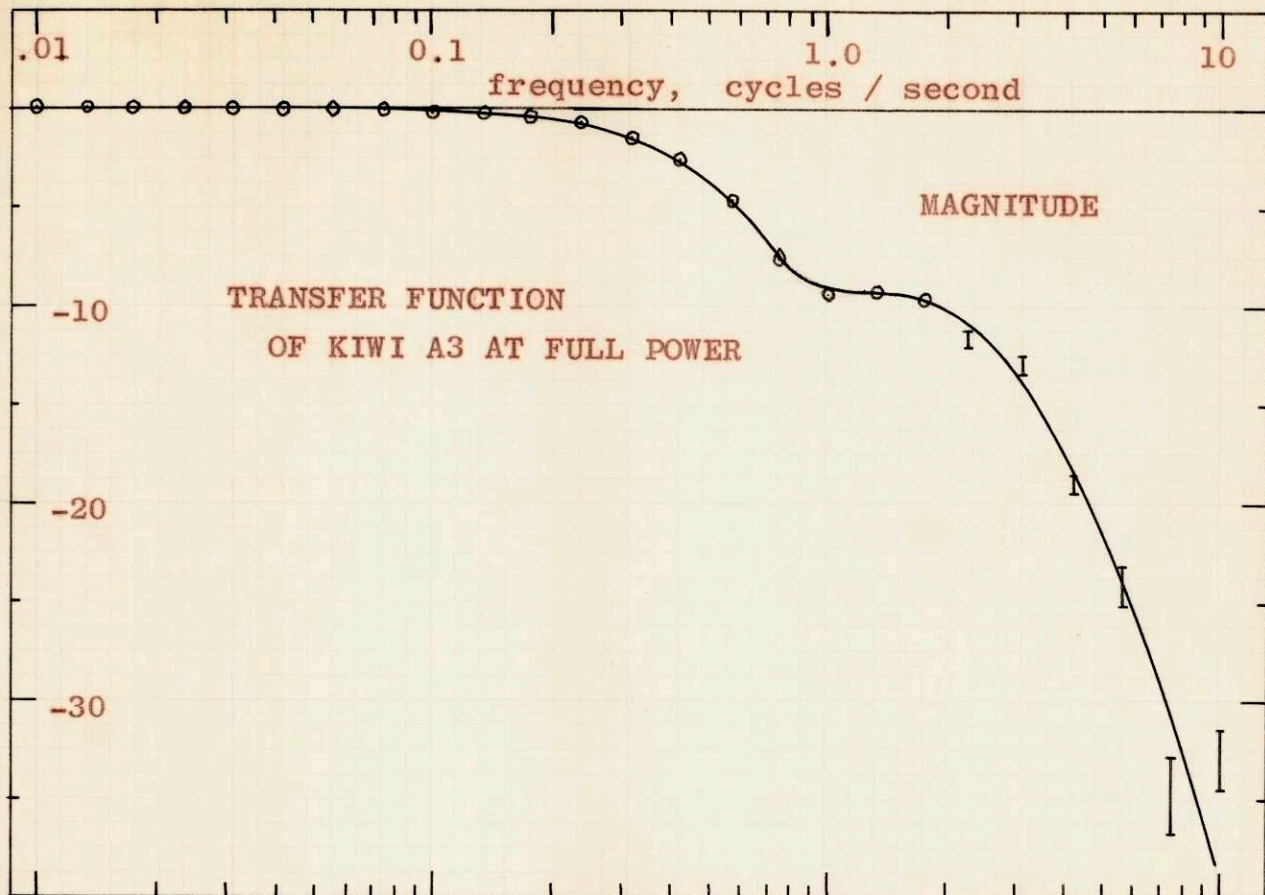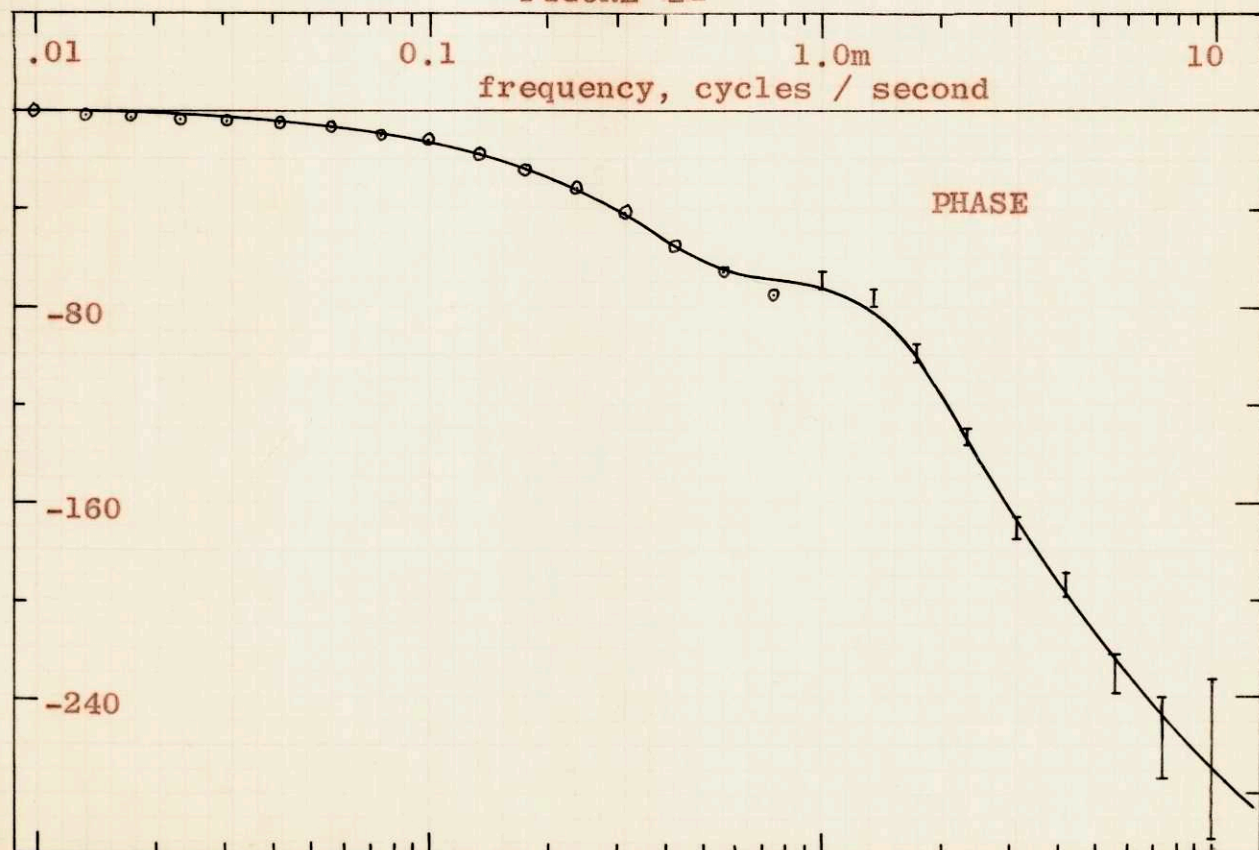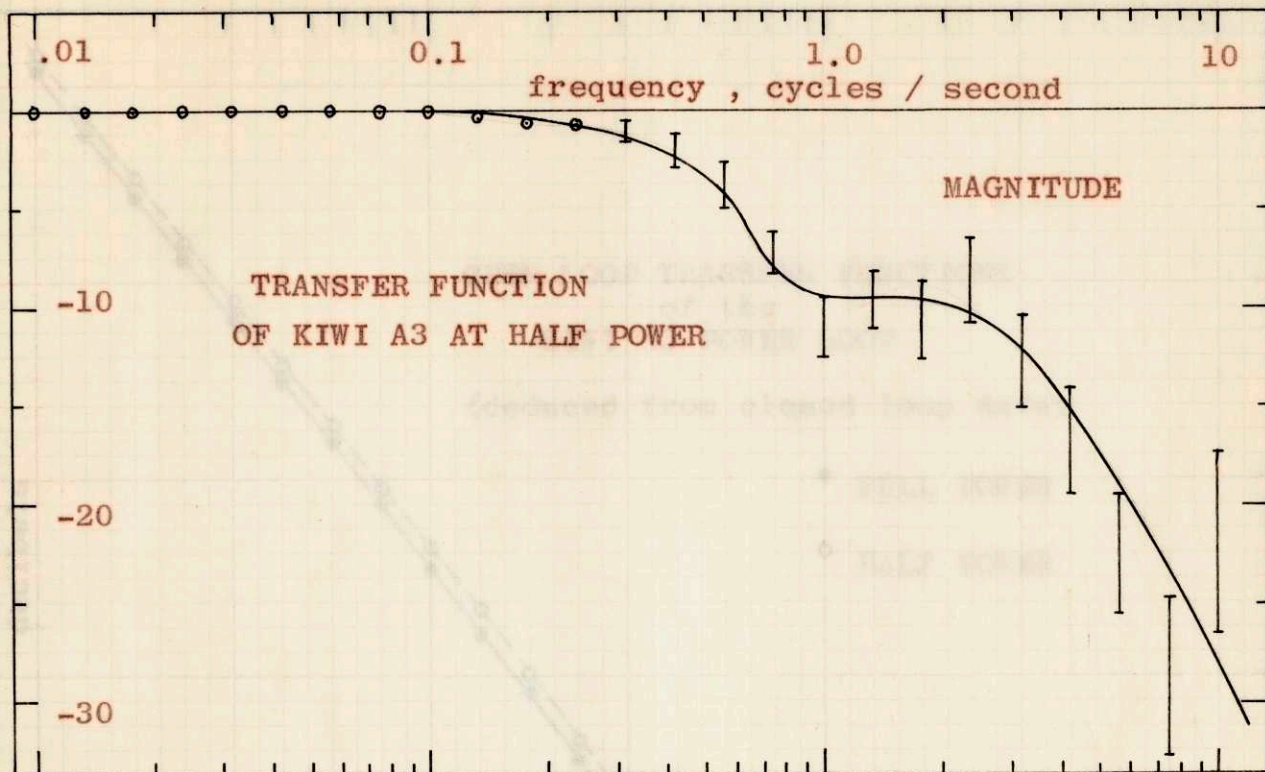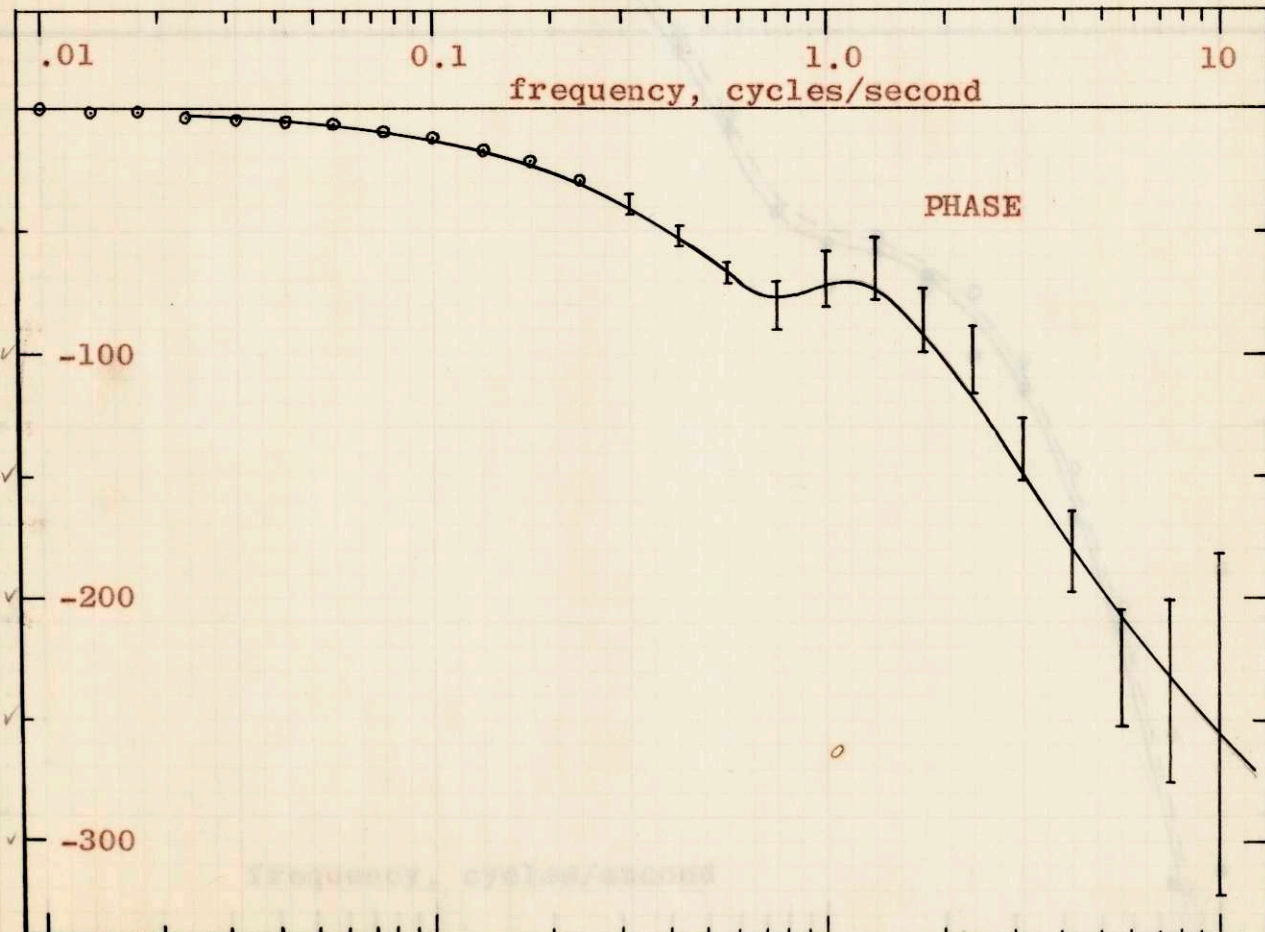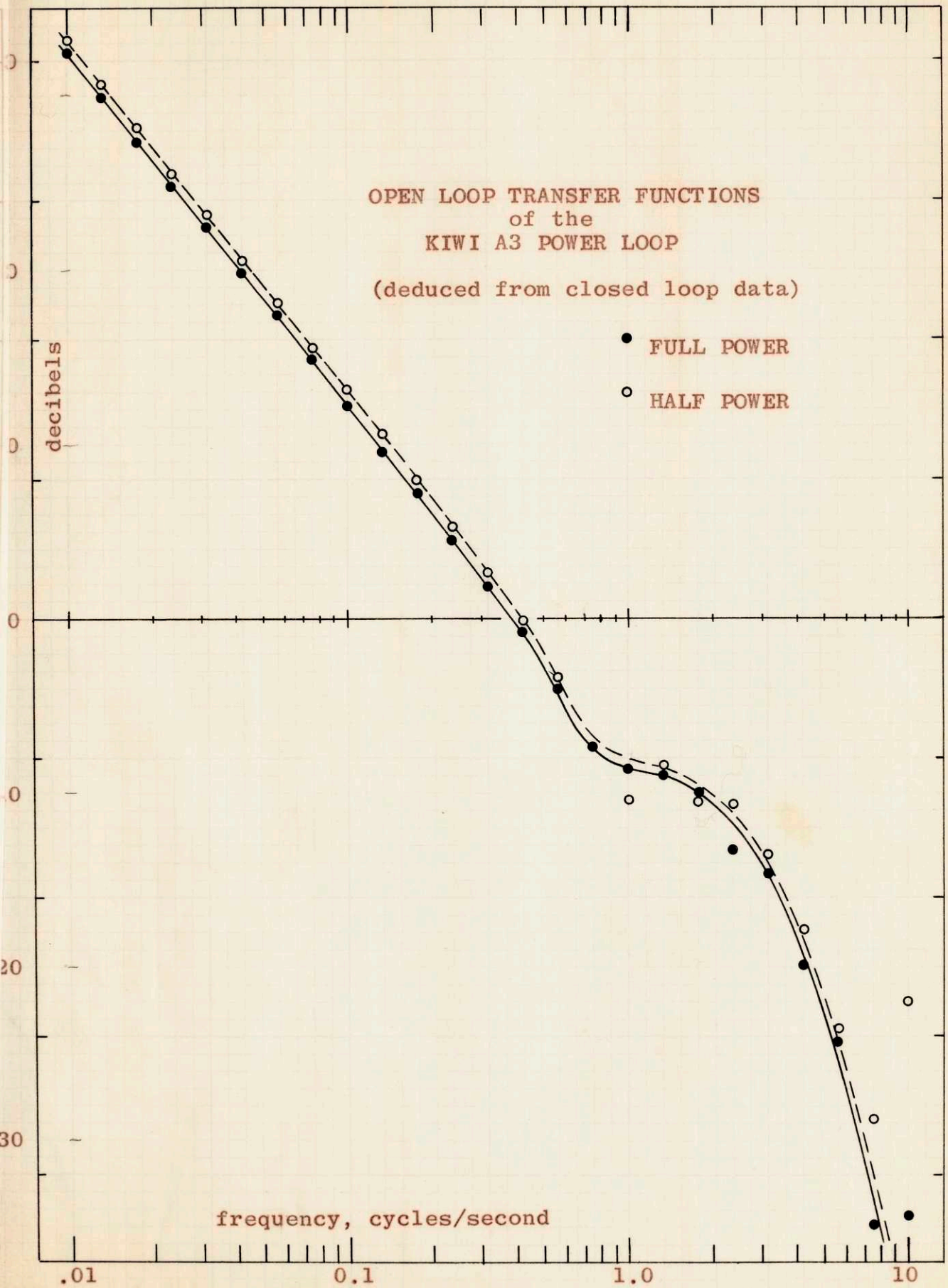
will be proportional to the "cents per inch" worth of the control rod. The control rod calibrations are given in the following table:

Power	Observed Shim Bank Position	Worth cents/inch
"half"	11.1″	16.85
full	12.8″	15.30

Thus, there is an expected decrease in open loop gain of 15.30/16.85 = 0.90 in going from "half" power to full power. In Figure 23 the observed decrease in open loop gain is 0.92 (-0.7 decibels) in very good agreement with 0.9.

3. Significance of the Kiwi-A3 Results

This is the first time dynamics measurements of control system performance have been made on a rocket reactor at full power. The suggestion that the cross-correlation method be applied to rocket reactors was first made in full knowledge that it was perhaps the only practical method of making such measurements.[*] The results indicate:

a) The control system performed essentially as expected.

b) The crosscorrelation method can produce useful dynamics data from reactor systems of this general power and bandwidth.

[*] Dr. George K. Hess, Jr., Bendix Corporation, Research Laboratory

CHAPTER   V

CONCLUSIONS

From the work that has been presented in the preceding
chapters, the following primary conclusions can be drawn.
  1) The crosscorrelation method has the following
      advantages:
            a) It yields the entire information about the
                impulse response of the system in the
                shortest possible time, that is, the
                system settling time.
            b) The method requires only small amplitude
                perturbations. Consequently it is not
                hazardous, not limited by system non-
                linearities, and does not interfere with
                normal system operation.
            c) It can be used even in the presence of strong
                noise sources provided that the cross-
                correlation time is increased beyond the
                system settling time.
  2) The crosscorrelation method is a useful reactor
      diagnostic technique.
  3) The crosscorrelation method is probably the best
      dynamics measurement tool for some reactor systems
      including rocket propulsion reactors.
  4) The method is promising enough to warrant further
      expenditure of time and money. Professional
      equipment is being designed for future experiments
      on rocket propulsion reactors.
  5) No disagreement with the theory has been found.
  6) The original purposes of the thesis have been
      achieved:

a)   The feasibility of the crosscorrelation
     method for use on reactor systems has
     been demonstrated.

b)   Data of the performance of a control
     system of a rocket propulsion reactor
     have been obtained.

Both the theoretical considerations and experimental
results described in the foregoing chapters show that the
listed advantages can be realized in the application of
the crosscorrelation method to reactor systems. The Kiwi-A3
experiment is a demonstration of the compatibility of the
crosscorrelation method with normal system operation.
The presence of the ± 1% rms fluctuations of reactor
power in no way interfered with the many other objectives
of the Kiwi-A3 full power run. The fluctuations represen-
ted only a factor of two increase over normal system
noise and were themselves noiselike; the power meter
fluctuations were barely noticeable to the reactor opera-
tors.

A major advantage of the crosscorrelation method is
that small input signals can be used. This is a result
of the ability of the method to produce usable results
even in the presence of strong noise sources. The cross-
correlator behaves (in the mean-square sense) as a pass-
band filter which attenuates all frequencies contained
in the system response signal which do not lie roughly
within the frequency spectrum of the input signal. The
noise frequencies which remain appear as random errors
in the measured impulse response (but spread out over
the entire crosscorrelation integration time interval).
The magnitude of these errors, relative to the data, can
be decreased by increasing the crosscorrelation time.
In order to estimate the crosscorrelation time needed the

concept of an "improvement factor" has been proposed.
The "improvement factor" is defined as the increase in
rms signal-to-noise ratio from the crosscorrelator input
to the crosscorrelator output. It is greater than or
equal to unity if the crosscorrelation time is just
equal to the system settling time; it increases propor-
tional to the square root of the crosscorrelation time
as the crosscorrelation time is increased beyond the
system settling time. This theory has been successfully
used to predict the errors in the data of the Kiwi-A3
"half" power run.

From the results of an analog computer study there
is evidence that the method tends to measure a linearized
reactor impulse response despite fluctuations which go
outside the range of linearity of the reactor kinetics
equations.

A basic purpose of this project has been to demon-
strate experimentally the feasibility of the crosscorela-
tion method for use on reactor systems. The experimental
results which have been obtained prove this feasibility.
The proof consists of two parts: first, detailed verifi-
cation of the validity of the method through analog com-
puter studies, and second, more general verification of
the practical ability to apply the method on two widely
differing types of reactor systems. Godiva II is a
fast reactor which operates at powers of a few watts.
It is conceptually the simplest kind of reactor. Kiwi-A3
on the other hand, is a thermal reactor operating at many
orders of magnitude higher power. It is only a part of
a complex system. The crosscorrelation method has pro-
duced correct impulse response data from both of these
systems. The obvious implication is that the method is
feasible for use on all reactor systems. However, the

advantages of the method are most clearly manifested
for the more complex reactor systems, since it is for
such systems that the requirements of small input sig-
nals and short experiment time are likely to be imposed.

The other basic purpose of the project has been to
obtain data of the control system performance of rocket
propulsion reactors at full power. This information
has not been available before. The results from Kiwi-A3
are presented graphically in Figures 19 to 23 of Chapter
II.

Three secondary conclusions are:

1)   The advantages of the idealized binary input
     signal are two. First, there are no random
     errors introduced by fluctuations in the
     statistics of the input signal such as would
     occur with a random input signal. Second,
     the fact that the signal is binary is a com-
     putational asset. The necessary storage, delay,
     and multiplication operations are much easier
     than with a continuously variable signal.

2)   Three conclusions can be drawn from the exper-
     ience of building the equipment which implements
     the crosscorrelation method and which is de-
     scribed in Chapter III.

     a)   Relays are not adequate for binary multi-
          plication much beyond ten bits per second;
          diode gates are adequate to at least 500
          bits per second.

     b)   The use of a punched paper tape input and
          delay system is limited to measurements
          on systems of bandwidth less than 16 cps
          (corresponding to 200 bits per second)
          with the present state of development of

reading devices. In any case a punched
paper tape is seriously limited as to the
possible number of crosscorrelation chan-
nels.

c) All other equipment described will perform
adequately in the range below 100 cps.

3) System transfer functions can be obtained from
impulse response data by numerical techniques
although the number of calculations involved
justifies the use of a digital computer. A
general code has been written for the purpose
and is described in detail in Appendix B and
more generally in II-E. A Monte Carlo method
for estimating the standard deviations of a
transfer function due to errors in the impulse
response data has been devised and shown to
give reasonable answers.

In any project as involved as this one has been, there
are a few things left undone and a few questions left un-
answered. Of these, one question is perhaps the most important
and the most difficult: what is the crosscorrelation function
when the system under test is non-linear? There is one bit of
empirical evidence presented in this thesis which suggests
that in a certain type of non-linearity, that of the reactor
kinetics equations, the effect of the non-linearity tends
to cancel out and a linearized impulse response is measured.
Perhaps it will follow that the crosscorrelation method does
tend to measure a linearized impulse response for most non-
linear systems. It is felt that this question warrants
further study.

APPENDIX A.

DISCUSSION OF POSSIBLE IMPLEMENTATIONS
OF
THE CROSSCORRELATION METHOD

The idea and the basic equations of the crosscorrelation method, put forth in the Introduction, were originally suggested by Y.W.Lee[8]. The technique has been used in the general field of Electrical Engineering for measuring the dynamics of systems.

In applying the method to the measurement of reactor dynamics, a great variety of possible implementations present themselves. First, there is a choice of input signals. The only condition limiting the choice is the requirement that the power spectrum be flat over the range of interest.

There is also a wide choice in the method of performing the crosscorrelation. The purpose of this appendix is to present some pros and cons of some possible implementations.

Input signals can be classified by two properties:
1) Predetermined or stochastic
2) Discrete level or continuous level

If the input is known in advance then the values of the delayed inputs are also known in advance and these can be used directly in the crosscorrelation calculation. Hence, no pure time delay device is required. In addition, specific inputs, having an optimized autocorrelation function, can be utilized. A stochastic input, on the other hand, has the advantage that it does not have to be stored prior to the experiment; and it can easily be

generated by a wide-band noise generator.

A discrete level signal has as main advantages ease of storage, ease of delay, and ease of multiplication. These advantages are particularly significant if the signal is just two level (binary); for this case digital techniques can be employed. The use of diode switching circuits to implement multiplication, for example, is a considerable equipment savings over the circuitry needed for multiplication of two continuous level signals, particularly if many values on the crosscorrelation function are to be computed simultaneously. One major advantage of being able to handle continuous level inputs is that any signal, perhaps deep within the system, can be regarded as the input signal and any other signal, further on in the system, can be regarded as the output signal. In addition, if the input signal is generated by a simple wide-band noise generator, it will usually be a continuous level signal.

To implement the crosscorrelation calculation, three operations must be performed: time delay, multiplication, and integration. One can implement the delay with a paper tape, magnetic storage, padé networks, a digital shifting register, etc. The paper tape system was used by the author mainly as a matter of convenience: a paper tape reader was on hand and a computer to punch the tapes was available. The main disadvantage of the paper tape system is the limited speed of operation.

A magnetic tape or drum delay can be used to delay either discrete or continuous level signals; and it can be used either to store predetermined delay signals or to actually delay a stochastic signal.

The Aeronutronic Company,[9] in applying the crosscorrelation method as the diagnostic component of a self-optimizing airplane controller, had a great deal of

success with drum storage. The basic advantage over
tape storage, which is cheaper, is freedom from tape
fluctuations: wow and flutter. The Aeronutronic
Company reported considerable trouble in attempting to
use a tape machine. On the other hand, Rajagopal,[13]
in applying the crosscorrelation method to a reactor
claims to have surmounted tape wow and flutter problems
through the use of a tape looping device.

Padé networks,[7] which are nodal networks built to
approximate a pure time delay, have been tried out by
the Aeronutronic Company and discarded. The basic
difficulty is that a good approximation to a pure delay,
over a frequency span of four decades, must be realized.
It would require an impractical number of components to
accomplish this.

Multiplication of the output signal by the delayed
input signal is the second step in the crosscorrelation.
Implementation of this multiplication has already been
considered in discussing the choice of the input signal.
If the input is a continuous level signal, then a con-
tinuous level multiplier must be used. If the input
is binary then semi-digital multiplication can be used
as described in Chapter III. In this connection it
should be mentioned that an attempt was made to use relays
for the switching; the fastest relays available proved
too slow. Diode gates are much faster, more reliable,
and can be made sufficiently accurate.

The integration is fairly easy. If precision is
desired, a standard analog computer integration network
can be used. These utilize a very high gain amplifier
with capacitive feedback. The amplifier output will be
the integral of the input current. Approximate integra-
tion can be obtained inexpensively from a simple R-C
network:
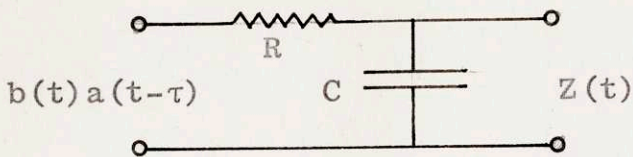
$$Z(t) = \frac{1}{RC} \int_{-\infty}^{t} d\lambda \; b(\lambda) \; a(\lambda-\tau) \; e^{(\lambda-t)/RC}$$

This method has the advantage of producing a continuous output. The average value of $Z(t)$ is proportional to $\phi_{ab}(\tau)$. The fluctuation can be decreased by increasing the integration time constant ($\sigma_\phi \sim \sqrt{1/RC}$).

Thus far, the possibility of calculating the cross-correlation function completely on a digital computer has been ignored. For some applications, this appears to be a very practical technique. All that is required for the experiment itself is a tape recorder and a noise generator. The input noise signal and the output response are recorded together on the tape. Later, these signals are sampled at regular intervals and digitized. A digital computer can then calculate the crosscorrelation directly. There are two main disadvantages to this technique. First, there is considerable time delay between the experiment and the results, and second, the analog-to-digital conversion is a difficult operation requiring expensive equipment not generally available.

In the previous discussion it was mentioned that a time delay between experiment and result is a serious drawback. This is true for two reasons. First, because the input and output signals are noise-like, one cannot tell very easily, while an experiment is in progress, whether they are reasonable. About the only observable fact is that the output noise increases when the input is applied. It is a great advantage, in setting up an

experiment, to try it out, perhaps on a simulation of the
real system, just to see that everything is working proper-
ly. Second, the crosscorrelation results are very quickly
available.

This leads to the concept of a reactor stability
monitor. If the crosscorrelator is set up to display the
impulse response continuously (on a oscilloscope, for
example), then the system dynamics can be continuously
observed. This can be a very useful tool either for
making adjustments to optimize system performance or
just to keep an eye on system stability. A tendency
toward instability is easily recognizable from a change
in the impulse response. A convenient implementation
of this monitor might utilize a binary input, diode
switching multiplication, and R-C circuit integration.

APPENDIX B

IMP - A CODE TO COMPUTE A SYSTEM TRANSFER FUNCTION

FROM IMPULSE RESPONSE DATA

(IBM-704, FORTRAN)

The code is largely self-explanatory. It is written as master program (TRAN) plus several subroutines.

TRAP - this subroutine computes the transfer function according to equation (II-84). This assumes a trapizoidal curve (straight line segments between the data points). The area and squared-area are computed and the transfer function is normalized by dividing by the area.

CORECT - this subroutine performs the iteration procedure discussed in II-C to correct for finite Δt. Equation (II-17) is used to calculate the successive points.

SIGMA - this subroutine calculates the theoretical standard deviations of the transfer function from the standard deviations of the impulse response. The equations for the transfer function from TRAP have been differentiated with respect to each data value and put into the form of equation (II-85).

TABLE - this subroutine calculates and stores a table of the error function.

NORMAL - this subroutine, given a point and a standard deviation, will calculate a new point which fits a normal distribution about the given point. It does this by selecting a random number between zero and unity using a standard RANDOM function and interpolating in TABLE to find the corresponding value on a normal distribution. Extensive chi-square tests have been performed by the author to show that the resulting distribution is indeed

normal.

BAZFAZ - this subroutine calculates the magnitude and phase of a complex number from the real and imaginary parts.

The master program, TRAN, allows for a wide variety of external decisions which are controlled by indexes as follows.

L1 $\neq$ 0 (=0) Correct (Do not correct) the data for finite Δt

L2 $\neq$ 0 (=0) Calculate (Do not calculate) the error function table

L3 $\neq$ 0 (=0) Proceed (Return to the start and read more data)

L4 $\neq$ 0 (=0) Use (Do not use) the corrected data instead of the original data

L5 $\neq$ 0 (=0) Interpolate (Do not interpolate) more points in between the given data points

L6 $\neq$ 0 (=0) Frequency correct for finite Δt by dividing the transfer function by $\bar{\Phi}_{aa}(\omega)$. (See equation (II-19) and Figure 6 of Chapter II)

L7 $\neq$ 0 (=0) Compute (Do not compute) the open loop transfer function

L8 $\neq$ 0 (=0) Use (Do not use) SIGMA

L9 $\neq$ 0 (=0) Compute (Do not compute) an ensemble of M new data curves (using NORMAL) and their transfer functions and compute the averages and standard deviations of the ensemble of transfer functions at each specified frequency

L10 $\neq$ 0 (=0) Print (Do not print) each of the M curves and transfer functions calculated

The input is on cards. The output is on tape. Sample printouts follow the listings.

IMP : LOGIC FLOW DIAGRAM

```
┌────────────────────────┐     ┌──────────────┐     ┌──────────────┐
│ READ INPUT CROSS-      │     │ SCALE THE    │     │ SHOULD       │   NO
│ CORRELATION DATA PAIRS │────▶│ DATA BY THE  │────▶│ WE           │─────────▶
│ AND STANDARD DEVIATIONS│     │ GIVEN        │     │ CORRECT?     │
│ CONSTANTS AND INDEXES  │     │ CONSTANTS    │     └──────────────┘
└────────────────────────┘     └──────────────┘           │
                                                          YES
                                                           │
                                                           ▼
┌────────────────────────┐  ┌────────────────────────┐  ┌──────────────────┐
│ IS THE CHANGE GREATER  │◀─│ CALCULATE THE NEXT BEST │  │ MAKE THE FIRST   │
│ THAN THE NUMBER E?     │  │ GUESS OF THE IMPULSE    │  │ APPROXIMATION:   │
└────────────────────────┘  │ RESPONSE ACCORDING TO   │  │ IMPULSE RESPONSE │
                            │ THE EQUATION (II-17)    │  │ EQUALS CROSSCOR- │
    NO        YES           └────────────────────────┘  │ RELATION FUNCTION│
                                                         └──────────────────┘
                            ┌────────────────────┐
                            │ HAVE WE MADE 100   │   NO
                            │ ITERATIONS YET?    │──────
                            └────────────────────┘
   (CONVERGENCE)                     │
                                    YES

                               (DIVERGENCE)
```

SET THE IMPULSE RESPONSE DATA EQUAL TO THE CROSSCORRELATION FUNCTION

PRINT OUT RESULTS SO FAR

ARE WE GOING TO NEED TO CALCULATE THE ERROR FUNCTION TABLE?

NO   YES

CALCULATE TABLE

NO   DO   WE WANT TO COMPUTE TRANSFORMS?

YES   HAVE WE CALCULATED ALL THE TRANSFORMS WE WANT TO?   ◀──── (A)

NO

READ IN NEEDED PARAMETERS AND CONSTANTS

COMPUTE THE LIST OF FREQUENCIES

SHOULD WE INTERPOLATE MORE POINTS ON THE IMPULSE RESPONSE CURVE?

YES   NO

```
┌────────────────────────────────┐     ┌──────────────────────────┐
│ USE STANDARD INTERPOLATION     │     │ CALCULATE THE AREA AND   │
│ FUNCTION TO CALCULATE NZ       │────▶│ SQUARED AREA OF THE      │
│ EQUALLY SPACED POINTS USING    │     │ IMPULSE RESPONSE CURVE   │
│ K-TH ORDER INTERPOLATION       │     │ (TRAPIZOIDAL INTEGRATION)│
└────────────────────────────────┘     └──────────────────────────┘
```

```
┌──────────────────────────────────────────────────────┐
│ CALCULATE THE TRANSFER FUNCTION (MAGNITUDE AND PHASE  │────▶ ( B )
│ AT EACH DESIRED FREQUENCY) ACCORDING TO EQUATION(II-84)│
└──────────────────────────────────────────────────────┘
```

(NEXT PAGE)

B

PRINT OUT TRANSFER FUNCTION

SHOULD WE CALCULATE THE OPEN LOOP TRANSFER FUNCTION?

YES

NO

CALCULATE THE OPEN LOOP TRANSFER FUNCTION AND PRINT OUT RESULTS

SHOULD WE CALL SIGMA?

YES

NO

COMPUTE THE THEORETICAL ERRORS IN THE TRANSFER FUNCTION. SEE THE #2 DO LOOP IN SIGMA FOR THE EQUATIONS. PRINT OUT RESULTS

A

NO

SHOULD WE USE THE MONTE CARLO METHOD TO ESTIMATE THE ERRORS IN THE TRANSFER FUNCTION?

YES

SET RMS SUMS TO ZERO

REPLACE EACH IMPULSE DATA POINT WITH A NEW POINT SELECTED AT RANDOM ON A NORMAL DISTRIBUTION CENTERED ABOUT THE ORIGINAL POINT USING A RANDOM FUNCTION AND LINEAR INTERPOLATION IN THE ERROR FUNCTION TABLE

CALCULATE THE TRANSFER FUNCTION OF THE NEW CURVE USING EQUATION (II-84)

SHOULD WE PRINT OUT THIS DATA?

YES

NO

PRINT OUT RANDOMIZED IMPULSE RESPONSE CURVE DATA AND ITS TRANSFER FUNCTION

INCREASE RMS SUMS (MAGNITUDE, MAGNITUDE IN DECIBELS, AND PHASE AT EACH DESIRED FREQUENCY) BY THE SQUARE OF THE DIFFERENCE BETWEEN THE CALCULATED TRANSFER FUNCTION VALUES AND THE ORIGINAL TRANSFER FUNCTION VALUES.

YES

HAVE WE CALCULATED M CURVES YET?

NO

COMPUTE $\sqrt{\dfrac{RMS\ SUMS}{M}}$. THESE ARE THE RMS VARIATIONS IN THE MAGNITUDE AND PHASE OF THE TRANSFER FUNCTION AT EACH DESIRED FREQUENCY. PRINT OUT RESULTS.

RETURN

A

```
C       IMP TRAN DOUG BALCOMB N4 82327
        DIMENSION H(72),T(72),SH(72),C(72),X(51),Y(51),S(100),D(72),FR(100
       1),FI(100),FM(100),FDB(100),FP(100),OM(100),ODB(100),OP(100),SM(100
       2),SDB(100),SP(100),SRM(100),SRDB(100),SRP(100),R(72),RM(100),RDB(1
       300),RP(100),RR(100),RI(100),AM(100),ADB(100),AP(100),DM(100),
       4DDB(100),DP(100)
  101 FORMAT(72H1
      1                      )
  102 FORMAT(5I5,4F10.5)
  103 FORMAT(3F14.5)
  104 FORMAT(2I3,E6.2,3I3,7I1)
  201 FORMAT(9H0DELTA T=F8.3,5H  L1=I2,5H  L2=I2,5H  L3=I2)
  202 FORMAT(12H0ITERATIONS=I3,17H    MAXIMUM ERROR=F8.5)
  203 FORMAT(39H0  TIME        DATA        SIGMA    CORRECTED/1H )
  204 FORMAT(47H0  FREQUENCY        MAGNITUDE      DECIBELS       PHASE/1H0)
  205 FORMAT(1H0I3,27H POINTS INTERPOLATED-ORDER=I3)
  206 FORMAT(14H0THIS IS CURVEI3,3H OFI3,18H RANDOMIZED CURVES)
  207 FORMAT(4H0L4=I2,5H  L5=I2,5H  L6=I2,5H  L7=I2,5H  L8=I2,5H  L9=I2,
      16H  L10=I2)
  208 FORMAT(7H0 AREA=F8.3,17H      SQUARED AREA=F10.3)
  209 FORMAT(22H0PROPAGATION OF ERRORS)
  210 FORMAT(28H0OPEN LOOP TRANSFER FUNCTION)
  211 FORMAT(33H0RANDOMIZED RMS ERRORS          M=I3)
  212 FORMAT(F8.3,F10.3,F10.3,F10.3)
  213 FORMAT(F12.5,F14.6,F11.3,F10.2)
  214 FORMAT(F12.5,F14.8,F11.5,F10.5)
  215 FORMAT(44H0AVERAGED RANDOMIZED TRANSFER FUNCTION    M=I3)
  216 FORMAT(25H0STANDARD DEVIATIONS     M=I3)
    1 READ 101
      READ 102,N,NGROUP,L1,L2,L3,SPAN,E,CH,CT
      READ 103,(H(I),T(I),SH(I),I=1,N)
      DO 28 I,1,N
      H(I)=CH*H(I)
      SH(I)=CH*SH(I)
   28 T(I)=CT*T(I)
      SH(N)=0.
      WRITE OUTPUT TAPE 9,101
      WRITE OUTPUT TAPE 9,201,SPAN,L1,L2,L3
      IF(L1)2,3,2
    2 CALL CORECT(H,C,T,N,SPAN,E,INDEX)
      WRITE OUTPUT TAPE 9,202,INDEX,E
    3 WRITE OUTPUT TAPE 9,203
      WRITE OUTPUT TAPE 9,212,(T(I),H(I),SH(I),C(I),I=1,N)
      IF(L2)4,1,4
    4 IF(L3)5,6,5
    5 CALL TABLE(X,Y)
    6 DO 7 I1=1,NGROUP
      READ 104,NPD,ND,S(1),K,M,NZ,L4,L5,L6,L7,L8,L9,L10
      IF(L4)8,9,8
    8 DO 10 I=1,N
   10 D(I)=C(I)
      GO TO 11
    9 DO 12 I=1,N
   12 D(I)=H(I)
   11 NS=1+NPD*ND
      F=10.**(1./FLOATF(NPD))
      DO 13 I=2,NS
   13 S(I)=F*S(I-1)
      CALL TRAP(D,T,N,S,NS,L5,NZ,K,L6,SPAN,A,SQ,FR,FI,FM,FDB,FP)
      WRITE OUTPUT TAPE 9,101
      WRITE OUTPUT TAPE 9,208,A,SQ
      WRITE OUTPUT TAPE 9,207,L4,L5,L6,L7,L8,L9,L10
```

```
      IF(L5) 14,15,14
   14 WRITE OUTPUT TAPE 9,205,NZ,K
   15 WRITE OUTPUT TAPE 9,204
      WRITE OUTPUT TAPE 9,213,(S(I),FM(I),FDB(I),FP(I),I=1,NS)
      IF(L7) 16,17,16
   16 DO 18 J=1,NS
      B=(1.-FR(J))**2+FI(J)**2
      OR=(FR(J)*(1.-FR(J))-FI(J)**2)/B
      OI=FI(J)/B
   18 CALL BAZFAZ(OR,OI,OM(J),ODB(J),OP(J))
      WRITE OUTPUT TAPE 9,101
      WRITE OUTPUT TAPE 9,210
      WRITE OUTPUT TAPE 9,204
      WRITE OUTPUT TAPE 9,213,(S(I),OM(I),ODB(I),OP(I),I=1,NS)
   17 IF(L8)19,20,19
   19 CALL SIGMA(SH,T,N,S,NS,FR,FI,A,SM,SDB,SP)
      WRITE OUTPUT TAPE 9,101
      WRITE OUTPUT TAPE 9,209
      WRITE OUTPUT TAPE 9,204
      WRITE OUTPUT TAPE 9,214,(S(I),SM(I),SDB(I),SP(I),I=1,NS)
   20 IF(L9) 21,7,21
   21 DO 22 J=1,NS
      AM(J)=0.
      ADB(J)=0.
      AP(J)=0.
      SRM(J)=0.
      SRDB(J)=0.
   22 SRP(J)=0.
      DO 23 I=1,M
      DO 24 J=1,N
   24 CALL NORMAL(D(J),SH(J),R(J),X,Y)
      CALL TRAP(R,T,N,S,NS,O,NZ,K,L6,SPAN,A,SQ,RR,RI,RM,RDB,RP)
      IF(L10) 25,26,25
   25 WRITE OUTPUT TAPE 9,101
      WRITE OUTPUT TAPE 9,206,I,M
      WRITE OUTPUT TAPE 9,203
      WRITE OUTPUT TAPE 9,212,(T(J),R(J),SH(J),D(J),J=1,N)
      WRITE OUTPUT TAPE 9,101
      WRITE OUTPUT TAPE 9,206,I,M
      WRITE OUTPUT TAPE 9,208,A,SQ
      WRITE OUTPUT TAPE 9,204
      WRITE OUTPUT TAPE 9,213,(S(J),RM(J),RDB(J),RP(J),J=1,NS)
   26 DO 23 J=1,NS
      AM(J)=AM(J)+RM(J)
      ADB(J)=ADB(J)+RDB(J)
      AP(J)=AP(J)+RP(J)
      SRM(J)=SRM(J)+(FM(J)-RM(J))**2
      SRDB(J)=SRDB(J)+(FDB(J)-RDB(J))**2
   23 SRP(J)=SRP(J)+(FP(J)-RP(J))**2
      DO 27 J=1,NS
      AM(J)=AM(J)/FLOATF(M)
      ADB(J)=ADB(J)/FLOATF(M)
      AP(J)=AP(J)/FLOATF(M)
      DM(J)=SQRTF(SRM(J)/FLOATF(M)-(AM(J)-FM(J))**2)
      DDB(J)=SQRTF(SRDB(J)/FLOATF(M)-(ADB(J)-FDB(J))**2)
      DP(J)=SQRTF(SRP(J)/FLOATF(M)-(AP(J)-FP(J))**2)
      SRM(J)=SQRTF(SRM(J)/FLOATF(M))
      SRDB(J)=SQRTF(SRDB(J)/FLOATF(M))
   27 SRP(J)=SQRTF(SRP(J)/FLOATF(M))
      WRITE OUTPUT TAPE 9,101
      WRITE OUTPUT TAPE 9,211,M
      WRITE OUTPUT TAPE 9,204
      WRITE OUTPUT TAPE 9,214,(S(I),SRM(I),SRDB(I),SRP(I),I=1,NS)
```

```
      WRITE OUTPUT TAPE 9,101
      WRITE OUTPUT TAPE 9,215,M
      WRITE OUTPUT TAPE 9,204
      WRITE OUTPUT TAPE 9,213,(S(I),AM(I),ADB(I),AP(I),I=1,NS)
      WRITE OUTPUT TAPE 9,101
      WRITE OUTPUT TAPE 9,216,M
      WRITE OUTPUT TAPE 9,204
      WRITE OUTPUT TAPE 9,214,(S(I),DM(I),DDB(I),DP(I),I=1,NS)
    7 CONTINUE
      GO TO 1
      END(0,1,0,1,1)


C     IMP TRAPIZOIDAL DOUG BALCOMB N4 82327
      SUBROUTINE TRAP(H,T,N,S,NS,L1,NZ,K,L2,SPAN,A,SQ,FR,FI,FM,FDB,FP)
      DIMENSIONH(72),T(72),S(100),FR(100),FI(100),FM(100),FDB(100),FP(10
     10),TZ(300),Z(300),B(300)
      IF(L1)2,1,2
    2 TZ(1)=T(1)
      Z(1)=H(1)
      IERR=0
      DELT=T(N)/FLOATF(NZ-1)
      NZ1=NZ-1
      DO 3 I=2,NZ1
      TZ(I)=TZ(I-1)+DELT
    3 Z(I)=INTRPF(TZ(I),N,K,XLOCF(T(1)),XLOCF(H(1)),1,1,XLOCF(IERR))
      TZ(NZ)=T(N)
      Z(NZ)=H(N)
      GO TO 4
    1 NZ=N
      DO 5 I=1,NZ
      TZ(I)=T(I)
    5 Z(I)=H(I)
    4 A=0.
      SQ=0.
      DO 6 I=2,NZ
      A=A+(Z(I)+Z(I-1))*(TZ(I)-TZ(I-1))/2.
    6 SQ=SQ+(Z(I)**2+Z(I-1)**2)*(TZ(I)-TZ(I-1))/2.
      N1=NZ-1
      B(1)=(Z(2)-Z(1))/TZ(2)
      DO 7 I=2,N1
    7 B(I)=(Z(I+1)-Z(I))/(TZ(I+1)-TZ(I))-(Z(I)-Z(I-1))/(TZ(I)-TZ(I-1))
      B(NZ)=-(Z(NZ)-Z(NZ-1))/(TZ(NZ)-TZ(NZ-1))
      DO 8 J=1,NS
      W=6.28318*S(J)
      FR(J)=0.
      FI(J)=-Z(1)*W
      DO 9 I=1,NZ
      FR(J)=FR(J)-B(I)*COSF(W*TZ(I))
    9 FI(J)=FI(J)+B(I)*SINF(W*TZ(I))
      FR(J)=FR(J)/(A*W**2)
      FI(J)=FI(J)/(A*W**2)
      IF(L2)10,8,10
   10 C=(2.*SINF(W*SPAN/2.)/(W*SPAN))**2
      FR(J)=FR(J)/C
      FI(J)=FI(J)/C
    8 CALL BAZFAZ(FR(J),FI(J),FM(J),FDB(J),FP(J))
      RETURN
      END(0,1,0,1,1)
```

```
IMP   SIGMA DOUG BALCOMB N4 82327
SUBROUTINE SIGMA(SH,T,N,S,NS,FR,FI,A,SFM,SFDB,SFP)
DIMENSION SH(72),T(72),S(100),FR(100),FI(100),SFM(100),SFDB(100),S
1FP(100)
DO 1 J=1,NS
W=6.28318*S(J)
X=W*T(2)/2.
SR=((SINF(X)**2)*SH(1)/X)**2
SI=((SINF(X)*COSF(X)/X-1.)*SH(1))**2
N1=N-1
DO 2 I=2,N1
X=W*(T(I)-T(I-1))/2.
Y=W*(T(I)+T(I-1))/2.
A=W*(T(I+1)-T(I))/2.
B=W*(T(I+1)+T(I))/2.
SR=SR+((SINF(A)*SINF(B)/A-SINF(X)*SINF(Y)/X)*SH(I))**2
2 SI=SI+((SINF(A)*COSF(B)/A-SINF(X)*COSF(Y)/X)*SH(I))**2
SR=SQRTF(SR)/(A*W)
SI=SQRTF(SI)/(A*W)
X=SQRTF(FR(J)**2+FI(J)**2)
SFM(J)=SQRTF((FR(J)*SR)**2+(FI(J)*SI)**2)/X
SFDB(J)=8.68579*SFM(J)/X
1 SFP(J)=57.295*SQRTF(FR(J)*SI+FI(J)*SR)/(X**2)
RETURN
END(0,1,0,1,1)


IMP TAB   DOUG BALCOMB N4 82327
SUBROUTINE TABLE(X,T)
DIMENSION X(51),T(51)
T(1)=-4.
T(2)=-3.
DO 10 I=3,49
10 T(I)=T(I-1)+.125
T(50)=3.
T(51)=4.
X(1)=0.
X(51)=1.
X(26)=.5
DO 11 I=27,50
X(I)=(ERRORF(T(I)/1.41421)+1.)/2.
J=52-I
11 X(J)=1.-X(I)
RETURN
END(0,1,0,1,1)
```

```
C        IMP   CORRECT DOUG BALCOMB N4 82327
         SUBROUTINE CORECT(H,C,T,N,SPAN,E,INDEX)
         DIMENSIONH(72),C(72),T(72)
         INDEX=0
         N1=N-1
         DO 30 I=1,N
30  C(I)=H(I)
36  FOM=0.
         INDEX=INDEX+1
         DO 31 I=2,N1
         DELH=(SPAN**2/(6.*(T(I+1)-T(I-1))))*((C(I+1)-
        1C(I))/(T(I+1)-T(I))-(C(I)-C(I-1))/(T(I)-T(I-1)))
         DIF=ABSF(H(I)-C(I)-DELH)
         C(I)=H(I)-DELH
         IF(DIF-FOM)31,31,32
32  FOM=DIF
31  CONTINUE
33  IF(FOM-E)34,34,35
35  IF(INDEX-100)36,37,37
37  DO 38 I=1,N
38  C(I)=H(I)
34  E=FOM
         RETURN
         END(0,1,0,1,1)
```

DELTA T=   0.020   L1= 1   L2= 1   L3= 1

ITERATIONS=   6   MAXIMUM ERROR= 0.00038

TIME	DATA	SIGMA	CORRECTED
0.	0.	0.	0.
0.020	1.200	0.900	0.383
0.040	11.000	0.900	10.573
0.060	25.400	0.900	25.884
0.080	35.000	0.900	35.390
0.100	40.100	0.900	40.221
0.120	43.200	0.900	43.603
0.140	42.100	0.900	42.145
0.160	40.100	0.750	40.147
0.180	37.300	0.750	37.588
0.200	31.700	0.900	31.577
0.220	27.300	0.900	27.041
0.240	25.400	1.300	25.611
0.260	21.600	0.900	21.645
0.280	17.400	0.900	17.135
0.300	15.400	0.900	15.806
0.320	10.200	1.300	9.602
0.340	10.500	0.900	10.572
0.380	10.000	0.900	9.918
0.400	10.800	0.900	11.069
0.420	9.400	0.750	8.990
0.440	11.700	0.900	11.835
0.460	13.000	0.750	13.064
0.480	13.500	1.300	13.522
0.540	13.200	0.900	13.288
0.560	11.300	1.300	11.100
0.580	11.300	1.300	11.316
0.640	10.800	1.300	10.792
0.700	11.100	0.900	11.150
0.740	8.400	1.300	8.394
0.760	7.300	1.300	7.122
0.780	8.000	1.300	7.990
0.840	11.100	1.300	11.294
0.860	7.800	1.300	7.732
0.940	1.700	1.300	1.677
0.960	0.900	1.300	0.851
1.040	3.500	1.300	3.416
1.060	6.500	1.300	6.565
1.240	0.	1.300	-0.009
1.260	-0.200	1.300	-0.204
1.340	-0.500	1.300	-0.501
1.560	0.	0.	0.

KIWI A3 FULL POWER MIDRANGE POST-MORTEM

AREA= 15.373   SQUARED AREA=   347.486

L4= 1   L5= 0   L6= 0   L7= 1   L8= 0   L9= 0   L10= 0

FREQUENCY	MAGNITUDE	DECIBELS	PHASE
0.01000	0.999682	-0.003	-1.38
0.01334	0.999691	-0.003	-1.84
0.01778	0.999379	-0.005	-2.46
0.02371	0.999042	-0.008	-3.28
0.03162	0.998367	-0.014	-4.37
0.04217	0.997126	-0.025	-5.84
0.05623	0.994883	-0.045	-7.78
0.07499	0.990928	-0.079	-10.36
0.10000	0.983917	-0.141	-13.80
0.13335	0.971543	-0.251	-18.36
0.17783	0.949847	-0.447	-24.37
0.23714	0.912243	-0.798	-32.22
0.31623	0.848465	-1.427	-42.27
0.42170	0.744850	-2.559	-54.54
0.56234	0.591700	-4.558	-67.52
0.74989	0.416990	-7.597	-74.47
1.00000	0.344016	-9.268	-69.24
1.33352	0.348484	-9.156	-78.74
1.77828	0.338966	-9.397	-93.27
2.37137	0.258291	-11.758	-131.38
3.16228	0.223987	-12.995	-169.37
4.21696	0.113485	-18.901	-194.11
5.62341	0.063080	-24.002	-230.79
7.49894	0.018245	-34.777	-256.81
9.99999	0.019108	-34.375	-266.87

KIWI A3 FULL POWER MIDRANGE POST-MORTEM

AREA= 15.373   SQUARED AREA=   347.486

L4= 1   L5= 0   L6= 0   L7= 1   L8= 0   L9= 0   L10= 0

RANDOMIZED RMS ERRORS   M= 25

FREQUENCY	MAGNITUDE	DECIBELS	PHASE
0.00100	0.01071946	0.09305	0.51916
0.00178	0.00442055	0.03832	0.23168
0.00316	0.00187583	0.01630	0.08175
0.00562	0.00042669	0.00371	0.04239
0.01000	0.00015704	0.00136	0.06126
0.01778	0.00011598	0.00101	0.10551
0.03162	0.00029204	0.00254	0.18704
0.05623	0.00091675	0.00800	0.32915
0.10000	0.00283186	0.02496	0.56683
0.17783	0.00832805	0.07579	0.90879
0.31623	0.02075004	0.20973	1.11713
0.56234	0.02699865	0.38789	1.19105
1.00000	0.01572697	0.39030	3.00801
1.77828	0.01217780	0.31010	3.28116
3.16228	0.01151776	0.44109	3.61052
5.62341	0.00812363	1.13058	8.89536
10.00000	0.00624689	3.05971	231.10238

RANDOMIZED RMS ERRORS   M= 25

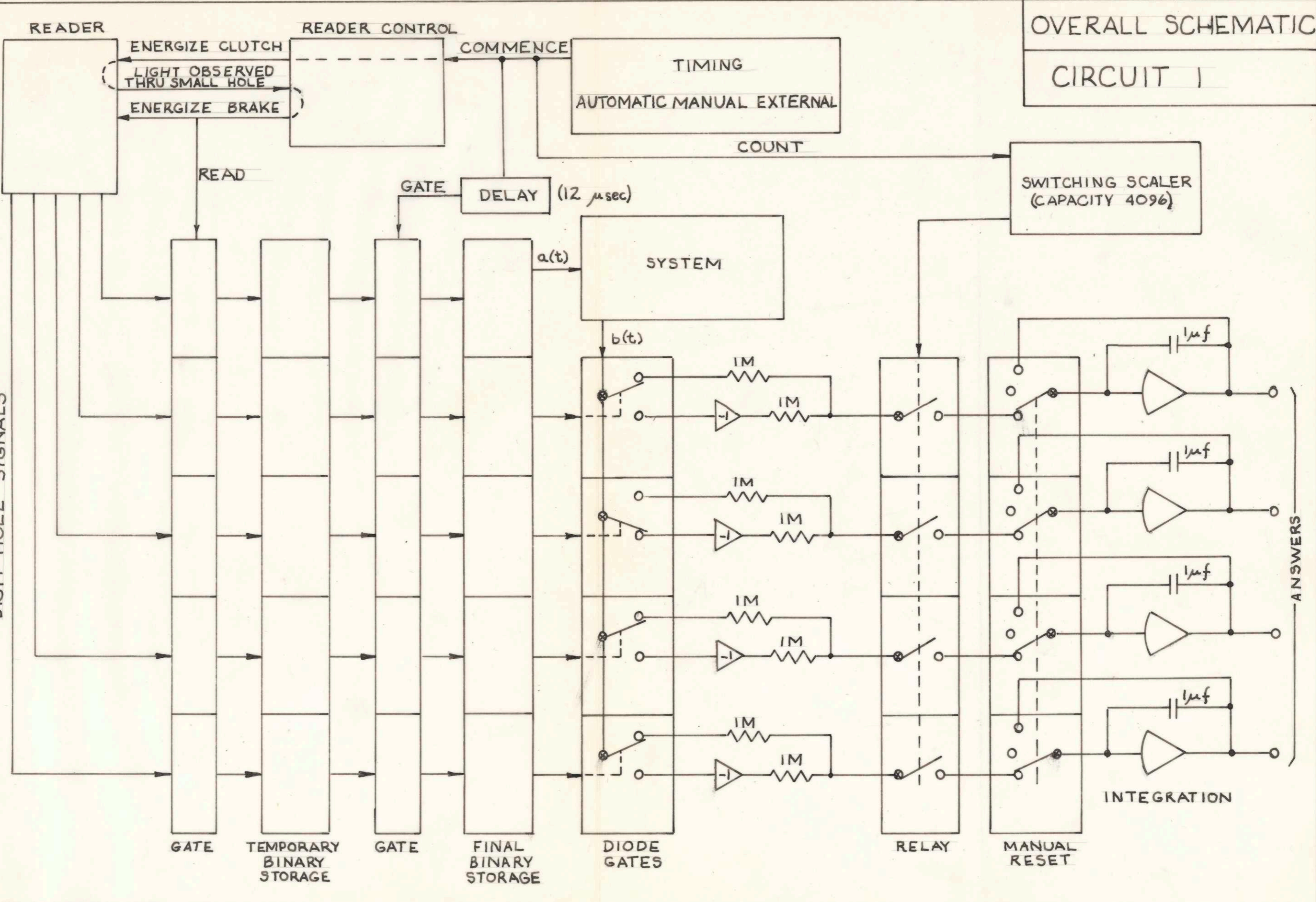FREQUENCY   MAGNITUDE   DECIBELS   PHASE

APPENDIX C

CIRCUIT DIAGRAMS

Diagram No. 1 is a schematic showing how Diagrams No. 2 through No. 7 fit together.

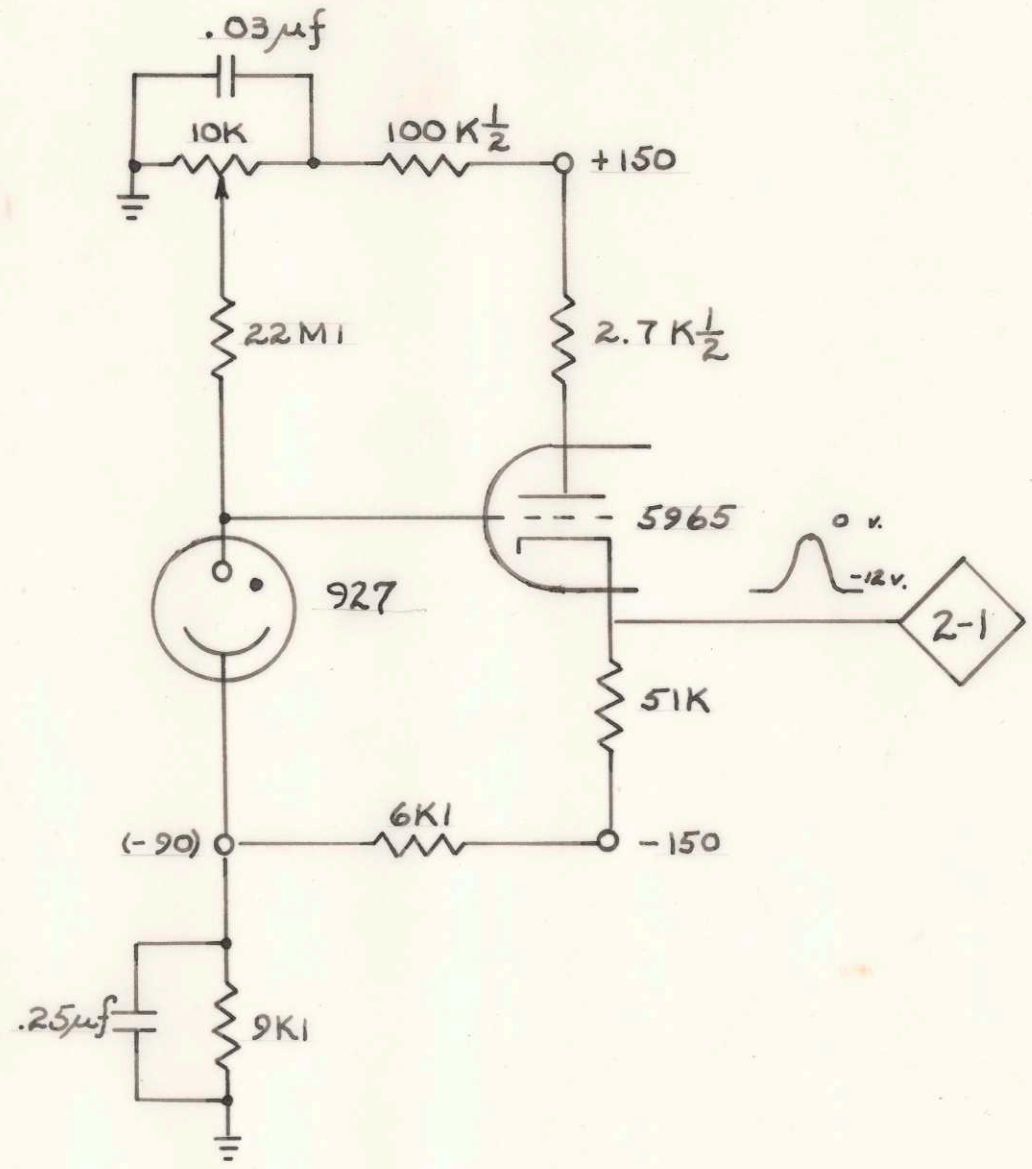Diagram No. 8 is the delay circuit for the Godiva rabbit transfer device.
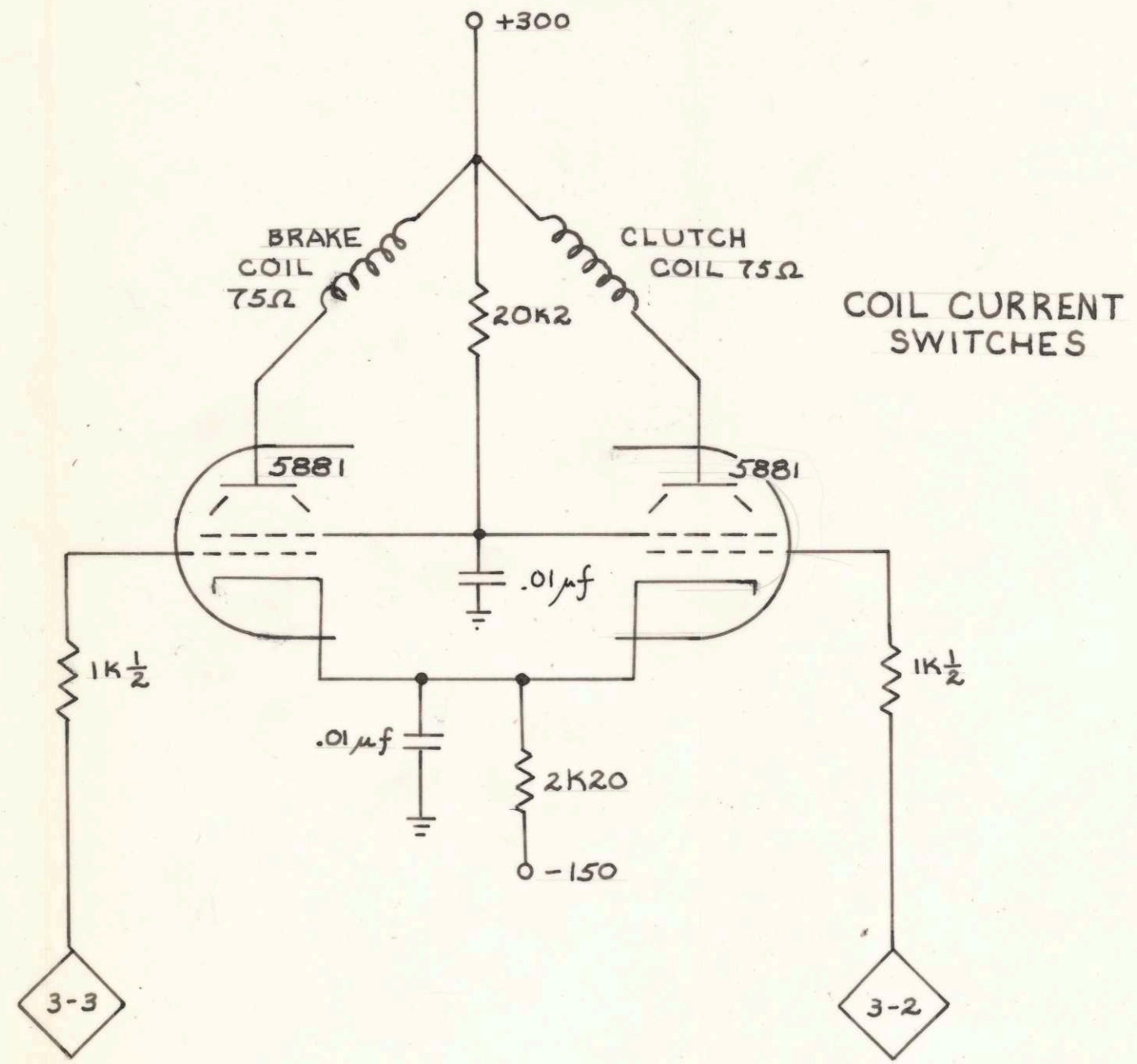
OVERALL SCHEMATIC CIRCUIT 1

.03μf

10K

100 K ½

+150

22 MI

2.7 K ½

5965

0 v.
-12 v.

2-1

927

51K

(-90)

6KI

-150

.25μf

9KI

LIGHT TRANSDUCER —
6 IDENTICAL CIRCUITS

+300

BRAKE
COIL
75Ω

CLUTCH
COIL 75Ω

20K2

COIL CURRENT
SWITCHES

5881

5881

.01μf

1K ½

1K ½

.01μf

2K20

-150

3-3

3-2

TIMING CIRCUIT
CIRCUIT 3

MULTIVIBRATOR

+150

12K2   12K2

20μμf   TIMED

100K

100K

40μf
4μf
.4μf
.4μf
.04μf

.04μf
.4μf
4μf
40μf

MANUAL

INVERTER

+150

12K2   20μμf   3K

10K

TRIGGER

+15

+300

BLOCKING
OSCILLATOR

30μμf
1K½   1000μμf

2.7K

-15

100Ω

+5

PULSE TRANSFORMER
PIC PQ 401

STEPPING FLIP FLOP

+150

12K2   12K2

20μμf

30μμf   39K   39K   30μμf

75K   75K

-150

MICROSWITCH
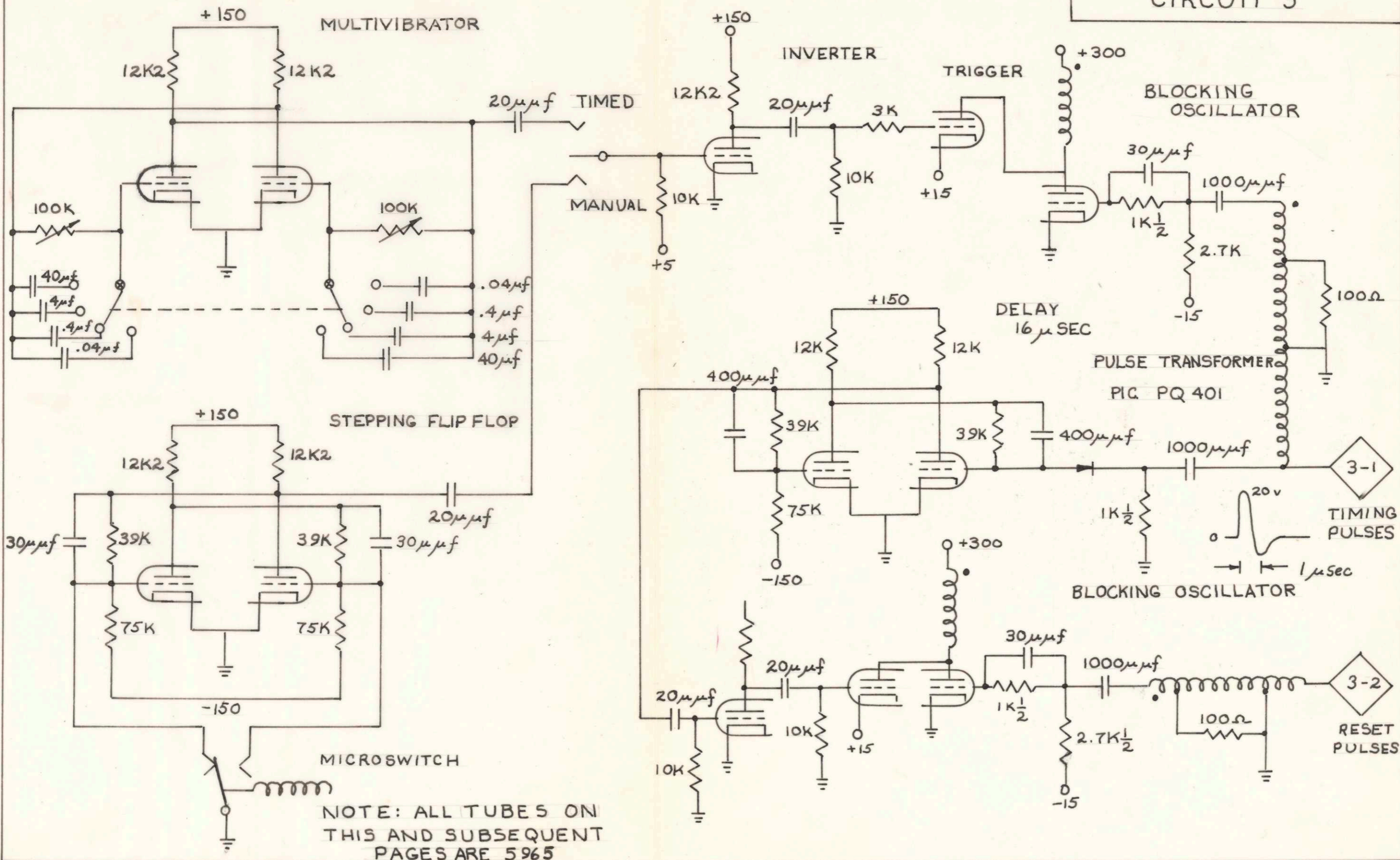
NOTE: ALL TUBES ON
THIS AND SUBSEQUENT
PAGES ARE 5965

DELAY
16 μ SEC

+150

12K   12K

400μμf

39K   39K   400μμf   1000μμf

75K

-150

1K½

BLOCKING OSCILLATOR

3-1

20v

0   1μsec

TIMING
PULSES

+300

20μμf   20μμf

30μμf   1000μμf

20μμf

10K   +15   1K½   100Ω

10K   2.7K½

-15

3-2

RESET
PULSES

131

READER CONTROL
CIRCUIT 4
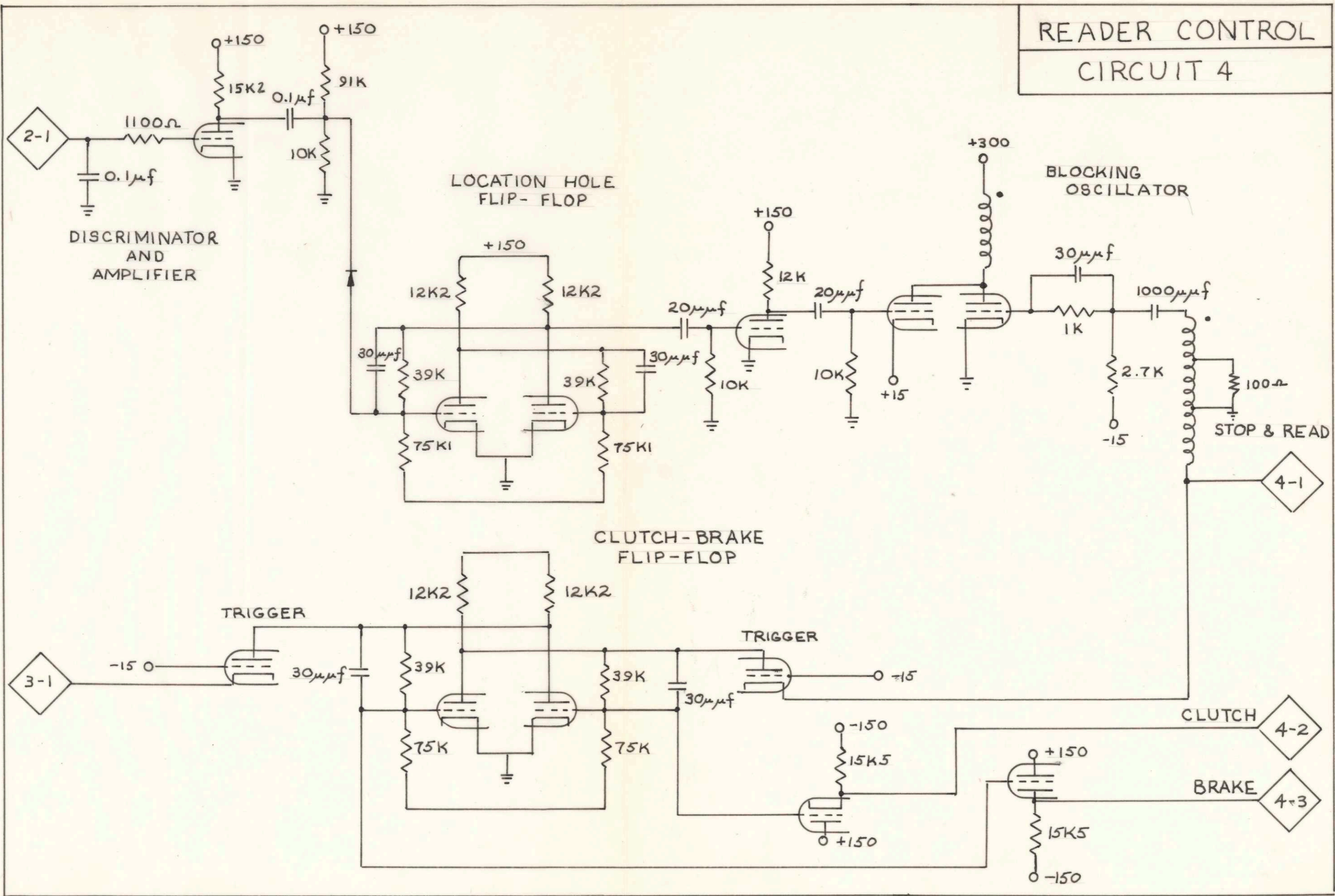
DIGIT HOLE FLIP-FLOPS(5)

CIRCUIT 5

FIVE IDENTICAL CIRCUITS

3-2 RESET

DIGITAL HOLE FLIP-FLOP   STORAGE   OUTPUT FLIP-FLOP

4-1 READ

3-1 TIMING

SCALER
CIRCUIT 6

DISCRIMINATOR

INPUT JACK (3-1)

BLOCKING OSCILLATOR

ELEVEN OTHER IDENTICAL FLIP FLOPS IN HERE STAGES 2 THRU 12

TO GRIDS OF THE NEXT STAGE

ALL DIODES 1N143
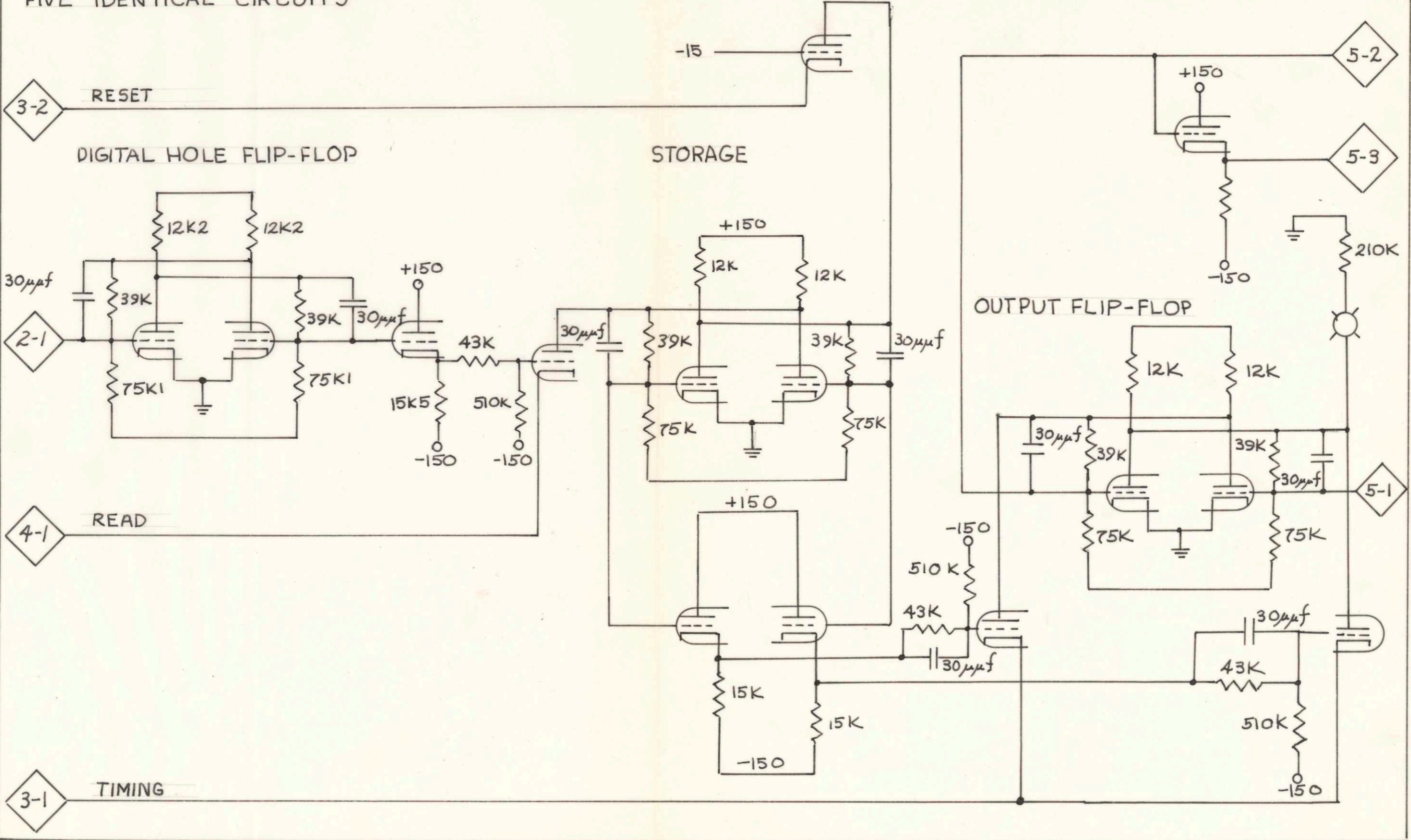
CROSSCORRELATION
CIRCUIT 7
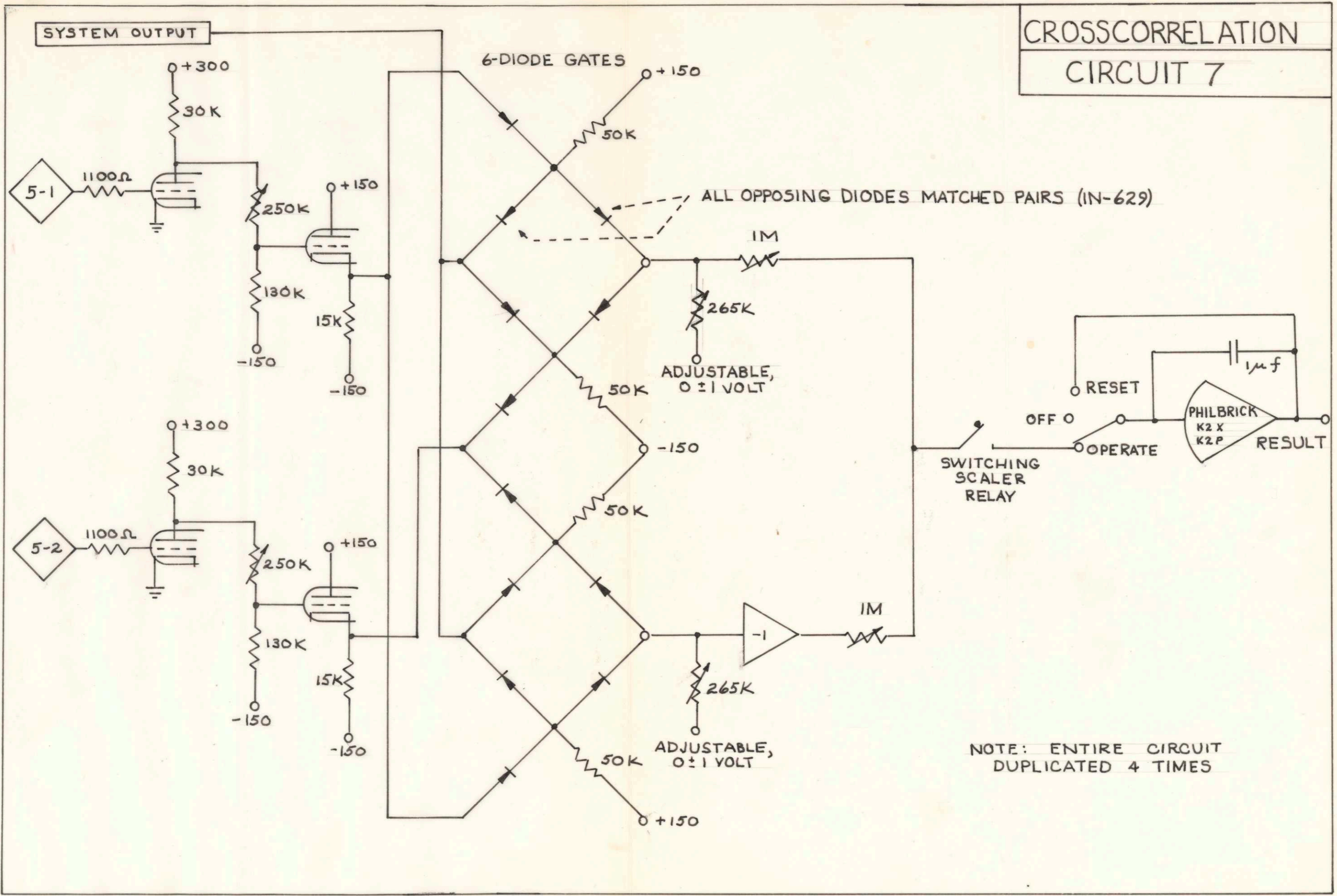
CIRCUIT 8
RABBIT CONTROL CIRCUIT
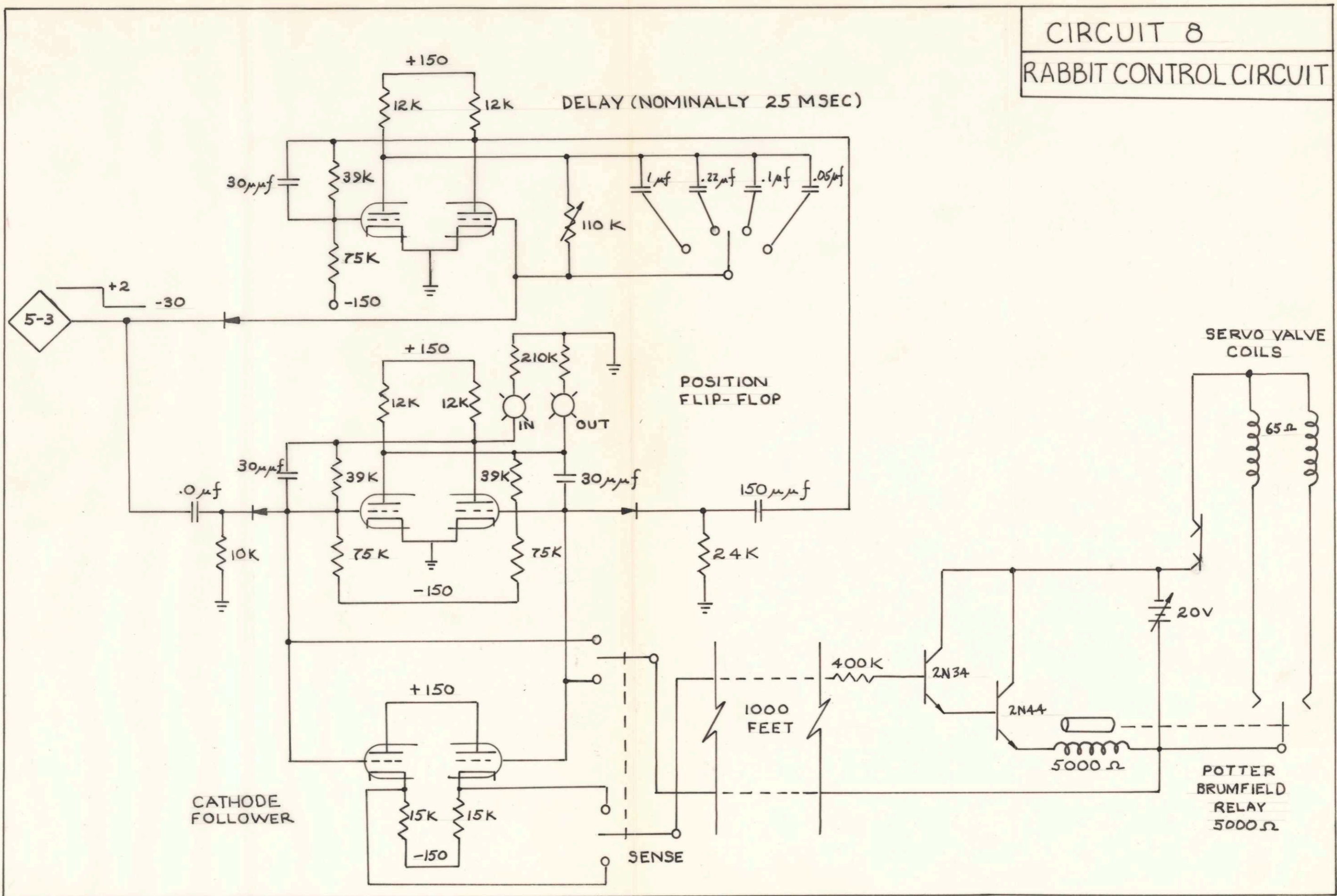
REFERENCES

1. Other, less complete descriptions of work described in this thesis:

    J. D. Balcomb, E. P. Gyftopoulos, H. B. Demuth, "The Use of Stochastic Inputs to Measure the Dynamic Response of Reactor Systems," Trans. Amer. Nuclear Soc.: 3, #2, Paper 27-3 (1960).

    J. D. Balcomb, E. P. Gyftopoulos, H. B. Demuth, "A Crosscorrelation Method for Measuring the Impulse Response of Reactor Systems," Nuclear Sci. and Eng. submitted for publication (1961).

2. F. Feiner, R. T. Frost, H. Hurwitz, Jr., "Pile Oscillator Techniques and the Error Analysis of Oscillator Measurements," KAPL-1703 (1956).

3. J. F. Boland, R. R. Smith, R. E. Rice, "A Measurement of the Transfer Function of a Fast Critical Assembly," ANL-5782 (1957).

4. A. F. Henry, "The Application of Reactor Kinetics to the Analysis of Experiments," Nuclear Sci. and Engr.: 3, 52-70 (1959).

5. E. D. Courant and P. R. Wallace, "Fluctuation of the Number of Neutrons in a Pile," Phys. Rev.: 72, 1038-1048 (1947).

6. C. Velez, "Autocorrelation Functions of Counting Rate in Nuclear Reactors and Their Application to the Design of Reactor Control Instrumentation," Ph.D. Thesis, Univ. of Mich. (1959).

7. J. G. Truxal, "Control System Synthesis," McGraw-Hill, New York (1955) pp 437-438, 550

8. Y. W. Lee, "Application of Statistical Methods to Communications Problems," Technical Report #181, R.L.E., MIT (1950).

9. Aeronutronic Systems, Inc., "A Study to Determine the Feasibility of a Self-Optimizing Automatic Flight Control System," WADD-TR-60-201 (1960).

10. A. E. Hastings and J. E. Meade, "A Device for Computing Correlation Function," Rev. Sci. Instr.: 23, 347-349 (1952).

11. F. E. Brooks, Jr. and H. W. Smith, "A Computer for Correlation Functions," Rev. Sci. Instr.: 23, 121-126 (1952).

12. H. E. Singleton, "A Digital Electronic Correlator," Proc. I.R.E: 38, 1422-1428 (1950).

13. V. Rajagopal, "Measurements on Internal Noise and Response to Random Inputs of a Reactor," Trans. Amer. Nuclear Soc: 3, #2, 27-4 (Dec. 1960).

14. J. H. Lanning, Jr. and R. H. Battin, "Random Processes in Automatic Control," McGraw-Hill, New York (1955).

15. G. W. Anderson, Aeronutronic Systems, Inc., private communication.

16. V. V. Solodovnikov, Yu. I. Topcheev, and G. V. Krutikova, "Transient Response from Frequency Response," Infosearch Limited, London (1955).

17. S. O. Rice, "Mathematical Analysis of Random Noise", from N. Wax, "Selected Papers on Noise and Stochastic Processes," pp 168, Dover, New York (1954).

18. J. G. Truxal, "Automatic Feedback Control System Synthesis," McGraw-Hill, pp 379-390, New York (1955).

19. G. R. Keepin, "Period Reactivity Relations Determined Directly from Prompt-Burst Neutron Decay Data," Nuclear Sci. and Eng: 5, 132-136 (1959).

20. G. A. Korn and T. M. Korn, "Electronic Analog Computers," McGraw-Hill, New York (1956).

21. T. E. Springer, personal communication, (these are intermediary numbers of a study to determine an optimum set of two delayed neutron groups).

22. T. F. Wimett, R. H. White, W. R. Stratton, and D. P. Wood, "Godiva-II, An Unmoderated Pulse Irradiation Reactor," Nuclear Sci. and Eng: 8, 691-708 (1960).

23. M. A. Schultz, "Control of Nuclear Reactors and Power Plants," McGraw-Hill, New York (1955) pp 43-44.

24. G. E. Hansen, Proc. 2nd Intern. Conf. on Peaceful Uses of Atomic Energy, Geneva: 10, 449-460 (1958).

25. G. K. Hess, Jr., H. B. Demuth, E. A. Brown, R. R. Mohler, "Control Systems for the Kiwi-A Nuclear Reactor Rocket Engines," I.R.E. transactions on Nuclear Science, to be published.